LA-6971-PR
Progress Report

Special Distribution
Issued: September 1977

c. 3

Applied Nuclear Data Research and Development

April 1—June 30, 1977

Compiled by

C. I. Baxman
P. G. Young

los alamos
scientific laboratory
of the University of California
LOS ALAMOS, NEW MEXICO 87545

An Affirmative Action/Equal Opportunity Employer

UNITED STATES
ENERGY RESEARCH AND DEVELOPMENT ADMINISTRATION
CONTRACT W-7405-ENG. 36

The four most recent reports in this series, unclassified, are LA-6560-PR, LA-6723-PR, LA-6754-PR, and LA-6893-PR.

This work was performed under the auspices of the Nuclear Regulatory Commission, the Electric Power Research Institute, the Air Force Weapons Laboratory, and the US Energy Research and Development Administration's Divisions of Military Application, Reactor Development and Demonstration, Physical Research, and Magnetic Fusion Energy.

CONTENTS

I. THEORY AND EVALUATION OF NUCLEAR CROSS SECTIONS..... 1

A. Four-Nucleon R-Matrix Analysis..... 1

B. Particle-Exchange Contributions to the R-Matrix... 1

C. Neutron Cross Sections for Yttrium and Titanium Isotopes..... 3

D. Excited State Cross Sections for the $^{169}Tm^{*}(n,\gamma)$ Reaction..... 10

E. General Development of the GNASH Code..... 13

F. Optical Model and Coupled-Channel Analysis..... 13

G. Cross-Section Evaluations for Version V of ENDF/B. 19

H. Electron and Photon Spectra Following a Fission Burst..... 19

II. NUCLEAR CROSS-SECTION PROCESSING..... 21

A. Nuclear Heating and ENDF/B Consistency..... 21

B. Cross Sections for Thermal Power Reactors..... 23

C. NJOY Code Development..... 24

D. Fission Partials in TRANSX..... 25

E. Monte Carlo Cross Sections..... 26

F. Two New Basic Computational Tools for Routine Use. 27

III. DATA FOR MAGNETIC FUSION ENERGY--ESTIMATION OF UNCERTAINTIES IN SECONDARY SPECTRA..... 30

IV. FISSION PRODUCTS AND ACTINIDES: YIELDS, YIELD THEORY, DECAY DATA, DEPLETION, AND BUILDUP..... 33

A. Fission-Yield Theory..... 33

B. ENDF/B Phenomenological Yield Model Improvements.. 34

C. Preliminary Yields for ENDF/B-V..... 34

D. Library for Processed ENDF/B Aggregate Fission-Product Spectra..... 47

E. Delayed Neutron Precursors..... 50

F. Comparisons of Calculated and Experimental Delayed Fission-Product Beta and Gamma Spectra..... 55

G. Processing of Preliminary ENDF/B Actinide Cross Sections..... 55

H. Few-Group Cross Sections for Fission-Product Absorption Calculations..... 55

V. SHIELD DESIGN FOR MEDIUM ENERGY NEUTRON RADIOTHERAPY... 61

REFERENCES..... 61

APPLIED NUCLEAR DATA RESEARCH AND DEVELOPMENT
QUARTERLY PROGRESS REPORT
April 1 - June 30, 1977

Compiled by

C. I. Baxman and P. G. Young

ABSTRACT

This progress report describes the activities of the Los Alamos Nuclear Data Group for the period April 1 through June 30, 1977. The topical content is summarized in the contents.

I. THEORY AND EVALUATION OF NUCLEAR CROSS SECTIONS

A. Four-Nucleon R-Matrix Analysis (G. Hale and D. Dodder)

New experimental data have been included in our analysis of the elastic scattering of protons on ^{3}He at energies up to 20 MeV.[1] These include measurements made with polarized protons on ^{3}He (Ref. 2) and with protons on polarized ^{3}He targets[3] at energies between 2.7 and 10 MeV. A good fit to these data has been achieved, while generally maintaining an excellent representation of the other data in the analysis. The addition of the new data has strengthened earlier indications that the low-energy polarization measurements of Drigo[4] are in error.

The revised R-matrix parameters, although not much different from the previous values, will be used to fix the isospin-1 part of our larger analysis of the ^{4}He system.

B. Particle-Exchange Contributions to the R-Matrix (G. Hale)

It is possible to account for part of a binary reaction process by imagining that one of the incident particles is a bound pair, one of which in the course of the reaction is attracted to the other incident particle to form (in general) a different bound pair in the final state. This "particle-exchange" process is illustrated diagrammatically in Fig. 1.

The contributions from such processes may be calculated approximately from the asymptotic forms of the bound-state wave functions without specific knowledge of the nuclear forces involved. Including these contributions has improved the phenomenological analysis of data for several reactions, including nucleon-nucleon[5] and p-^{3}He scattering.[6]

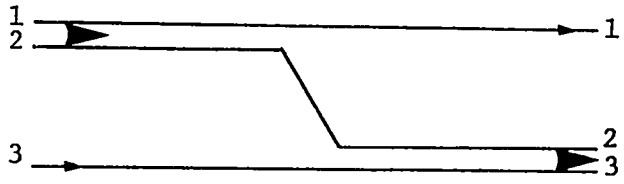

Fig. 1.
Particle-exchange diagram for the reaction (1,2) + 3 → 1 + (2,3).

We are investigating the possibility of including particle-exchange contributions explicitly in the R-matrix formulation of nuclear reactions. This would seem a natural place to include them, since the elements of R are essentially the channel-surface matrix elements of the Green's function, $G = (H-E)^{-1}$, for the total internal Hamiltonian, H, for an appropriate choice of boundary condition. If H_0 represents the sum of the kinetic-energy operators of the three particles plus the interaction in the (1,2) bound pair, then the lowest order term of the Green's function,

$$G_0 = (H_0-E)^{-1} \quad ,$$

cancels the hard-sphere contribution to the amplitude for (1,2) + 3 → (1,2) + 3 elastic scattering. Its contribution to the reaction (1,2) + 3 → 1 + (2,3) (Fig. 1) is proportional to

$$C_{23}\, C_{12}\, [F_0(ka)O_0(k'a') + F_0(k'a')O_0(ka)]\, \frac{d}{dx}\, Q_0\, (x)$$

for particle 2 exchanged in a relative S-state, where

C_{ij} is the coupling constant for (i,j) → i + j,

F_0 and O_0 are the $\ell = 0$ regular and outgoing spherical wave Coulomb functions, respectively,

k and k' are the initial and final center-of-mass wave numbers,

a and a' are the initial and final channel radii,

Q_0 is the $\ell = 0$ irregular Legendre function, and

$$x = \left(\frac{m_1}{m_1 + m_2} k^2 + \frac{m_1 m_2}{m_1} k'^2 + 2m_2 B/\hbar^2 \right) / kk' \quad ,$$

with B the binding energy of the (1,2) system.

Because of the large $^6Li \rightarrow \alpha + d$ coupling constant, we expect such terms to contribute strongly to the $^6Li(n,t)^4He$ reaction, and possibly account for a large portion of the 1/v cross section observed at low neutron energies. We are checking to see if some of the distant-level terms in our current R-matrix analysis for the ^7Li system[7] are approximating the effect of particle exchange terms.

C. Neutron Cross Sections for Yttrium and Titanium Isotopes (E. D. Arthur and P. G. Young

1. Cross Sections for n + $^{86-92}Y$ Reactions from 1 keV to 20 MeV. Cross sections for neutron-induced reactions on $^{86,87,88,88M,89,90,91,92}Y$ have been calculated from 1 keV to 20 MeV using the GNASH and COMNUC nuclear model codes. The results are available in the Los Alamos Scientific Laboratory (LASL) ENDF/B sub-library (photostore file FS=LASL405, OAC=TO2PGY).

For each target nucleus the following reactions were included in the calculation: (n,γ), (n,n'), (n,p), (n,α), (n,2n), (n,np), (n,nα), (n,pn) and (n,αn). A complete list of the reactions, thresholds, etc. is included as Table I.

The isomeric states for which explicit calculations were made are shown in Fig. 2. The n + ^{88}Y calculations were made for the $J^\pi = 1^+$ second excited state of ^{88}Y at $E_x = 0.393$ MeV. In the case of ^{89}Y, the capture cross section to the ^{90}Y $J^\pi = 7^+$ second excited state ($E_x = 0.682$ MeV) was calculated, as was the

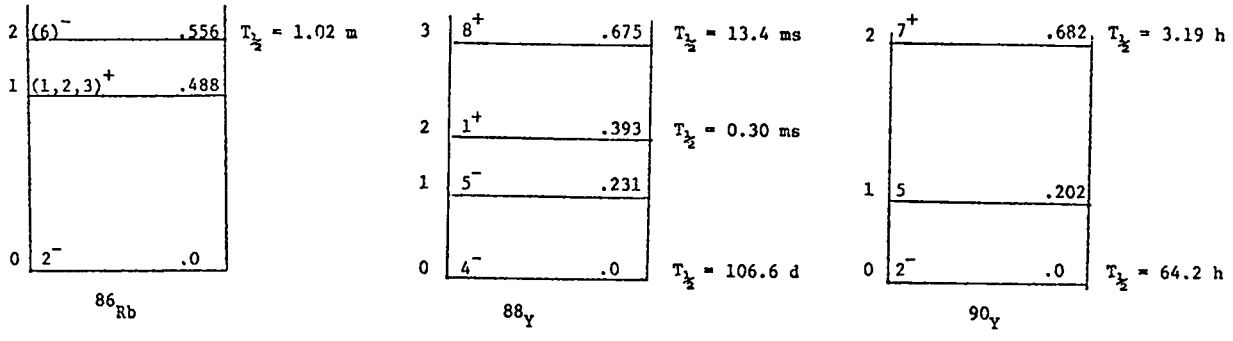

Fig. 2.
Low-lying states of ^{86}Rb, ^{88}Y, and ^{90}Y.

TABLE I

Q-VALUES AND THRESHOLD FOR YTTRIUM FRACTIONS

MAT	MT	Reaction	Initial State	Final State	Q (MeV)	E_{th} (MeV)
3986	4	$^{86}Y(n,n')^{86}Y$	0	0	-0.208	0.210
	16	$^{86}Y(n,2n)^{85}Y$	0	0	-9.473	9.584
	22	$^{86}Y(n,n\alpha)^{82}Rb$	0	0	-5.467	5.531
	28	$^{86}Y(n,np)^{85}Sr$	0	0	-5.430	5.494
	102	$^{86}Y(n,\gamma)^{87}Y$	0	0	11.819	-
	103	$^{86}Y(n,p)^{86}Sr$	0	0	6.055	-
	107	$^{86}Y(n,\alpha)^{83}Rb$	0	0	5.359	-
3987	4	$^{87}Y(n,n')^{87}Y$	0	0	-0.381	0.386
	16	$^{87}Y(n,2n)^{86}Y$	0	0	-11.819	11.956
	22	$^{87}Y(n,n\alpha)^{83}Rb$	0	0	-6.460	6.535
	28	$^{87}Y(n,np)^{86}Sr$	0	0	-5.764	5.831
	102	$^{87}Y(n,\gamma)^{88}Y$	0	0	9.377	-
	103	$^{87}Y(n,p)^{87}Sr$	0	0	2.665	-
	107	$^{87}Y(n,\alpha)^{84}Rb$	0	0	2.416	-
3988	4	$^{88}Y(n,n')^{88}Y$	0	0	-0.231	0.234
	16	$^{88}Y(n,2n)^{87}Y$	0	0	-9.377	9.484
	22	$^{88}Y(n,n\alpha)^{84}Rb$	0	0	-6.960	7.040
	28	$^{88}Y(n,np)^{87}Sr$	0	0	-6.712	6.789
	102	$^{88}Y(n,\gamma)^{89}Y$	0	0	11.468	-
	103	$^{88}Y(n,p)^{88}Sr$	0	0	4.401	-
	107	$^{88}Y(n,\alpha)^{85}Rb$	0	0	3.517	-

TABLE I (cont)

MAT	MT	Reaction	Initial State	Final State	Q (MeV)	E_{th} (MeV)
881	4	$^{88M}Y(n,n')^{88}Y$	2	0	0.393	-
	16	$^{88M}Y(n,2n)^{87}Y$	2	0	-8.894	9.087
	22	$^{88M}Y(n,n\alpha)^{84}Rb$	2	0	-6.567	6.642
	28	$^{88M}Y(n,np)^{87}Sr$	2	0	-6.319	6.392
	102	$^{88M}Y(n,\gamma)^{88}Y$	2	0	11.861	-
	103	$^{88M}Y(n,p)^{88}Sr$	2	0	4.794	-
	107	$^{88M}Y(n,\alpha)^{85}Rb$	2	0	3.910	-
304	4	$^{89}Y(n,n')^{89}Y$	0	0	-0.908	0.918
	16	$^{89}Y(n,2n)^{88}Y$	0	0	-11.468	11.598
	16	$^{89}Y(n,2n)^{88M}Y$	0	2	-11.861	11.996
	16	$^{89}Y(n,2n)^{88M}Y$	0	3	-12.143	12.281
	22	$^{89}Y(n,n\alpha)^{85}Rb$	0	0	-7.951	8.041
	28	$^{89}Y(n,np)^{88}Sr$	0	0	-7.067	7.147
	102	$^{89}Y(n,\gamma)^{90}Y$	0	0	6.860	-
	102	$^{89}Y(n,\gamma)^{90M}Y$	0	2	6.178	-
	103	$^{89}Y(n,p)^{89}Sr$	0	0	-0.707	0.715
	107	$^{89}Y(n,\alpha)^{86}Rb$	0	0	0.699	-
	107	$^{89}Y(n,\alpha)^{86M}Rb$	0	2	0.144	-
3990	4	$^{90}Y(n,n')^{90}Y$	0	0	-0.202	0.204
	16	$^{90}Y(n,2n)^{89}Y$	0	0	-6.860	6.937
	22	$^{90}Y(n,n\alpha)^{86}Rb$	0	0	-6.160	6.229
	28	$^{90}Y(n,np)^{89}Sr$	0	0	-7.567	7.652

TABLE I (cont)

MAT	MT	Reaction	Initial State	Final State	Q (MeV)	E_{th} (MeV)
3990	102	$^{90}Y(n,\gamma)^{91}Y$	0	0	7.947	-
	103	$^{90}Y(n,p)^{90}Sr$	0	0	0.237	-
	107	$^{90}Y(n,\alpha)^{87}Rb$	0	0	3.766	-
3991	4	$^{91}Y(n,n')^{91}Y$	0	0	-0.556	0.562
	16	$^{91}Y(n,2n)^{90}Y$	0	0	-7.946	8.034
	22	$^{91}Y(n,n\alpha)^{87}Rb$	0	0	-4.181	4.227
	28	$^{91}Y(n,np)^{90}Sr$	0	0	-7.709	7.795
	102	$^{91}Y(n,\gamma)^{92}Y$	0	0	6.557	-
	103	$^{91}Y(n,p)^{91}Sr$	0	0	-1.883	1.904
	107	$^{91}Y(n,\alpha)^{88}Rb$	0	0	1.902	-
3992	4	$^{92}Y(n,n')^{92}Y$	0	0	-0.241	0.244
	16	$^{92}Y(n,2n)^{91}Y$	0	0	-6.557	6.629
	22	$^{92}Y(n,n\alpha)^{88}Rb$	0	0	-4.655	4.706
	28	$^{92}Y(n,np)^{91}Sr$	0	0	-8.440	8.532
	102	$^{92}Y(n,\gamma)^{93}Y$	0	0	7.491	-
	103	$^{92}Y(n,p)^{92}Sr$	0	0	-1.129	1.141
	107	$^{92}Y(n,\alpha)^{89}Rb$	0	0	2.522	-

(n,α) cross section to the 6^- isomeric state in ^{86}Rb at 0.556 MeV. The (n,2n) cross sections to the isomeric states at 0.393 MeV (1^+) and 0.675 MeV (8^+) in ^{88M}Y were also included for ^{89}Y.

The following global optical parameter sets were used to obtain transmission coefficients used in the calculation:

neutrons - (1 keV-2 MeV) Moldauer[8]
neutrons - (2 MeV-20 MeV) Wilmore-Hodgson[9]
protons - Perey[10]
alphas - McFadden-Satchler[11]

The Gilbert-Cameron[12] level density form was used with no adjustment of the parameters given by Cook,[13] except as required to match the low-lying levels of each residual nucleus. A simplified pre-equilibrium model by Milazzo-Colli et al.[14] was used to account for multistep processes occurring before equilibrium is reached. Such semidirect effects are important in obtaining correct (n,p) (n,α), and (n,2n) cross sections at higher energies.

Because (n,γ) cross sections were of special concern, a fairly complete study of the parameters needed for calculations of capture cross sections in this mass region was made (see our previous progress report[15] for details). The Brink-Axel[16] giant dipole resonance model was used to provide the energy dependence of gamma-ray transmission coefficients. Gamma-ray cascades were followed in detail assuming all transitions to be electric dipole, magnetic dipole, or electric quadrupole in nature. A new formalism based on an approach similar to that used in pre-equilibrium particle decay was developed in order to account for direct-semidirect effects and the presence of the giant dipole resonance upon higher energy capture cross sections. These latter effects are clearly present in the calculations of the $^{89}Y(n,\gamma)$ cross sections (shown in Fig. 3) for energies around 14 MeV.

In Figs. 3-6 comparisons of the calculations with available experimental results are made for ^{89}Y reactions. The experimental data references in Figs. 4-6 are defined in the Lawrence Livermore Laboratory report UCRL-50400.

2. Cross Sections for n + $^{46-50}Ti$ Reactions from 8-20 MeV. Using the same techniques and model parameters described above, reaction cross sections were also calculated for neutron-induced reactions on $^{46,47,48,49,50}Ti$. The results are generally in good agreement with experimental data. The calculations are available in tabular form and have been provided to A. B. Smith of Argonne

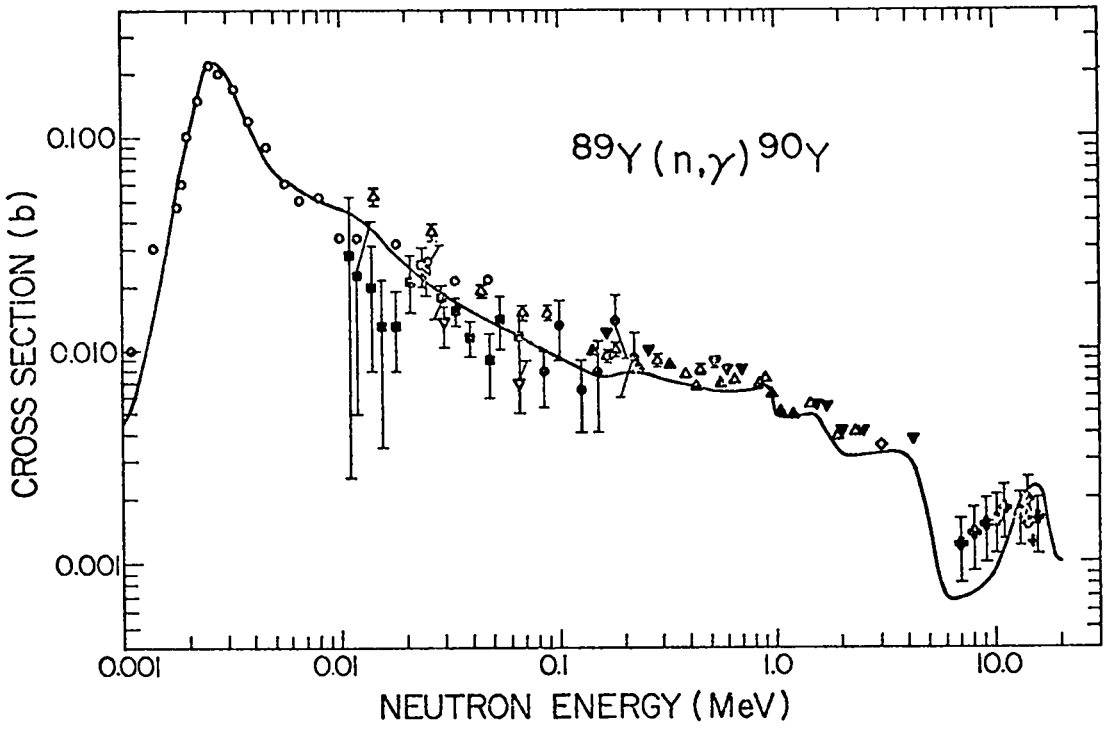

Fig. 3.
The $^{88}Y(n,\gamma)$ cross section from 1 keV to 20 MeV. The solid curve represents the evaluated data and the points are experimental results.

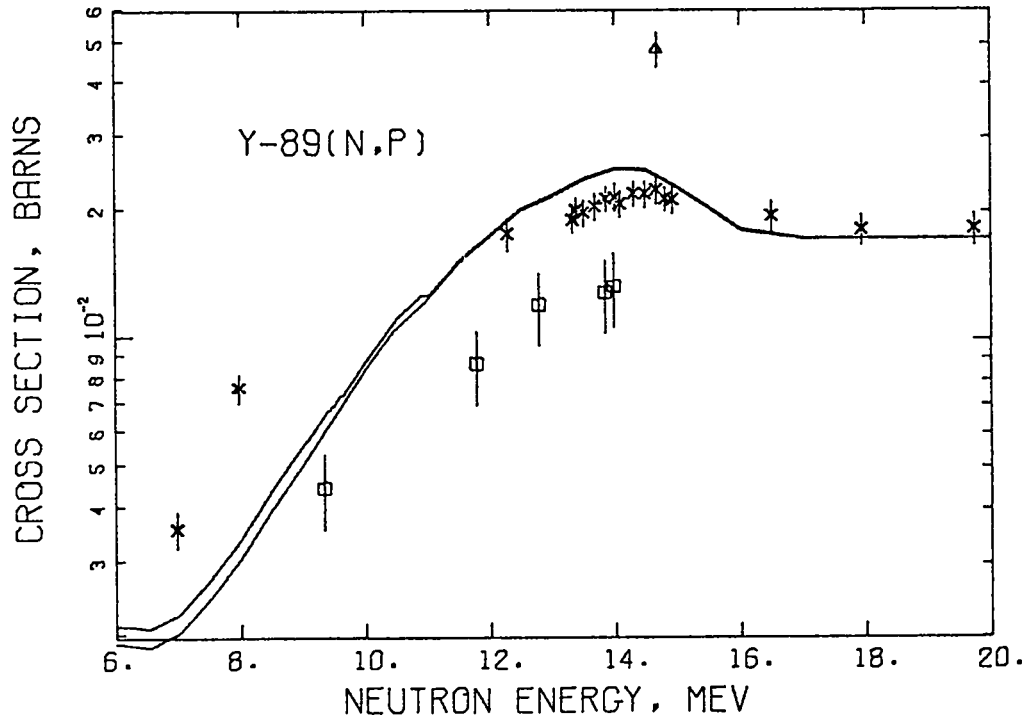

Fig. 4.
The $^{89}Y(n,p)$ cross section from 6 to 20 MeV. The solid curve represents the evaluated data and the points are experimental results.

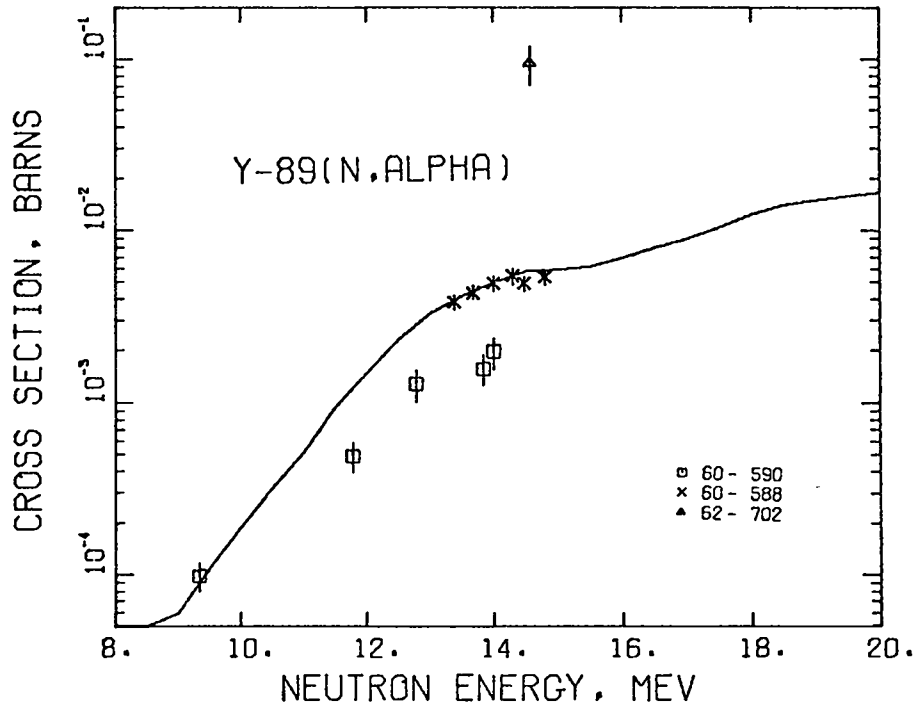

Fig. 5.
The $^{89}Y(n,\alpha)$ cross section from 8 to 20 MeV. The solid curve represents the evaluated data and the points are experimental results.

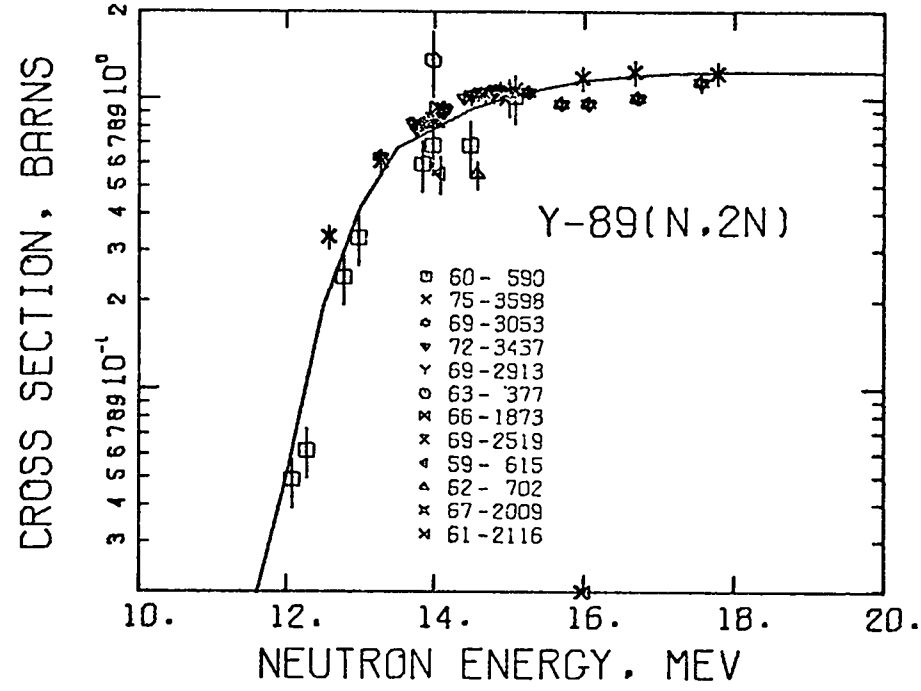

Fig. 6.
The $^{89}Y(n,2n)$ cross section from 10 to 20 MeV. The solid curve represents the evaluated data and the points are experimental results.

National Laboratory (ANL), who is evaluating titanium data for inclusion in the Evaluated Nuclear Data Files (ENDF/B).

D. Excited State Cross Sections for the $^{169}Tm^{*}(n,\gamma)$ Reaction (E. D. Arthur)

We have performed statistical-precompound-theory calculations of neutron-induced reaction cross sections on ^{169}Tm using the GNASH[17] and COMNUC[18] model codes, in which the target nucleus could be in its ground state or in one of several low-lying excited states. Destruction cross sections [(n,γ) and $(n,2n)$] were calculated from 5 keV to 2 MeV (for capture) and from threshold up to 15 MeV for the $(n,2n)$ reaction. Calculations were first made for ^{169}Tm in its ground state ($J^{\pi} = 1/2^{+}$) and first excited state ($J^{\pi} = 3/2^{+}$, $E_x = 0.0084$ MeV). The $(n,2n)$ cross sections calculated for ^{169}Tm in its ground and first excited states were found to be very similar. Only around the $(n,2n)$ thresholds for these two cases were there differences as large as 10%. However, reasonably significant differences did occur for the capture cross sections.

Figure 7 shows the experimental and calculated (n,γ) values for ^{169}Tm in its ground state. The solid histogram results from the recent measurements of D. M. Drake[19] (LASL P-3) made at the Oak Ridge Electron Linear Accelerator (ORELA). Other points are older measurements taken from the Brookhaven National Laboratory (BNL) report BNL-325. The dotted curve results from statistical calculations using the neutron-optical parameters of Auerbach[20] with the Weisskopf[21] approximation for the gamma-ray strength function. The discrepancy between the calculation and the experimental values for energies greater than 500 keV may be due in part to the fact that gamma-ray cascades were not considered in the calculation and that all gamma rays were assumed to result from capture (i.e., $n,n'\gamma$ contributions were ignored). Also, above approximately 1 MeV the systematic errors in the experimental results become greater because of gamma rays from the $(n,n'\gamma)$ reaction, which are detected in the experimental apparatus.

Using the same input parameters (optical model, gamma-ray strength, and normalization) as those used for the curve in Fig. 7, (n,γ) cross sections were calculated for ^{169}Tm in its first seven excited states. The ratios of the excited state cross sections to the ground-state cross section are given in Fig. 8. The excited state numbers are indicated for each curve, and the excitation energies, spins, and parities of the states are given in Table II. The results in Fig. 8 indicate that the excited state cross sections for the $^{169}Tm^{*}(n,\gamma)$ reactions are significantly higher than the ground state values over the neutron

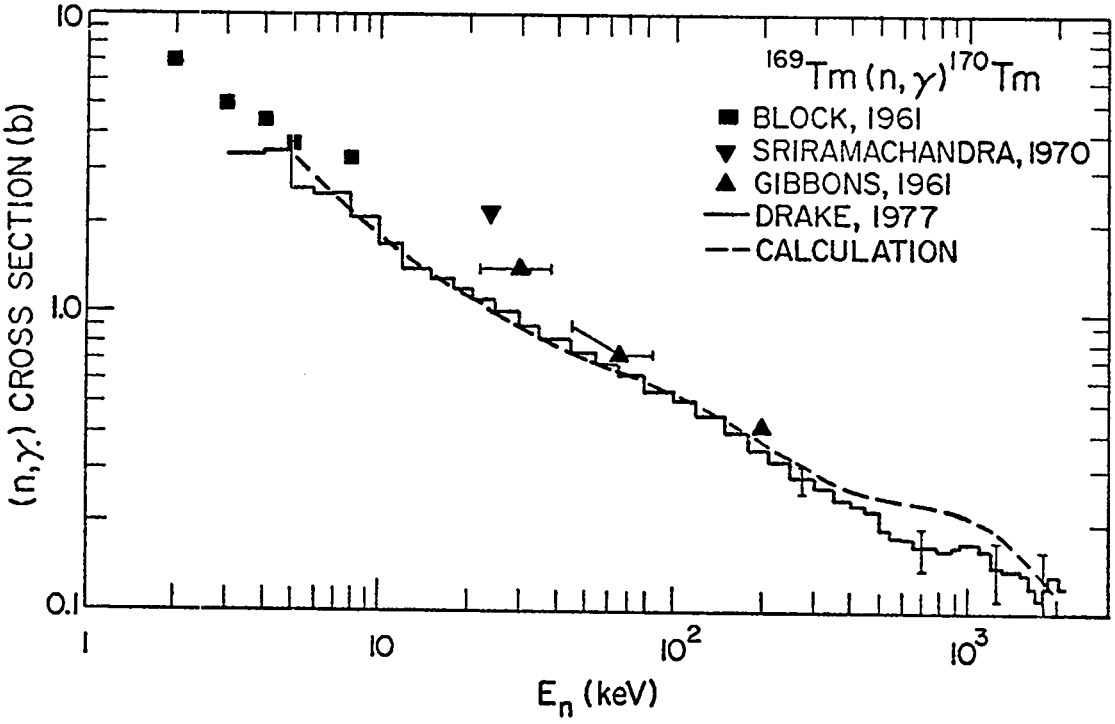

Fig. 7.

Theoretical and experimental cross sections for the $^{169}Tm(n,\gamma)$ reaction.

TABLE II

SPINS, PARITIES, AND EXCITATION ENERGIES OF THE LOW-LYING STATES OF ^{169}Tm

Excited State Number	Excitation Energy (keV)	Spin, Parity
(ground)	0	$1/2^+$
1	8.4	$3/2^+$
2	118.2	$5/2^+$
3	139.0	$7/2^+$
4	316.2	$7/2^+$
5	332	$9/2^+$
6	368	$11/2^+$
7	379	$7/2^-$

energy range 5 keV to 2 MeV. The largest effect occurs for the $11/2^+$ sixth excited state, whose cross section is a factor of 3 higher at 1 MeV than the ground state cross section.

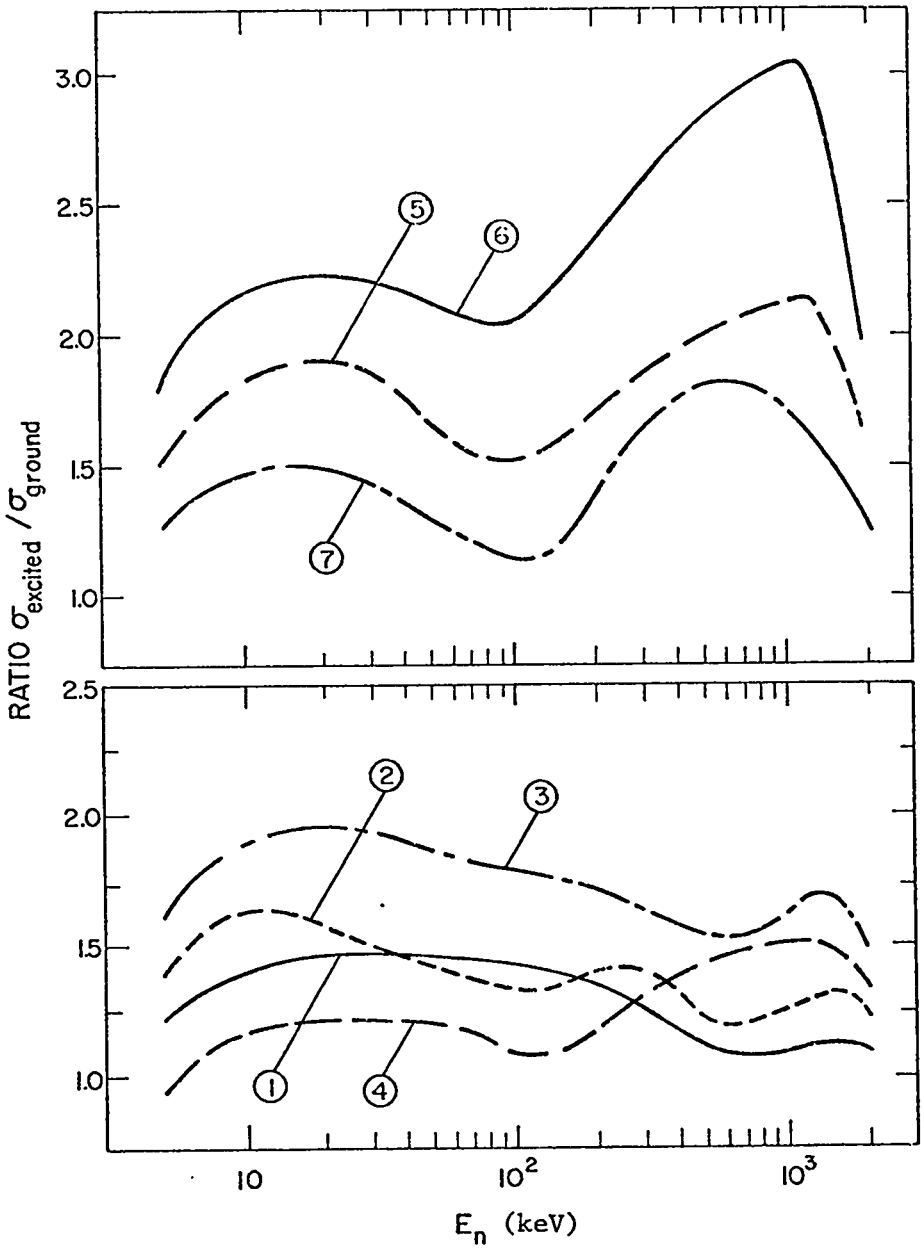

Fig. 8.
Ratios of $\sigma_{excited}$ to $\sigma_{ground\ state}$ for $^{169}Tm(n,\gamma)$ reactions calculated for the first seven excited states of ^{169}Tm.

E. General Development of the GNASH Code (E. D. Arthur and P. G. Young)

Papers were presented this quarter at the New York American Nuclear Society (ANS) meeting describing calculations with the GNASH[17] code of 15-MeV neutron-induced charged-particle spectra on stainless steel 316[22] and of proton and alpha-production cross sections from n + ^{59}Co reactions up to 40 MeV.[22] In addition, a paper summarizing GNASH capabilities, calculations, and limitations was presented at the Brookhaven National Laboratory symposium on neutron cross sections in the 10-40 MeV range.[23]

In preparation for these papers, several calculations of cross sections and secondary-energy distributions as functions of incident-neutron energy were carried out, primarily for stainless steel components. Calculated (n,p) cross sections using the Wilmore-Hodgson[9] global optical parameters for neutrons and the Perey[10] parameters for protons are compared to experiment in Fig. 9 for ^{54}Fe, ^{56}Fe, ^{58}Ni, and ^{60}Ni. Figure 10 compares experimental and calculated (n,2n) cross sections for ^{52}Cr and ^{56}Fe using the same model parameters. Finally, calculated gamma-ray emission spectra from 14-MeV neutron bombardment of ^{56}Fe and ^{93}Nb are compared to recent LASL measurements in Fig. 11. Parameter optimization was not used for any of these calculations.

F. Optical Model and Coupled-Channel Analysis (D. G. Madland, D. C. George, and P. G. Young)

1. Code Development. The optical model search code RAROMP[24] (spin 0 and spin 1/2 projectiles) has been modified to calculate certain quantities pertinent to neutron-nucleus elastic scattering analysis. These are the reaction cross section σ_R, the total inelastic cross section σ_E, and the total cross section σ_T, together with their decomposition into channel spin ℓ, namely $\sigma_R^{(\ell)}$, $\sigma_E^{(\ell)}$, and $\sigma_T^{(\ell)}$ (a previous modification computes the transmission coefficient T_ℓ). In addition, the option of including an isotropic compound elastic (σ_{CE}) contribution to σ_E and σ_R is allowed; that is, $\sigma_E(\text{exp}) = \sigma_E$ (shape elastic optical model) + σ_{CE} and $\sigma_R(\text{exp}) = \sigma_R$ (optical model) - σ_{CE}. These modifications have all been made by direct use of the S-matrix elements generated by integration of the Schrodinger equation.

The optical model search code SNOOPY VI[25] (spin 0, 1/2, 1 projectiles) has been modified for production search-optimization of elastic angular distributions and/or polarization data by adapting the lineprinter plot routines to include the experimental data points and uncertainties, as well as the theoretical

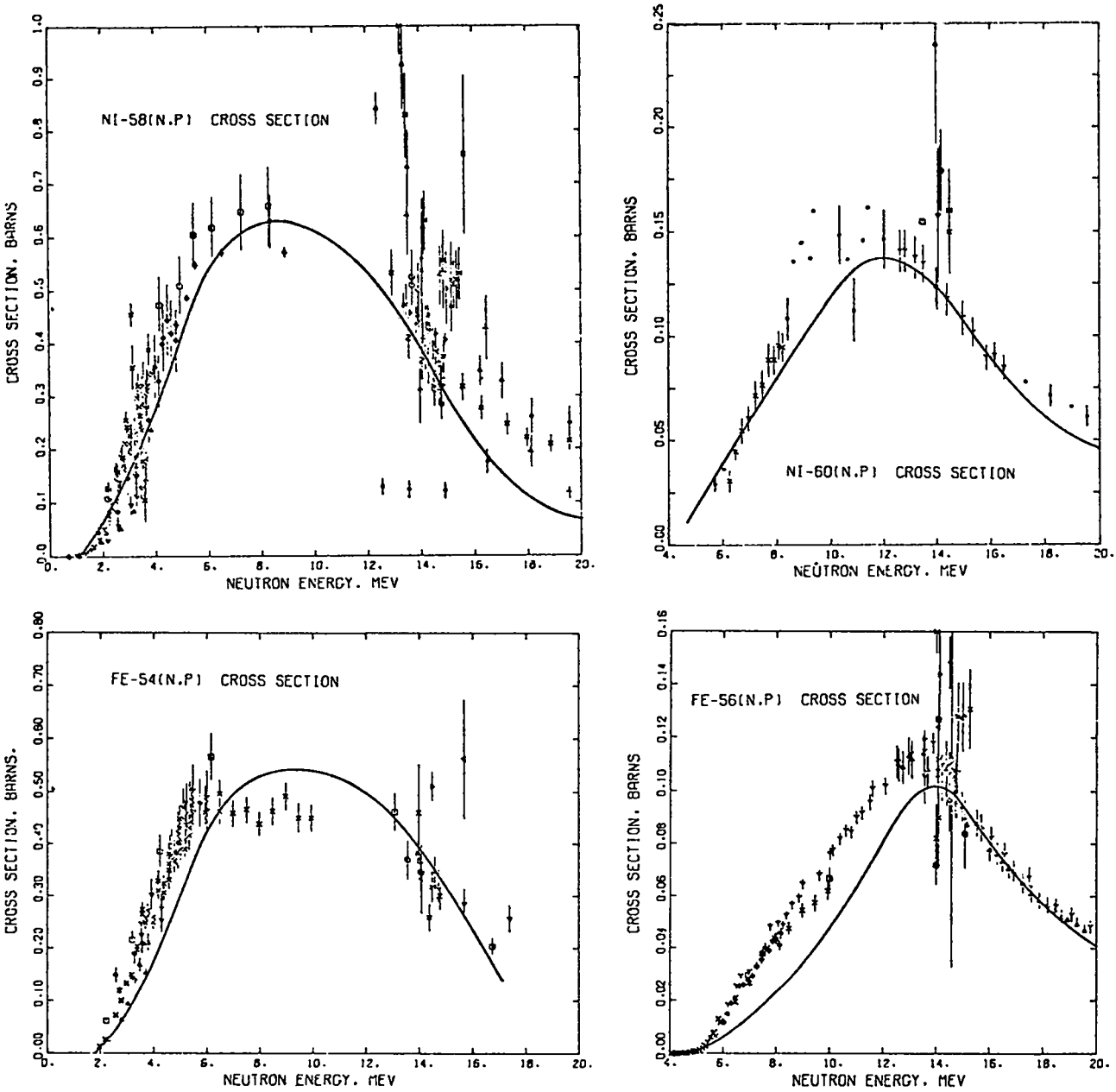

Fig. 9.
Calculated and experimental (n,p) cross section for ^{54}Fe, ^{56}Fe, ^{58}Ni, and ^{60}Ni. The solid curves indicate the GNASH calculations.

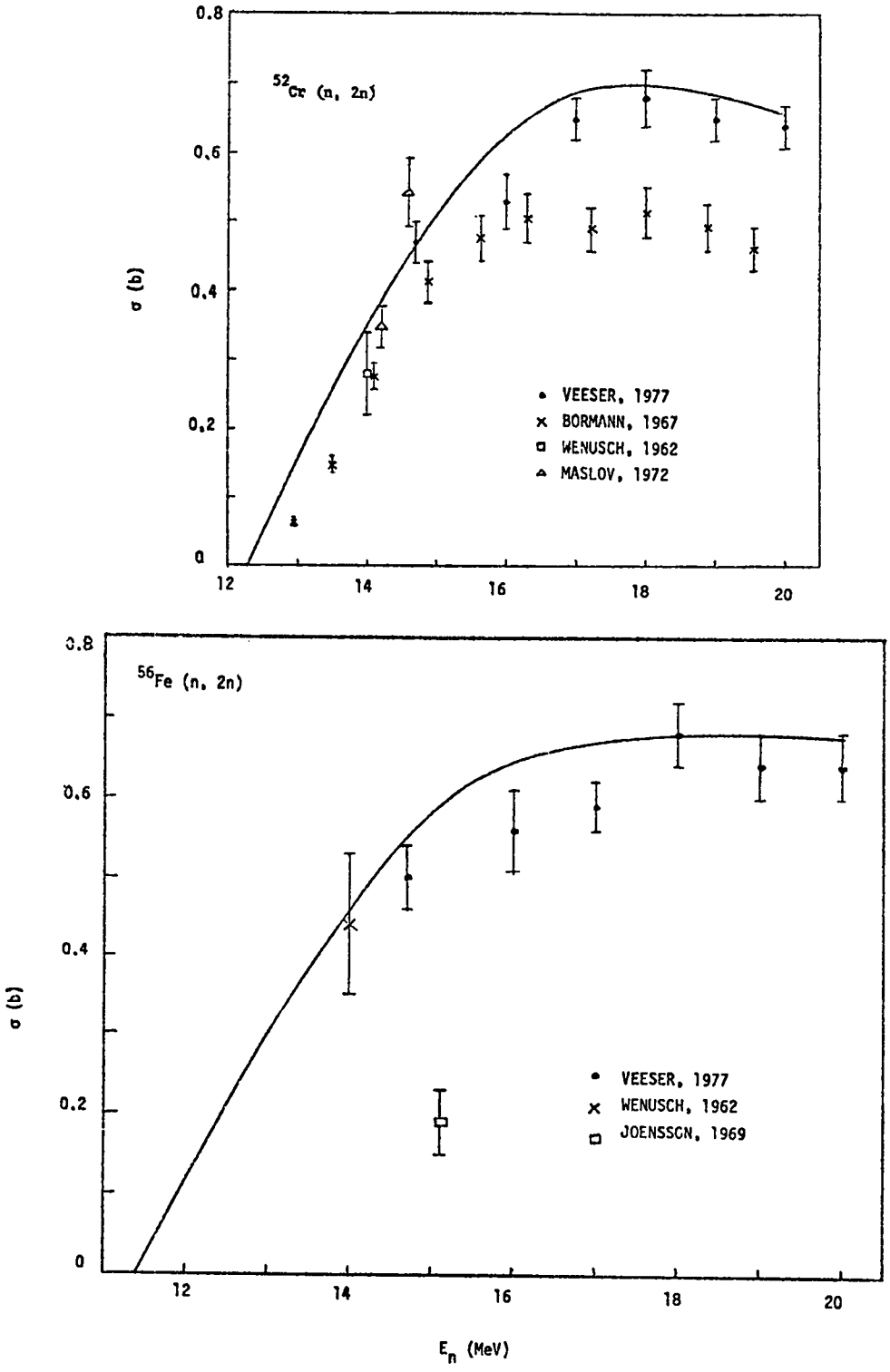

Fig. 10.
Calculated and experimental (n,2n) cross sections for ^{52}Cr and ^{56}Fe. The solid curves indicate the GNASH calculations.

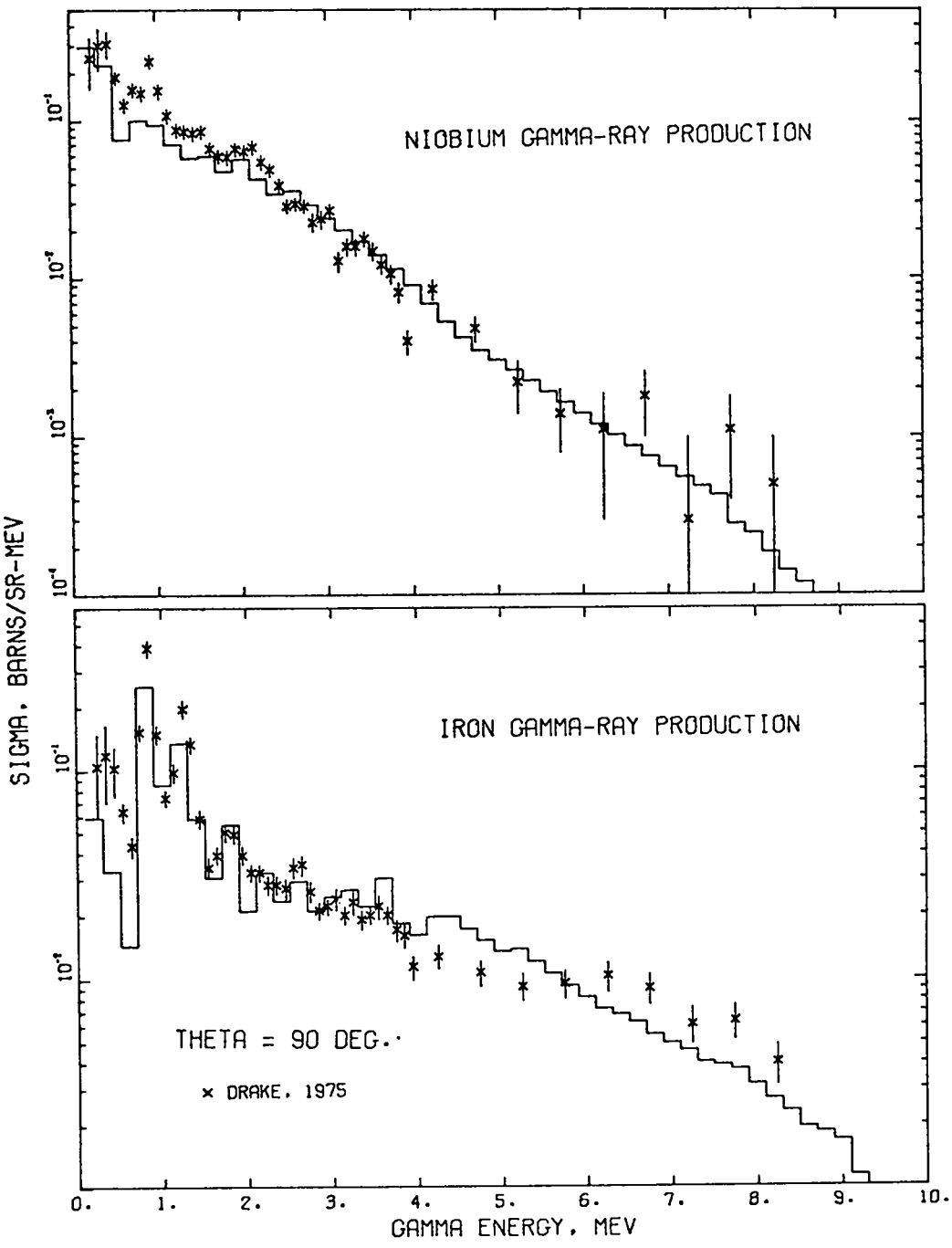

Fig. 11.
Calculated and experimental gamma-ray emission spectra induced by 14 MeV neutron bombardment of ^{56}Fe and ^{93}Nb. The solid histograms represent the GNASH calculations.

values. This revision allows a direct comparison of the data and the fit to the data as a function of the scattering angle. Previously, the goodness of fit could only be judged in terms of the total χ^2.

2. Optical Model Calculations for the n + ^{237}U Reaction. The total probability of forming the compound nucleus $^{238}U^*$ was calculated as a function of the neutron energy E_n from 10 keV to 40 MeV. The total probability of formation is just the absorption cross section σ_A which is equal to the sum of experimental reaction cross section σ_R (exp) and the compound elastic cross section σ_{CE}. This sum is, by definition, the optical model reaction cross section σ_R(optical model). In the absence of elastic neutron scattering data for ^{237}U, the calculations were carried out by using three different global optical model parameter sets: Wilmore-Hodgson[9] (W-H), Becchetti-Greenlees[26] (B-G), and Moldauer[8] (M). The results for eight bombarding energies are illustrated in Fig. 12 (reaction cross section), Fig. 13 (total elastic cross section), and Fig. 14 (total cross section). As Fig. 12 shows, there are strong disagreements, particularly below 1 MeV, in the optical model reaction cross section. This is due partly to the inadequacy of the spherical optical model for calculations in the deformed actinide region, but is mainly caused by differences in the data bases used to generate the three global sets: W-H is valid for $1 \leqslant E_n \leqslant 15$ MeV, B-G is valid for $1 \leqslant E_n \leqslant 40$ MeV, and M is valid for $E_n \leqslant 1$ MeV. Moreover, only the data base of M includes data for $A > 208$. The conclusion is that only semi-quantitative results can be obtained with these three global sets in the actinide region. Consequently, the calculation is being repeated by performing optical model searches on ^{235}U elastic scattering data, together with total cross-section data of other uranium isotopes. By doing so we hope to also improve the calculations of the elastic (Fig. 13) and total cross sections (Fig. 14) for other uranium isotopes. This work is to be followed by invoking coupled-channel calculations of the S-matrix to take into account the effects of the strongly collective ground state rotational band.

3. Transmission Coefficient Comparisons. A number of large discrepancies appear to exist between different laboratories in the calculation of transmission coefficients (for various particles) used in statistical model reaction codes. It was therefore decided to check the internal consistency of codes used in T-2 by computing several test cases with entirely independent codes. Transmission coefficients for neutrons, protons, and alpha particles were calculated for the mass 88 system at several different incident energies with TCCAL (a utility code

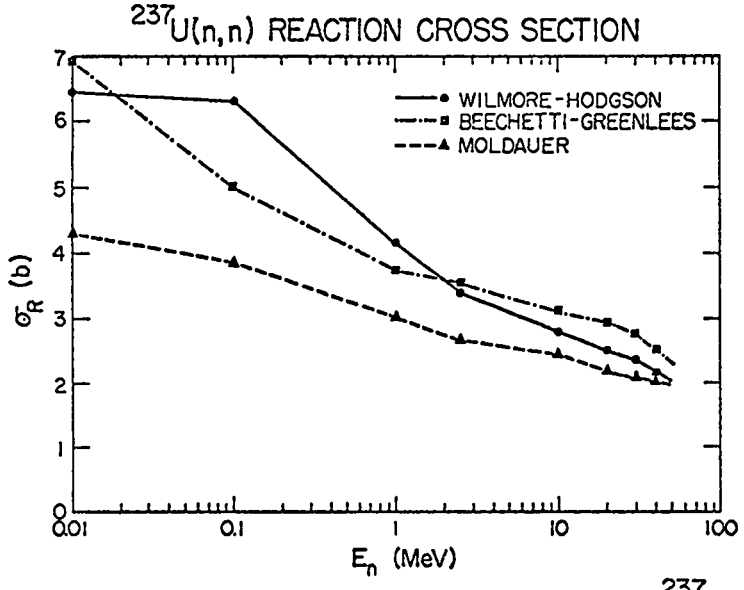

Fig. 12.
Optical model reaction cross section as a function of the neutron bombarding energy for three global optical potentials. The lines serve merely to guide the eye through the calculated points.

Fig. 13.
Optical model total elastic cross section as a function of the neutron bombarding energy, for three global potentials. The lines serve merely to guide the eye.

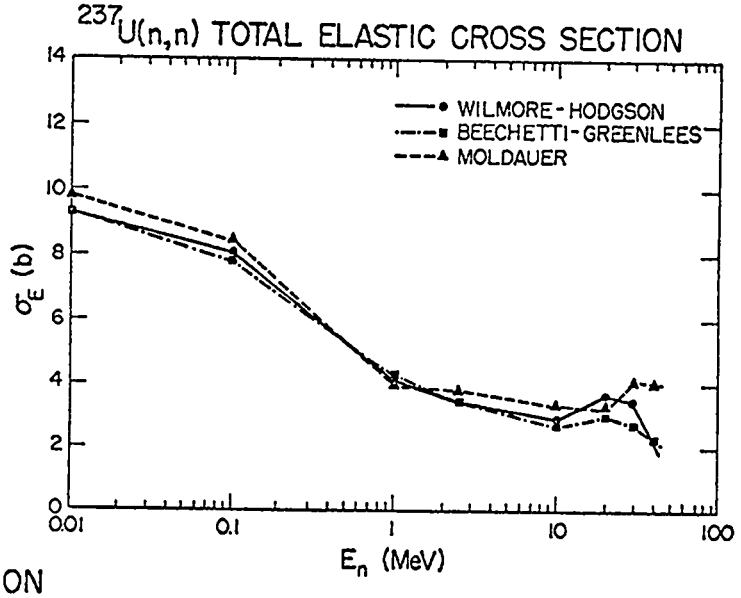

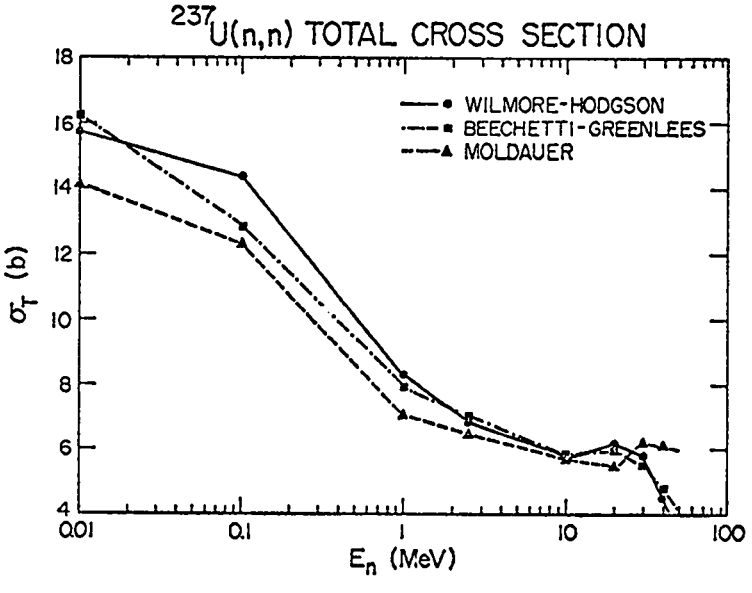

Fig. 14.
Optical model total cross section as a function of the neutron bombarding energy for three global optical potentials. The lines serve merely to guide the eye.

for generating GNASH input that uses optical routines by Ferguson[27]) and RAROMP (an optical model code developed at the University of Minnesota[24]). The largest discrepancy found is for alpha particles at 30 MeV and is about 1%. Since the differences are negligible for neutrons, very slight for protons, and ~1% for alpha particles, it is thought that the treatment of the Coulomb waves is the major source of the differences. For cross-section calculations however, 1% changes in T_ℓ are negligible, and we conclude that our transmission coefficient calculations are satisfactory for our purposes.

G. Cross-Section Evaluations for Version V of ENDF/B (E. D. Arthur, D. G. Foster, Jr., G. M. Hale, R. J. LaBauve, and L. Stewart)

Several evaluations are being updated and revised for Version V of ENDF/B. Thus far, revised data sets for ^{1}H, ^{2}H, ^{3}H, ^{10}B, and ^{15}N have been submitted to BNL. In addition to updating the formats for Version V, the following modifications were made:

- ^{1}H - Correlated error files added.
- ^{2}H - Elastic and total cross sections at low energies updated to include more recent measurements.
- ^{3}H - File 8 data provided.
- ^{10}B - New R-matrix analysis incorporated for standard cross sections and joined to the Version IV data above 1 MeV. Correlated error files added for cross sections below 1 MeV.
- ^{15}N - The preliminary data set submitted earlier to BNL was checked and several corrections made. File 4 elastic angular distributions were extensively thinned.

Updating of the ^{6}Li, ^{14}N, ^{16}O, and ^{27}Al evaluations is in progress.

H. Electron and Photon Spectra Following a Fission Burst (D. G. Foster, Jr., and N. L. Whittemore)

The short-term project to supply to the Air Force Weapons Laboratory (AFWL) a compact parameterization of time-dependent electron and photon spectra emitted following a fission burst[28] is almost completed. In consultation with AFWL, the time range has been extended down to 0.1 s after fission. Rather than add complicated provisions for holding selected parameters constant in overdetermined cases, as mentioned in the previous progress report, we have decided to use fixed decay constants which are averages of those obtained in free fits to several

sets of data and fit only the amplitudes in the final pass. Preliminary indications are that a single set of average parameters for all six output sets (fast and 14-MeV fission in ^{235}U, ^{238}U, and ^{239}Pu) leads to an increase in rms errors of the fits of less than a factor of 1.5.

The original free fits can now use up to six different methods of making the initial estimates for the decay constants. The first method is to use the constants obtained for the next lower energy group. The others depend on first searching the data for apparent regions of slowly changing decay constants. Wherever the fitted time range includes enough times, logarithms of the data in each group are fitted with a five-term Lagrange polynomial in order to calculate the logarithmic slope and its first two derivatives. The lowest and highest slopes are used to generate four different arbitrary sets of trial values with uniform logarithmic spacing. The sixth method is to use the points at which the product of the first and second derivatives of the logarithmic slope has relative minima (used in the order of the depth of the minima). We have found this rather ad hoc index to be quite effective. For cases with fewer than 10 times to be fitted, the sixth method does not work, and the limits for the uniformly spaced trial sets are found from the first and last pair of times. A novel method of generating the five-term Lagrange polynomials is described in Sec. II.F of this report.

The preliminary ENDF/B-V evaluated fission-product yields for 14-MeV neutrons on ^{239}Pu have been received, converted to individual-nuclide yields,[29] and used in CINDER calculations of the decay following a 100-μs burst at seven time steps per decade from 0.1 to 10^6 s. These have been reduced to normalized spectra in the manner described previously.[28] Free fits to the beta spectra have been completed. The average decay constants for betas have been calculated and final parameter sets will be sent to AFWL during July. Results for both beta and gamma emission can be punched out directly in the format selected by AFWL, in any desired group structure. An improved method for converting group structures was developed for this project and is described in Sec. II.F.

Preliminary exploration of fitting the more erratic photon spectra in as many as 38 groups has not revealed any new problems. FPSPFT has successfully fitted several cases that display growth followed by decay, without the required negative amplitudes generating any negative emission rates.

II. NUCLEAR CROSS-SECTION PROCESSING

A. Nuclear Heating and ENDF/B Consistency (R. E. MacFarlane, P. G. Young, and D. W. Muir)

Nuclear reactions deposit heat by means of charged secondary particles, including the recoiling residual nucleus itself. Unfortunately, the charged-particle spectra required for this direct calculation are not included in ENDF/B data files. An alternate approach is the energy-balance method. The energy carried away by neutrons and photons is simply subtracted from the energy available; the result has to be the total charged particle energy. This method uses data available in the ENDF/B neutron and photon files. Furthermore, it guarantees conservation of total energy for large systems. This is the method used by the HEATR module of NJOY.

The energy-balance method has two weaknesses. For all but the lightest isotopes the heating is a difference between large numbers; therefore, extreme care is required in the evaluation process to assure that neutron and photon spectra, yields, and cross sections are consistent with the reaction Q-values. Second, for element evaluations, the isotopic information required to compute the available energy is not available; only a single effective Q value can be defined. If the errors introduced by this problem are too large, evaluated heating numbers or new isotopic evaluations will be required.

The sensitivity of the method to neutron/photon consistency can be turned to the advantage of the evaluator. For many reactions, kinematic estimates of the recoil can be computed (e.g., capture and two-body scattering). For particle producing reactions, conservative kinematic limits can be established. In the simplest form, the lower limit assumes that the particles exit with zero energy, and the upper limit assumes that the particles take all the available energy with no photons being emitted. In this manner, a band of kinematically allowed heating numbers can be defined. If the energy-balance heating number computed by HEATR lies outside this band, an inconsistency in the evaluation may be indicated.

The HEATR module has been revised to accumulate and print these kinematic limits. Portions of a sample listing for ^{184}W from ENDF/B-IV follow on page 22.

Column 301 (MT=300+1) is the total kerma, 304 is inelastic, and 402 is capture (elastic heating is not shown). In the low-energy region, capture dominates. The negative kerma violates the "MIN" limit (note the "HIGH" and "LOW" flags). An examination of the files shows that for 7.9921 eV and below,

FINAL KERMA FACTORS

E	301	302	304	402
MIN	-9.2164E+04	5.8869E-05	0.	-9.2164E+04
1.1955E-03	-5.2900E+03	5.8870E-05	0.	-5.2900E+03
MAX	9.3715E+04	5.8870E-05	0.	9.3715E+04
MIN	5.7371E+03	7.5203E+03	0.	-1.7832E+03
7.4999E+04	7.5205E+03	7.5203E+03	0.	1.6029E-01
MAX	9.4661E+03	7.5204E+03	0.	1.9456E+03
				LOW
MIN	9.9473E+03	1.0867E+04	2.2323E+02	-1.1434E+03
1.5000E+05	2.3732E+04	1.0868E+04	1.7474E+04	-4.6100E+03
MAX	1.2432E+04	1.0868E+04	2.2821E+02	1.3365E+03
	HIGH		HIGH	
				LOW
MIN	1.1865E+04	1.2175E+04	6.2427E+02	-9.3381E+02
1.9000E+05	3.9592E+04	1.2175E+04	3.4298E+04	-6.8807E+03
MAX	1.3941E+04	1.2175E+04	6.3400E+02	1.1318E+03
	HIGH		HIGH	
				LOW
MIN	1.4179E+04	1.3653E+04	1.2877E+03	-7.6228E+02
2.4000E+05	5.6392E+04	1.3653E+04	5.1677E+04	-8.9379E+03
MAX	1.5922E+04	1.3653E+04	1.3023E+03	9.6612E+02
	HIGH		HIGH	
	LOW			LOW
MIN	1.0517E+05	2.5221E+04	0.	2.0983E+01
3.9000E+06	-3.7048E+05	2.5222E+04		-1.9128E+05
MAX	1.0555E+05	2.5222E+04	0.	3.8297E+02
	LOW			LOW
MIN	1.5171E+05	2.9708E+04	0.	2.6108E+01
6.4000E+06	-1.4501E+06	2.9709E+04		-2.1483E+05
MAX	1.5183E+05	2.9709E+04	0.	1.4116E+02
	LOW			LOW
MIN	1.5683E+05	3.2140E+04	0.	2.0151E+01
8.0000E+06	-1.9252E+06	3.2140E+04		-2.2279E+05
MAX	1.7102E+05	3.2140E+04	0.	8.6624E+01
	LOW			LOW
MIN	8.8845E+04	3.3776E+04	0.	4.4635E+01
1.0000E+07	-2.2391E+05	3.3777E+04		-1.9958E+05
MAX	1.8568E+06	3.3777E+04	0.	1.6304E+02
	LOW		LOW	LOW
MIN	6.4471E+04	3.3839E+04	0.	1.1831E+02
1.2600E+07	-1.4241E+04	3.3839E+04		-1.9492E+05
MAX	6.1967E+06	3.3840E+04	0.	3.8160E+02
	LOW			LOW
MIN	5.7055E+04	3.2052E+04	0.	1.7748E+02
1.5750E+07	-4.5830E+05	3.2052E+04		-1.4667E+05
MAX	9.8160E+06	3.2052E+04	0.	5.2262E+02
	LOW			LOW
MIN	6.2107E+04	3.3874E+04	0.	2.8507E+02
2.0000E+07	-1.5426E+06	3.3874E+04		-1.4011E+05
MAX	6.4316E+06	3.3874E+04	0.	7.7875E+02

Q = 5.7500 MeV,

$\bar{E}$ = 2.0178 MeV,

and yield = 2.8500.

Since 2.0178 X 2.85 = 5.75073 > 5.75, the kerma is negative. A cosmetic adjustment could be applied to make the kerma positive (e.g., yield = 2.849).

It should be noted that internal conversion is not included in the kinematic limits. The conversion of gammas in the 100-keV range could increase the "MAX" kerma somewhat.

The second segment shows the onset of inelastic scattering. The large value in MT304 could be due to an inconsistent evaluation or to internal conversion of the 111-keV gamma. The negative capture kerma is due to a 3.3% inconsistency in photon energy.

In the high-energy segment, (n,2n) and particle-emitting reactions become important. The kinematic limits define a range of allowed heating numbers. It becomes much more difficult to disentangle the sources of error. However, model codes can be used to good advantage. Table III compares GNASH[17] calculations to the ENDF results. The column labeled "charged particles" and $\sigma_p\bar{E}_p$ is equivalent to total kerma as discussed above. The other columns show how the ENDF "errors" are divided among neutrons and gammas. This table suggests that a reevaluation with careful attention to consistency will be required to remove the conflicts.

This code is being made available to the National Nuclear Data Center (NNDC) at BNL to be used in the review process for the ENDF/B-V evaluations now being submitted. In addition, the existing ENDF/B-IV materials are being tested to evaluate their usefulness for heating calculations.

B. Cross Sections for Thermal Power Reactors (R. E. MacFarlane)

A program to produce cross-section libraries for the analysis of thermal power reactors has been completed under the support of the Electric Power Research Institute (EPRI) and the U. S. Energy Research and Development Administration (ERDA).

Two new modules for NJOY were developed. THERMR generates incoherent thermal-scattering matrices for free atoms or for atoms bound in solids or liquids. It also produces coherent scattering cross sections for hexagonal materials (e.g., graphite). The results are written to an interface file in ENDF-like

TABLE III

^{184}W KERMA FACTORS BY MODEL CALCULATIONS

	Neutrons			Gammas			Charged Particles				
E_n	σ_n	$\bar{E}_n$	$\sigma_n\bar{E}_n$	σ_γ	$\bar{E}_\gamma$	$\sigma_\gamma\bar{E}_\gamma$	σ_p	$\bar{E}_p$	$\sigma_p\bar{E}_p$	Sum	Method
3.75	6.634	2.619	17.377	7.200	1.112	8.009			-0.408	24.978	ENDF
	6.575	2.561	16.835	7.287	1.150	8.381	6.645	0.015	1.103	25.319	GNASH
6.0	5.554	3.678	20.431	9.542	1.475	14.078			-1.148	33.361	ENDF
	5.535	3.550	19.650	10.130	1.353	13.704	5.557	0.021	0.116	33.470	GNASH
7.6	5.195	4.303	22.353	10.973	1.655	18.154			-1.983	38.524	ENDF
	5.120	4.309	22.063	11.650	1.447	16.855	5.131	0.027	0.136	39.054	GNASH
9.5	6.862	3.928	26.959	7.554	1.251	9.436			-1.003	35.392	ENDF
	6.611	4.350	28.761	7.235	1.147	8.296	5.100	0.038	0.192	37.249	GNASH
12.0	7.493	5.097	38.194	8.313	0.977	8.124			0.059	46.377	ENDF
	7.363	5.456	40.174	6.503	1.068	6.945	5.250	0.043	0.225	47.344	GNASH

format and are then available to be processed by other modules such as GROUPR or PLOTR. The POWR module takes output from GROUPR and formats it for either EPRI-CELL or EPRI-CPM.

These modules have been used to prepare new cross-section libraries for EPRI-CELL using ENDF/B-IV. Heavy-water and the thorium-cycle nuclides were added to the list of isotopes. Self-shielding data were added for all the fissile and fertile isotopes. The technical features of the new libraries have been discussed in previous quarterlies; they include group-to-group scattering matrices, pointwise flux calculation, accurate Doppler broadening, multilevel effects, and improved transport cross sections.

In order to test these libraries, a cell calculation has been set up based on a fuel element run for two cycles in the Carolina Light and Power H. B. Robinson Pressured Water Reactor (PWR). The EPRI-CELL calculation was run for 19 time steps or 32.0 MWD/kg. The isotopic composition at two different times is compared with experiment in Table IV. The results using the existing Nuclear Associates International (NAI) library are also given. The spread in these results is similar to the spread observed between the results using other processing codes.[30]

C. NJOY Code Development (R. E. MacFarlane, R. J. Barrett, D. W. Muir, and R. M. Boicourt)

Validation of NJOY has continued. Several minor errors in the heating factor module (HEATR) were found and corrected during the course of the development

TABLE IV

COMPARISON OF ISOTOPIC RATIOS FOR CP&L TEST PROBLEM

Ratio[a]	Experiment	NAI	NJOY (mod)[b]
Wt% U235/U	.604 ± .052	.602	.628 (+4.3)
Wt% Pu239/Pu	54.11 ± 1.15	53.72	54.04 (+6.0)
Wt% Pu240/Pu	25.14 ± .32	24.95	24.08 (-3.5)
Wt% Pu241/Pu	13.07 ± .30	15.21	15.97 (+5.0)
Wt% Pu242/Pu	6.02 ± .50	6.12	5.93 (-3.1)
Wt Pu239/Pu238	5.20-3 ± 0.01-3	4.77-3	4.58-3 (-4.0)

a. For 30.92 MWD/kg burnup,

b. Numbers in parentheses are percent differences with respect to the NAI results.

described in Sec. II.A. Additional modifications needed to process ENDF/B-V were incorporated, and the preliminary Version V actinide files have been processed. NJOY was compiled successfully under both FTN and CHAT on the LTSS operating systems. Small test problems have been run.

Major portions of the code have been sent to the Oak Ridge National Laboratory (ORNL) for IBM compatibility testing and to BNL for testing small machine compatibility (PDP-10). The NJOY report is being written.

D. Fission Partials in TRANSX (R. J. Barrett and R. E. MacFarlane)

There are several fissionable isotopes for which the cross sections for direct fission (n,f), secondary fission (n,n'f), tertiary fission (n,2nf), and quaternary fission (n,3nf) are given separately in ENDF/B-IV. For some applications, it is of interest to separate the secondary neutron distributions for each of these reactions into two parts, adding the fission neutrons to the nu and chi vectors and distributing to the scattering matrix those neutrons that are emitted before fission. Because the group-averaged fission matrix from NJOY contains both components, new coding has been added to TRANSX to make the separation.

The separation is made on the assumption that the true fission spectrum for each of the reactions has the same shape as the spectrum of direct fission (n,f). The resulting equations for the contribution to the scattering matrix are:

$$\sigma^{scatt}_{g\to g} = \sigma_{g\to g'} - \left\{ \sum_{g'} \sigma_{g\to g''} - \sigma_g \right\} \frac{\sigma_{(n,f),g\to g'}}{\sum_{g''} \sigma_{(n,f),g\to g''}} \qquad \text{(for (n,n'f)} \quad ,$$

$$\sigma^{scatt}_{g\to g} = \sigma_{g\to g'} - \left\{ \sum_{g''} \sigma_{g\to g''} - 2\sigma_g \right\} \frac{\sigma_{(n,f),g\to g'}}{\sum_{g''} \sigma_{(n,f),g\to g''}} \qquad \text{(for (n,2nf)} \quad ,$$

$$\sigma^{scatt}_{g\to g} = \sigma_{g\to g'} - \left\{ \sum_{g''} \sigma_{g\to g''} - 3\sigma_g \right\} \frac{\sigma_{(n,f),g\to g'}}{\sum_{g''} \sigma_{(n,f),g\to g''}} \qquad \text{(for n,3nf)} \quad .$$

This formulation allows for upscatter and is therefore turned off for $g'>g$. It can also result in negative valued matrix elements. These are typically very small ($<10^{-8}$ b) and are suppressed by the code.

Results produced with the new coding have been checked against hand calculation.

E. Monte Carlo Cross Sections (R. J. Barrett, R. J. LaBauve, and R. E. MacFarlane)

Elemental titanium from ENDF/B-IV was processed at 300 K with gamma production matrices for the LASL Monte Carlo library. The file was processed simultaneously with both the ETOPL-MCENDF package and the NJOY-MCNJOY sequences. The final results of the two calculations were subjected to extensive comparisons, and with few exceptions they agreed quite well.

The principal difference showed up in the calculation of local heating in the neutron-energy region from 2 to 20 MeV. The NJOY-MCNJOY results showed continuous behavior, while the ETOPL-MCENDF numbers showed discontinuities at the neutron-group boundaries (Fig. 15). The heating calculation in both codes is done by subtracting the total outgoing neutron energy E_n and the total outgoing gamma energy E_γ from the available energy, which is the sum of the incident neutron energy and the reaction Q-value: $H = E_n + Q - E'_n - E_\gamma$. The discontinuities in the ETOPL-MCENDF numbers result from the fact that, within the boundaries of each neutron group, E_γ is held constant and equal to the average E_γ for that neutron group.

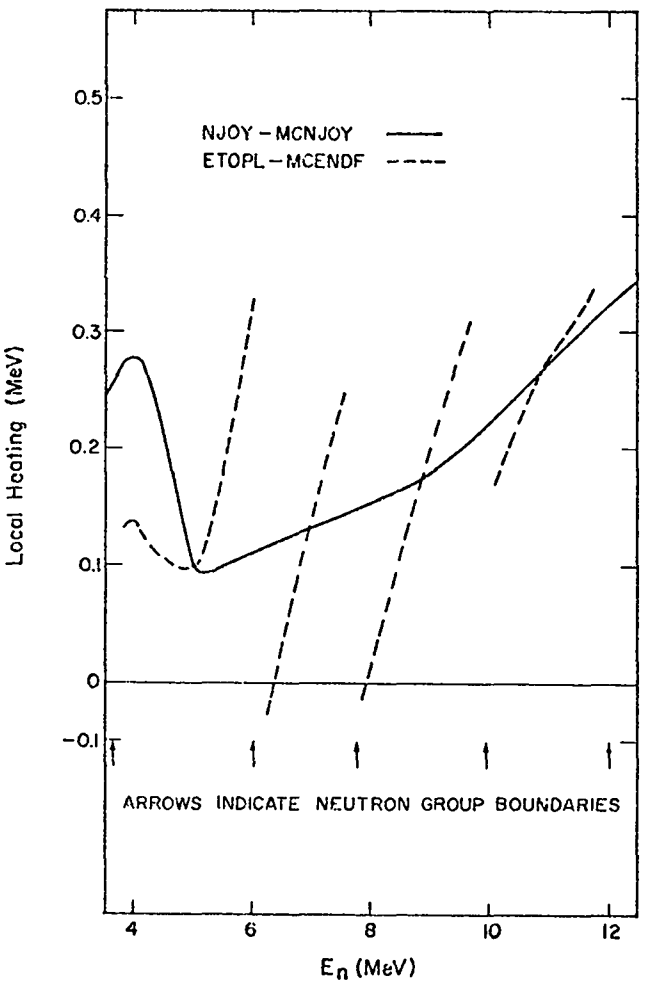

Fig. 15.
Titanium local heating from 4-12 MeV.

The other major difference was a discrepancy in the elastic cross sections in the thermal region. The NJOY results were judged more reasonable.

As a result of these comparisons, the file produced by NJOY-MCNJOY was added to the recommended Monte Carlo library. This is the first NJOY-processed isotope to be included in that file.

F. Two New Basic Computational Tools for Routine Use (D. G. Foster, Jr.)

Certain basic computational problems occur again and again in the evaluation and handling of nuclear data. Those that are not sufficiently universal to have their solutions embodied in the operating-system library for a computer are usually solved by individually written subroutines that evolve over the course of time as need and experience dictate. For example, in least-squares fitting a matrix-inversion routine is a basic tool found in every system library, but

we found it useful several years ago to rewrite one in COMPASS to achieve a major reduction in computing time and expense.[31]

During the course of fitting exponential series to time-dependent beta and gamma spectra of fission products for AFWL (Sec. I. H), two such chronic tasks were reduced to much improved subroutines. These are described below:

1. Explicit Lagrange Polynomials -- Subroutine LAGRNG. Lagrange's interpolation polynomial of degree n - 1 is a standard method of interpolating between n data points. For values y_i at points x_i $(1 \leqslant i \leqslant n)$, the polynomial can be written explicitly for any value of x in the form

$$y = \sum_{i=1}^{n} y_i \prod_{j=1}^{n}{}' \frac{(x-x_j)}{(x_i-x_j)} \quad , \tag{1}$$

where the product $\prod'$ excludes the factor in which i = j. This form can be generated easily on a computer for any particular n, whether or not the x_i are uniformly spaced. It has the disadvantage, however, that the actual coefficients of powers of x are never generated explicitly. Accordingly, the entire calculation must be repeated for each new value of x, even though the same set (x_i,y_i) is being fitted. In addition, it is not straightforward to generate the derivatives of y with respect to x when the explicit coefficients are not generated. Finally, the need often arises to reuse a particular set of x_i for several different sets of y_i (for example, in fitting time-dependent spectra in order to interpolate them). In short, it is useful to be able to express the coefficient of each power of x explicitly as a linear combination of the set y_i ; that is, to calculate the values of A_{ij} in the expansion

$$y = \sum_{i=1}^{n} x^{i-1} \sum_{j=1}^{n} A_{ij} y_j \quad . \tag{2}$$

To accomplish this evaluation, we note that the numerator of the ith term in Eq. (1) is a polynomial in x of degree n - 1, and the denominator is just the numerator evaluated at x_i. The coefficient of the jth term in this polynomial is equal to $(-1)^{j-1}$ times the sum of all possible products of the x_k taken j - 1 at a time, with x_i excluded from the set. Thus, the central problem is to

generate all of these possible products and add them to their appropriate coefficients in as efficient and general a way as possible. To do this, we identify each x_k with the kth bit in a binary number b containing n bits. By setting b = 1 initially and adding 1 successively until the number reaches 2^n-1 we can pass through the entire set of possible products exactly once. The exclusion of x_i is accomplished by subsequently masking b to remove the ith bit.

The subroutine LAGRNG is actually coded in the CROS dialect of FORTRAN-4 for a CDC-7600 computer. This dialect includes an in-line function BITCNT that exploits the population-count 7600 instruction (CX in COMPASS). This permits us to determine the number of 1-bits in the masked b efficiently, and thus to assign the product to its corresponding sum. The output of the main part of the subroutine is the array A_{ij} of Eq. (2). A second entry point LAGCOF performs the calculation of $\sum_{j=1}^{n} A_{ij}y_j$ for any specified set of y_j.

Clearly, there are other ways of obtaining the same result as the population count on computers that do not have this instruction, and for 7600's it would be useful to rewrite LAGRNG in COMPASS to eliminate dependence on the CROS dialect. The original motivation for using this approach was to avoid the need for a nest of n + 1 loops to generate the polynomial for n points. LAGRNG will handle any value of n, using a fixed triple loop to calculate A_{ij}.

2. Rebinning of Histograms -- Subroutines HISTFT and REBIN. Practical nuclear data, whether or not they can be described analytically, frequently must be reduced to integrals over groups (i.e, to histogram form) for use in a computer. Indeed, many measurements originate in multichannel analyzers and are in histogram form from the outset. The eventual user of such data is frequently faced with the need to convert such a histogram into an equivalent histogram with different boundaries between groups. Unless the functional form of the data is known, some information has inevitably been lost in the original binning, but it is often the case that the integrals over the bins are quite accurate, so that a means of rebinning that preserves this original accuracy in the integrals is required.

A simple and obvious procedure is to replace the original smooth function of x by a polynomial in x. We choose this polynomial so that it exactly reproduces the integrals over several adjacent bins of the original histogram. The contents of any old bin that lies wholly within a new bin are of course transferred *in toto*. When an old bin straddles the boundary between two new bins,

the integral over the old bin is divided between the adjacent new bins in accordance with the integral of the fitted polynomial.

We have implemented this simple procedure with a subroutine HISTFT, which fits a three-term polynomial to the integrals over three adjacent bins, and a subroutine REBIN, which keeps track of the boundaries and moves the fitted region as required. The two subroutines reproduce exactly the integral between any two boundaries that are common to the two bin structures. In addition, they restore reasonable-looking facsimiles of fine structure that has been obliterated by the original binning. Obviously they cannot restore more than one partly obliterated peak or valley within each original bin.

III. DATA FOR MAGNETIC FUSION ENERGY -- ESTIMATION OF UNCERTAINTIES IN SECONDARY SPECTRA (D. W. MUIR)

Work continues on the Experimental Power Reactor Covariance Data Library[32] for the LASL quantitative data assessment program. During this quarter we have initiated an effort to incorporate uncertainties in secondary energy spectra into the covariance library.

The effect of spectrum uncertainty on calculated results can be estimated by an integral perturbation technique proposed in Ref. 33 and further developed in Ref. 34. The usual perturbation expansion for the change δR in a calculated quantity due to changes $\delta\sigma_{g'}$ in the secondary spectrum from some reaction is

$$\frac{\delta R}{R} = \sum_{1}^{G} \frac{\partial R/R}{\partial \sigma_{g'}/\sigma_{g'}} \frac{\delta \sigma_{g'}}{\sigma_{g'}} , \qquad (3)$$

where g' runs over all secondary energy groups. A similar contribution to $\delta R/R$ is obtained for each initial neutron energy and for each nuclear reaction (or groups of reactions).

Because of the large number of reactions and initial energy groups involved in any practical sensitivity analysis, it is not feasible to evaluate the uncertainties in the detailed shapes of secondary spectra. For this reason, we shall focus our attention on "gross" features of the spectra. In particular, we shall be interested in variations in the integral of these spectra above and below E_c, where E_c is some conveniently chosen energy cut-point. For the discussions to follow, E_c is taken to be the median secondary energy. That is, we introduce

a new group boundary $E_{g',m}$, such that if

$$\sigma = \sum_{1}^{G} \sigma_{g'} \quad ,$$

then

$$\sum_{1}^{g'_m} \sigma_{g'} = 1/2 \ \sigma . \tag{4}$$

We now apply an "integral perturbation" f to this energy spectrum as follows:

$$\frac{\delta\sigma_{g'}}{\sigma_{g'}} = \begin{cases} + f, \text{ if } g' \leqslant g'_m \\ - f, \text{ if } g' > g'_m \end{cases} . \tag{5}$$

Substitution of this particular set of $[\delta\sigma_{g'}]$ into Eq. (3) gives

$$\frac{\delta R}{R} = S^{SED} \cdot f \quad , \tag{6}$$

$$S^{SED} = \sum_{1}^{g'_m} \frac{\partial R/R}{\partial\sigma_{g'}/\sigma_{g'}} - \sum_{g'_m+1}^{G+1} \frac{\partial R/R}{\partial\sigma_{g'}/\sigma_{g'}} \quad . \tag{7}$$

The significance of Eq. (6) is that uncertainties in spectra can be propagated into uncertainties in calculated results [Var(R)] the same way we have previously propagated uncertainties in cross sections.[35] The tools required for these calculations are sensitivities calculated according to Eq. (7) and covariance matrices of f. More explicitly, if f_i represents the value of f for a particular nuclear reaction at a particular incident energy and f_j corresponds to some different reaction-energy combination, then the uncertainty in R due to uncertainties in secondary energy spectra is given by

$$\frac{Var(R)}{R^2} = \sum_{i,j} S_i^{SED} \, S_j^{SED} \, Cov(f_i, f_j) \quad .$$

To illustrate our procedure for evaluating the uncertainty in f, consider the case where one has available the data from N-independent measurements of the secondary neutron spectrum emitted from some target at some interesting incident neutron energy such as 14 MeV. In this case, the usual problem of constructing a cross-section probability distribution reduces to assigning a set of weights (w_n; n=1,N) to the measurements. One can then use this set of weights to calculate $\bar{\sigma}$, the expected value of the energy-integrated cross section, as well as $\overline{E'_m}$, the median energy of the expected secondary energy spectrum. Recalling the meaning of f as an "integral perturbation" [Eq. (5)], one can calculate the value of f for the nth measurement.

$$f^n = \frac{\sigma_H^n - \sigma_C^n}{\bar{\sigma}} \quad ,$$

where σ_H^n is the integral of the measured spectrum above $\overline{E'_m}$ and σ_C^n is the integral below. From the definition of E'_m [Eq. (4)], one can easily show that $\bar{\sigma}_H = \bar{\sigma}_C = \bar{\sigma}/2$, so that the expected value of f is zero. This simplifies the calculation of Var(f):

$$\mathrm{Var}(f) \equiv \overline{(f-\bar{f})^2} = \overline{f^2}$$

or

$$\mathrm{Var}(f) = \sum_n w_n \frac{\left(\sigma_H^n - \sigma_C^n\right)^2}{\bar{\sigma}^2} \quad .$$

The standard deviation (i.e., the "uncertainty") of f is just $[\mathrm{Var}(f)]^{1/2}$.

We have written a short program SPEC that performs the numerical operations described above on a set of input energy spectra. In order to test the method on some data of practical interest, we have input to the SPEC program the 14-MeV total inelastic scattering spectra for several different elements. Basic data were taken from ENDF/B-IV for the elements Ti, V, Cr, Mn, Fe, Co, Ni, Cu, Zr, Nb, Mo, Ta, W, and Pb. Individual values of $\sigma_H^n - \sigma_C^n = f^n \cdot \bar{\sigma}$ are shown in Fig. 16. Assuming uniform weights $w_n = 1$, the standard deviation of f for this collection of spectra is 54%.

Inspection of the data in Fig. 16 reveals that the variability of f^n is not closely correlated with the obvious nuclear variables such as atomic mass, odd-even effects, or shell closure. For this reason, we feel that the variability seen in Fig. 16 results primarily from spectral uncertainty in the individual evaluations.

IV. FISSION PRODUCTS AND ACTINIDES: YIELDS, YIELD THEORY, DECAY DATA, DEPLETION, AND BUILDUP

A. Fission-Yield Theory [D. G. Madland, R. E. Pepping (University of Wisconsin), C. W. Maynard (University of Wisconsin), T. R. England, and P. G. Young]

During this quarter, the yield calculation code has been rewritten to utilize the expression of Gilbert and Cameron[12] for the density of states of the fission fragments. The density function consists of two formulas, one based on the Fermi gas model and applied only at high fragment excitation (~4 MeV) where the model is presumably more valid, and a second phenomenological formula applied at lower

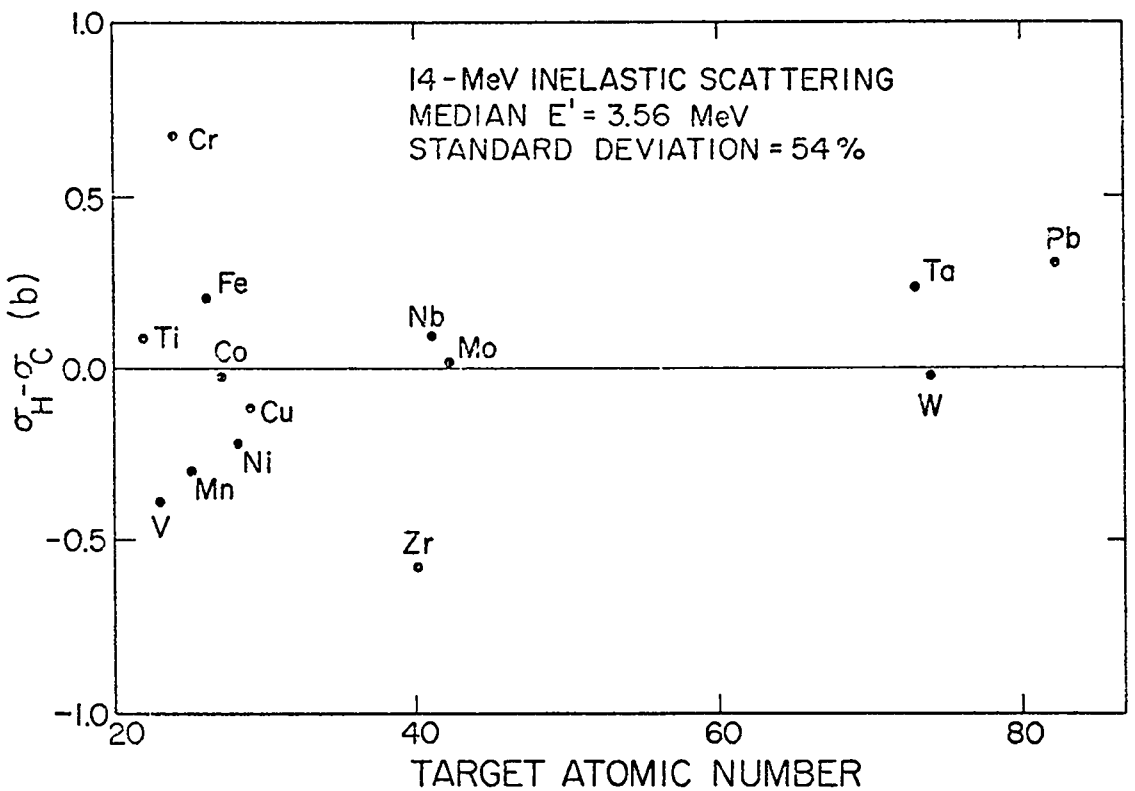

Fig. 16
Spectrum shape parameter ($\sigma_H - \sigma_C$) calculated from ENDF/B-IV evaluations for several important structural materials.

excitation. The level density is allowed to exhibit shell effects through the density parameter a.

Currently the expression for the density parameter is being studied to give best agreement with experimental measurements of observed level spacing (the reciprocal of the level density). Such data are available at about one neutron binding energy of excitation. The form of the expression for the density parameter is essentially that of Ignatyuk et al.[36] with a slight alteration to insure that $a > 0$ for large S, where S is the shell-correction term to the fragment binding energy expression. Also under consideration are models for the separation parameter δ which appears in the expression for the Coulomb energy and may be interpreted as a measure of the separation of the charge distributions of the nascent fragments.

B. ENDF/B Phenomemological Yield Model Improvements

1. Zp Values for Neutron-Induced Fission [D. G. Madland and R. E. Pepping (University of Wisconsin)]. Work is continuing on the use of the prompt neutron distribution of Terrell[37] to determine Zp values for fission products from those calculated for fission fragments by use of the semiempirical mass formula of Seeger.[38]

2. Ternary Fission Probabilities and Charge Distributions (D. G. Madland and Leona Stewart. This work is complete and a report[39] has been issued. A paper summarizing this work has been submitted for presentation at the American Nuclear Society Winter Meeting.

C. Preliminary Yields for ENDF/B-V [T. R. England, D. G. Madland, B. F. Rider (General Electric), and R. E. Schenter (Hanford Engineering Development Lab)]

A total of 20 fission-product yield sets for 11 fissionable nuclides were proposed in December 1976 for inclusion in ENDF/B-V by the Cross-Section Evaluation Working Group (CSEWG) Yield Committee. The sets are identified in Table V. ENDF/B-IV contains ten sets for six fissionable nuclides.

A preliminary evaluation, labeled ENDF/B-VC, is complete and is now included with a preliminary ENDF/B-V actinide evaluation in the format structure of Version IV. Accordingly, these sets contain independent yields (~1100 yields per set).

Table VI lists the cumulative yields for each mass chain (in percent). Each set has been adjusted to achieve charge balance and to sum to 200%, but no nucleon

or energy conservation is used in the evaluation. Several integral conservation tests have been completed, and additional tests are in progress.

Table VII lists several yield-weighted quantities; these can be used to compute the integral results in Table VIII (except for the delayed neutrons discussed in Sec. IV.E). In general, the Q value for fission, delayed, and prompt neutrons is improved for those yield sets common to Version IV, and most quantities are within a few percent of measured or evaluated values.

The preliminary yields incorporate improved models for pairing[40] and isomeric effects[41] and recent, unpublished cumulative yields.

The preliminary yield sets (cumulative and independent) are evaluated values after delayed neutron emission. The final independent sets for ENDF/B-V will apply before delayed neutrons are emitted.

TABLE V

PROPOSED FISSION PRODUCT YIELD SETS FOR ENDF/B[a]

Fissionable Nuclide	Yield Set: Spontaneous	Thermal	Fast	High Energy (14 MeV)
^{232}Th			XX	X
^{237}Np			X	
^{233}U		XX	X	X
^{235}U		XX	XX	XX
^{236}U			X	
^{238}U			XX	XX
^{239}Pu		XX	XX	X
^{240}Pu			X	
^{241}Pu		XX	X	
^{242}Pu			X	
^{252}Cf	X			

[a] XX denotes sets in Versions IV and V.

TABLE VI

TOTAL MASS YIELDS IN PERCENT IN ENDF/B-VC

MASS	TH232F	TH232HE	NP237F	U233T	U233F
66	1.20943E-06	1.28534E-04	1.82759E-07	2.60232E-07	4.48094E-07
67	4.16025E-06	2.21673E-04	3.64892E-07	1.18279E-06	1.79671E-06
68	1.33590E-05	7.31190E-04	1.82732E-06	3.63995E-06	5.48031E-06
69	3.10267E-05	1.46238E-03	9.67351E-06	9.99845E-06	1.49823E-05
70	6.21982E-05	2.67246E-03	2.38702E-05	3.91084E-05	5.97881E-05
71	1.58101E-04	5.10554E-03	6.05062E-05	1.72776E-04	2.58550E-04
72	4.25797E-04	7.86876E-03	1.47482E-04	5.00348E-04	7.66317E-04
73	6.42439E-04	1.61964E-02	3.61404E-04	1.09173E-03	1.69224E-03
74	1.15654E-03	2.90639E-02	6.47642E-04	2.72928E-03	4.17976E-03
75	2.94450E-03	5.10530E-02	1.29166E-03	8.18620E-03	1.24431E-02
76	7.20648E-03	8.71965E-02	5.87752E-03	1.45593E-02	2.21055E-02
77	1.22302E-02	1.23523E-01	1.06654E-02	2.58328E-02	4.03683E-02
78	3.63238E-02	2.45395E-01	2.44389E-02	6.08444E-02	6.96763E-02
79	8.58910E-02	1.22731E+00	5.63697E-02	1.45532E-01	1.09491E-01
80	2.07177E-01	1.20128E+00	1.11761E-01	2.36500E-01	1.99080E-01
81	4.27507E-01	1.50718E+00	2.06838E-01	4.48783E-01	3.69702E-01
82	1.09705E+00	1.68819E+00	3.15882E-01	5.46624E-01	5.82142E-01
83	2.19207E+00	1.72942E+00	3.45156E-01	1.01828E+00	9.94742E-01
84	4.03330E+00	2.19820E+00	5.50205E-01	1.70386E+00	1.63956E+00
85	4.19017E+00	3.88800E+00	7.49182E-01	2.19667E+00	2.16332E+00
86	6.60542E+00	4.72448E+00	9.76066E-01	2.85965E+00	2.78110E+00
87	7.04487E+00	4.85337E+00	1.89762E+00	4.02253E+00	3.80820E+00
88	7.36536E+00	5.42071E+00	1.86372E+00	5.50354E+00	5.11557E+00
89	7.35318E+00	5.86392E+00	2.20519E+00	6.27567E+00	5.87315E+00
90	7.74753E+00	5.94336E+00	3.42497E+00	6.80892E+00	6.44826E+00
91	7.31302E+00	5.78211E+00	4.04546E+00	6.53796E+00	6.46208E+00
92	6.81209E+00	6.20535E+00	4.00183E+00	6.59238E+00	6.49941E+00
93	7.42253E+00	5.70600E+00	5.05175E+00	7.01087E+00	6.88577E+00
94	5.73293E+00	6.94611E+00	5.96126E+00	6.81292E+00	6.73820E+00
95	5.32826E+00	4.43445E+00	5.84965E+00	6.19660E+00	6.27246E+00
96	4.42206E+00	3.41523E+00	6.49415E+00	5.66313E+00	5.70394E+00
97	4.43610E+00	3.10617E+00	6.13590E+00	5.44878E+00	5.45006E+00
98	3.74260E+00	2.72487E+00	5.55573E+00	5.15633E+00	5.13862E+00
99	2.91281E+00	1.98918E+00	6.33153E+00	4.86707E+00	4.68643E+00
100	1.39643E+00	1.55974E+00	5.59839E+00	4.40651E+00	4.37900E+00
101	7.42931E-01	1.49847E+00	5.59853E+00	3.23009E+00	3.73702E+00
102	3.75673E-01	1.22297E+00	5.68956E+00	2.44960E+00	2.82774E+00
103	1.60652E-01	9.55645E-01	5.83026E+00	1.66227E+00	1.78950E+00
104	8.96935E-02	1.04348E+00	5.24186E+00	1.02885E+00	1.23901E+00
105	3.42519E-02	9.64895E-01	3.55707E+00	4.77157E-01	8.86266E-01
106	4.45240E-02	1.07975E+00	2.46078E+00	2.58570E-01	2.95250E-01
107	5.23821E-02	1.03342E+00	1.70067E+00	1.15909E-01	1.49831E-01
108	6.24082E-02	1.04573E+00	1.03812E+00	6.24158E-02	1.09492E-01
109	5.88116E-02	1.18061E+00	4.22624E-01	4.37436E-02	9.24851E-02
110	7.15993E-02	1.12719E+00	2.84772E-01	2.58025E-02	8.95904E-02
111	6.96982E-02	1.21854E+00	9.46992E-02	1.90917E-02	7.71651E-02
112	6.94581E-02	1.24001E+00	7.22286E-02	1.41983E-02	6.88075E-02

TABLE VI (cont)

MASS	TH232F	TH232HE	NP237F	U233T	U233F
113	7.10546E-02	1.21305E+00	5.15464E-02	1.36522E-02	6.67868E-02
114	7.63666E-02	1.21287E+00	5.16489E-02	1.28104E-02	6.27076E-02
115	8.54435E-02	1.29603E+00	5.25792E-02	1.23231E-02	5.79523E-02
116	7.45975E-02	1.57855E+00	4.85260E-02	1.41585E-02	6.37596E-02
117	6.06024E-02	1.51671E+00	4.37574E-02	1.13679E-02	5.35002E-02
118	6.50720E-02	1.50993E+00	5.56952E-02	1.21948E-02	5.35104E-02
119	5.89139E-02	1.44353E+00	5.60677E-02	1.25349E-02	6.22538E-02
120	5.59217E-02	1.39291E+00	5.57875E-02	1.37917E-02	6.87446E-02
121	5.27209E-02	1.00046E+00	6.70053E-02	1.49458E-02	7.71717E-02
122	3.80573E-02	1.25790E+00	6.12479E-02	1.46586E-02	7.09634E-02
123	3.14300E-02	1.23989E+00	6.75443E-02	1.97375E-02	7.50091E-02
124	2.79410E-02	1.41001E+00	7.53981E-02	2.41871E-02	1.01831E-01
125	3.22089E-02	1.18669E+00	1.30985E-01	1.11735E-01	1.38566E-01
126	5.10276E-02	1.26802E+00	1.64967E-01	2.44391E-01	2.67877E-01
127	9.16519E-02	1.24508E+00	4.02128E-01	5.60807E-01	5.05516E-01
128	1.89870E-01	1.50204E+00	6.68262E-01	7.56488E-01	1.11488E+00
129	3.96572E-01	1.69333E+00	1.14508E+00	1.62763E+00	1.69478E+00
130	8.45553E-01	2.13419E+00	2.36782E+00	2.10801E+00	2.52701E+00
131	1.61793E+00	2.53786E+00	3.87299E+00	3.65193E+00	3.73440E+00
132	2.89181E+00	2.91221E+00	5.31263E+00	4.96148E+00	4.96538E+00
133	3.81064E+00	3.95355E+00	7.04929E+00	6.02613E+00	6.00261E+00
134	5.39679E+00	6.87892E+00	7.84528E+00	6.35030E+00	6.22670E+00
135	5.40849E+00	5.10218E+00	7.41633E+00	6.22275E+00	6.36461E+00
136	5.64412E+00	5.50234E+00	7.78806E+00	7.14034E+00	6.99185E+00
137	6.64959E+00	5.37521E+00	6.17908E+00	6.80118E+00	6.64151E+00
138	7.11203E+00	5.39534E+00	6.37285E+00	5.91351E+00	6.48421E+00
139	7.03574E+00	5.48034E+00	5.18570E+00	6.30709E+00	6.33499E+00
140	7.77146E+00	5.75577E+00	5.48464E+00	6.48361E+00	6.20388E+00
141	7.27006E+00	5.74916E+00	5.38877E+00	6.52547E+00	6.39057E+00
142	6.15709E+00	4.86472E+00	4.55350E+00	6.65107E+00	6.44534E+00
143	6.67084E+00	5.28992E+00	4.69589E+00	5.87608E+00	5.52982E+00
144	7.82959E+00	4.03386E+00	4.26663E+00	4.63504E+00	4.46768E+00
145	5.40314E+00	3.21245E+00	2.91584E+00	3.39102E+00	3.18242E+00
146	4.60814E+00	2.39368E+00	2.26676E+00	2.53598E+00	2.37686E+00
147	3.09433E+00	1.73133E+00	2.22048E+00	1.73156E+00	1.67852E+00
148	2.02364E+00	9.07737E-01	1.50692E+00	1.27158E+00	1.19314E+00
149	8.95420E-01	5.83634E-01	1.45240E+00	7.57701E-01	7.03708E-01
150	3.42633E-01	3.32756E-01	7.45164E-01	5.02509E-01	4.64406E-01
151	1.74688E-01	2.38798E-01	8.84271E-01	3.19306E-01	3.05067E-01
152	7.60979E-02	1.15852E-01	4.63327E-01	2.06015E-01	1.90946E-01
153	3.29895E-02	8.20533E-02	3.40923E-01	1.04056E-01	1.15993E-01
154	7.71314E-03	5.25871E-02	1.84750E-01	4.52624E-02	6.26673E-02
155	4.05026E-03	2.97007E-02	1.25817E-01	2.16189E-02	3.28821E-02
156	2.58151E-03	1.71527E-02	1.01575E-01	1.12417E-02	1.78550E-02
157	9.86832E-04	1.00451E-02	3.51485E-02	6.36232E-03	9.72177E-03
158	5.40562E-04	5.88539E-03	1.38794E-02	2.28720E-03	3.19146E-03
159	1.13879E-04	4.15498E-03	7.07940E-03	8.79244E-04	1.69764E-03
160	8.06506E-05	1.62627E-03	2.73638E-03	2.84574E-04	4.03456E-04
161	2.02065E-05	9.89859E-04	8.50286E-04	1.20208E-04	9.12071E-05

TABLE VI (cont)

MASS	TH232F	TH232HE	NP237F	U233T	U233F
162	9.29826E-06	4.79705E-04	3.30112E-04	1.54604E-05	2.19248E-05
163	5.41076E-06	2.40335E-04	1.40672E-04	7.22764E-06	1.00338E-05
164	2.37028E-06	1.24064E-04	6.13043E-04	2.37780E-06	3.37341E-06
165	3.95547E-07	6.84449E-05	2.07757E-05	7.52202E-07	1.12587E-06
166	1.61463E-07	2.77438E-05	1.22829E-05	4.57908E-07	6.48025E-07
167	1.13877E-07	1.50407E-05	1.69646E-06	6.40885E-08	9.03469E-08
168	6.14055E-08	7.52469E-06	4.34502E-07	1.64642E-08	2.37459E-08
169	3.05578E-08	3.41545E-06	1.40797E-07	5.57320E-09	7.93123E-09
170	1.14608E-08	1.28902E-06	4.43967E-07	1.64677E-09	2.36976E-09
171	4.13515E-09	4.14096E-07	1.31759E-07	5.43922E-10	7.23016E-10
172	1.57714E-09	9.84340E-08	5.10491E-07	1.76217E-10	2.62896E-10

MASS	U233HE	U235T	U235F	U235HE	U236F
66	7.16327E-04	7.66127E-08	8.91959E-07	2.94860E-04	7.87739E-07
67	1.63835E-03	3.92930E-07	2.86955E-06	6.55970E-04	1.96894E-06
68	2.02233E-03	6.63673E-07	4.96098E-06	8.97600E-04	3.94147E-06
69	3.25346E-03	1.43753E-06	1.07438E-05	1.33076E-03	8.85782E-06
70	5.27784E-03	3.30427E-06	2.32358E-05	2.39300E-03	1.97189E-05
71	8.35219E-03	7.74013E-06	5.77074E-05	3.98240E-03	4.92398E-05
72	1.38155E-02	2.69477E-05	2.04450E-04	6.11202E-03	1.77163E-04
73	2.28672E-02	1.17981E-04	8.42803E-04	1.11892E-02	6.88926E-04
74	3.43917E-02	3.63307E-04	1.97903E-03	1.69665E-02	1.67294E-03
75	5.97164E-02	1.18381E-03	1.68120E-02	2.68779E-02	1.27940E-02
76	8.48215E-02	3.87083E-03	2.80070E-02	3.98358E-02	2.16525E-02
77	1.19160E-01	8.35912E-03	4.48055E-02	6.61510E-02	4.35128E-02
78	1.87903E-01	2.16868E-02	7.09785E-02	9.91224E-02	5.51172E-02
79	2.63864E-01	4.48535E-02	1.12097E-01	1.71426E-01	1.08265E-01
80	3.91792E-01	1.33843E-01	1.77493E-01	2.58466E-01	1.77154E-01
81	6.12328E-01	1.96454E-01	2.89519E-01	2.89733E-01	2.55900E-01
82	9.40035E-01	3.21187E-01	4.01393E-01	6.27882E-01	3.64317E-01
83	1.31092E+00	5.37376E-01	5.72275E-01	1.13885E+00	5.43953E-01
84	2.06395E+00	1.00074E+00	1.02057E+00	1.55530E+00	9.88952E-01
85	2.34712E+00	1.30154E+00	1.32659E+00	1.65607E+00	1.48223E+00
86	2.73613E+00	1.96595E+00	1.92813E+00	2.54570E+00	1.67725E+00
87	3.14425E+00	2.55909E+00	2.46547E+00	2.42173E+00	2.25978E+00
88	3.84176E+00	3.63792E+00	3.48276E+00	3.40515E+00	2.89790E+00
89	4.65739E+00	4.89937E+00	4.52654E+00	4.28238E+00	3.85065E+00
90	4.78821E+00	5.93898E+00	5.44167E+00	4.80900E+00	4.60575E+00
91	5.45687E+00	5.97014E+00	5.65464E+00	4.99176E+00	5.52330E+00
92	5.66090E+00	5.97546E+00	5.73437E+00	5.22074E+00	6.08593E+00
93	5.68843E+00	6.34542E+00	6.12526E+00	5.28979E+00	5.54963E+00
94	5.46713E+00	6.43749E+00	6.18292E+00	5.11664E+00	5.69658E+00
95	5.46416E+00	6.49553E+00	6.38068E+00	5.02675E+00	6.26032E+00
96	5.09612E+00	6.27500E+00	6.08586E+00	5.17267E+00	5.88516E+00
97	5.00469E+00	5.94357E+00	5.95453E+00	5.78628E+00	4.96881E+00
98	4.19587E+00	5.77467E+00	5.86530E+00	4.18492E+00	5.88514E+00

TABLE VI (cont)

MASS	U233HE	U235T	U235F	U235HE	U236F
99	3.64829E+00	6.14922E+00	5.77920E+00	5.05673E+00	5.79522E+00
100	3.09106E+00	6.18094E+00	6.27634E+00	4.01894E+00	5.67015E+00
101	2.80697E+00	5.07524E+00	5.34780E+00	3.51100E+00	5.39171E+00
102	2.52330E+00	4.22518E+00	4.52457E+00	3.30717E+00	5.06142E+00
103	2.35096E+00	3.03954E+00	3.27031E+00	3.24859E+00	4.11014E+00
104	2.00475E+00	1.83377E+00	2.26463E+00	2.07684E+00	3.44375E+00
105	1.78478E+00	9.67557E-01	1.17219E+00	1.96752E+00	2.41827E+00
106	1.47581E+00	3.99968E-01	5.56189E-01	1.57251E+00	1.00126E+00
107	1.61373E+00	1.42047E-01	3.15645E-01	1.29566E+00	9.59397E-01
108	1.17364E+00	6.87718E-02	1.71149E-01	1.07930E+00	3.64165E-01
109	1.17411E+00	3.30062E-02	1.35597E-01	1.32312E+00	1.48357E-01
110	1.26992E+00	3.09224E-02	9.40900E-02	1.04549E+00	1.08262E-01
111	1.19745E+00	1.90598E-02	4.37040E-02	1.17541E+00	7.92492E-02
112	1.12579E+00	1.19868E-02	3.70070E-02	1.02929E+00	5.01948E-02
113	1.06639E+00	1.23284E-02	3.30405E-02	1.06303E+00	3.95577E-02
114	1.00766E+00	1.18327E-02	3.24564E-02	9.75979E-01	3.44481E-02
115	1.00335E+00	1.07467E-02	2.92361E-02	1.04914E+00	5.28454E-02
116	1.05595E+00	1.19278E-02	3.41050E-02	9.72296E-01	3.54351E-02
117	1.04213E+00	1.04318E-02	3.33435E-02	1.07216E+00	3.67198E-02
118	1.07631E+00	1.01525E-02	3.20979E-02	1.10453E+00	3.78439E-02
119	1.10766E+00	1.04882E-02	3.26640E-02	1.11606E+00	3.68461E-02
120	1.12856E+00	1.10036E-02	3.33937E-02	1.13457E+00	3.98339E-02
121	1.10799E+00	1.35054E-02	3.48139E-02	1.06269E+00	3.97579E-02
122	1.22343E+00	1.25258E-02	3.54919E-02	1.21370E+00	5.36715E-02
123	1.32710E+00	1.59317E-02	4.47891E-02	1.24050E+00	7.56843E-02
124	1.49841E+00	1.96546E-02	5.53344E-02	1.31595E+00	9.93987E-02
125	1.53940E+00	2.94686E-02	7.54556E-02	1.42357E+00	1.71252E-01
126	1.87790E+00	5.71285E-02	1.40060E-01	1.89908E+00	2.58894E-01
127	2.20334E+00	1.25263E-01	2.74414E-01	2.27786E+00	2.31518E-01
128	2.62382E+00	3.51102E-01	6.77022E-01	2.45373E+00	6.37292E-01
129	2.93034E+00	7.67347E-01	9.31481E-01	3.50670E+00	1.02354E+00
130	3.41086E+00	1.76464E+00	2.00512E+00	3.63553E+00	2.06459E+00
131	3.49660E+00	2.88418E+00	3.20146E+00	4.03833E+00	2.98773E+00
132	4.22799E+00	4.29779E+00	4.60887E+00	4.71359E+00	4.24137E+00
133	4.61061E+00	6.69609E+00	6.61800E+00	5.54988E+00	6.89946E+00
134	4.99919E+00	7.80107E+00	7.61161E+00	5.88754E+00	7.92055E+00
135	5.10750E+00	6.54920E+00	6.34726E+00	5.91133E+00	5.70413E+00
136	6.56232E+00	6.27937E+00	6.18171E+00	4.71546E+00	6.41000E+00
137	5.17874E+00	6.22240E+00	6.17536E+00	4.84606E+00	6.02764E+00
138	5.52884E+00	6.75860E+00	6.55409E+00	4.49200E+00	6.42306E+00
139	5.86622E+00	6.38397E+00	6.34064E+00	4.78472E+00	6.08395E+00
140	5.56387E+00	6.28154E+00	6.10118E+00	4.55878E+00	5.62216E+00
141	4.92240E+00	5.83273E+00	6.02198E+00	4.34698E+00	5.45137E+00
142	4.55035E+00	5.88764E+00	5.65989E+00	4.42428E+00	5.71957E+00
143	3.61120E+00	5.94404E+00	5.70095E+00	3.92364E+00	5.97783E+00
144	2.62646E+00	5.47873E+00	5.27666E+00	3.20198E+00	5.25927E+00
145	2.04505E+00	3.91584E+00	3.75551E+00	2.65945E+00	3.76340E+00
146	1.64059E+00	2.96940E+00	2.89918E+00	2.25731E+00	3.05195E+00

TABLE VI (cont)

MASS	U233HE	U235T	U235F	U235HE	U236F
147	1.25308E+00	2.23607E+00	2.09820E+00	1.65742E+00	2.30172E+00
148	9.81213E-01	1.67048E+00	1.67333E+00	1.24983E+00	1.80495E+00
149	6.31468E-01	1.07453E+00	1.02697E+00	6.45370E-01	1.35644E+00
150	4.61083E-01	6.48424E-01	6.86516E-01	5.42613E-01	7.85391E-01
151	3.08511E-01	4.16114E-01	4.08103E-01	3.57302E-01	4.24399E-01
152	2.28096E-01	2.68012E-01	2.79580E-01	2.76322E-01	4.17478E-01
153	1.53185E-01	1.61421E-01	1.77150E-01	2.08210E-01	2.68372E-01
154	1.04296E-01	7.35723E-02	7.65423E-02	8.34517E-02	1.39154E-01
155	6.92077E-02	3.20908E-02	5.56226E-02	6.65254E-02	9.93991E-02
156	4.42755E-02	1.32141E-02	2.12884E-02	5.45291E-02	4.07549E-02
157	2.80999E-02	6.19288E-03	1.47010E-02	3.93978E-02	2.48489E-02
158	1.97024E-02	2.94656E-03	8.08121E-03	2.42914E-02	1.19265E-02
159	1.15293E-02	1.01029E-03	2.96698E-03	1.21379E-02	4.67088E-03
160	8.29996E-03	3.21768E-04	1.33638E-03	7.44589E-03	2.08701E-03
161	5.02700E-03	8.55409E-05	3.35791E-04	5.26248E-03	8.94374E-04
162	3.17855E-03	1.95422E-05	2.74446E-04	2.91789E-03	5.36837E-04
163	1.97319E-03	7.82115E-06	5.94082E-05	1.65822E-03	1.19184E-04
164	1.20581E-03	2.44410E-06	2.42515E-05	1.02745E-03	4.76724E-05
165	7.23058E-04	1.18342E-06	9.17555E-06	5.63232E-04	1.79403E-05
166	2.59824E-04	5.41615E-07	5.60866E-06	2.68628E-04	1.09354E-05
167	2.52498E-04	3.05158E-07	2.65008E-06	1.93416E-04	5.16705E-06
168	1.53356E-04	6.97415E-08	6.86354E-07	1.11303E-04	1.29206E-06
169	8.94355E-05	2.84852E-08	1.62428E-07	7.66243E-05	3.18303E-07
170	4.94170E-05	5.98620E-09	4.86168E-08	3.40154E-05	9.63892E-08
171	2.70756E-05	2.84542E-09	1.62158E-08	1.84134E-05	3.17793E-08
172	1.92517E-05	9.77746E-10	4.35372E-09	1.61418E-05	8.52545E-09

MASS	U238F	U238HE	PU239T	PU239F	PU239HE
66	1.78209E-08	8.42071E-05	1.85681E-07	8.92750E-07	6.09964E-05
67	6.14526E-08	1.38035E-04	3.71465E-07	2.94572E-06	9.62668E-05
68	2.30824E-07	2.97730E-04	1.29950E-06	8.65834E-06	2.13714E-04
69	6.25131E-07	5.00586E-04	4.64311E-06	3.21254E-05	3.63333E-04
70	1.72801E-06	8.97581E-04	1.58286E-05	8.93487E-05	6.54349E-04
71	5.00526E-06	1.59323E-03	2.86806E-05	2.67548E-04	1.17184E-03
72	9.46341E-06	2.98217E-03	9.78289E-05	6.73808E-04	2.13294E-03
73	4.80257E-05	5.17460E-03	2.24801E-04	8.90979E-04	3.68045E-03
74	9.46516E-05	7.97689E-03	5.39880E-04	1.78512E-03	5.75013E-03
75	2.45036E-04	1.38031E-02	1.25879E-03	2.89425E-03	1.00173E-02
76	8.12561E-04	2.18822E-02	2.78711E-03	5.97714E-03	1.60068E-02
77	3.35411E-03	3.12521E-02	7.21495E-03	1.38947E-02	2.31581E-02
78	1.13965E-02	4.06427E-02	2.82816E-02	3.07211E-02	2.97555E-02
79	3.31803E-02	1.68692E-01	4.61839E-02	5.80163E-02	8.53401E-02
80	7.02092E-02	2.11836E-01	1.13783E-01	8.84090E-02	1.54098E-01
81	1.48278E-01	3.30830E-01	1.72441E-01	1.54291E-01	2.66262E-01
82	2.48637E-01	4.50912E-01	2.07192E-01	2.20821E-01	3.37841E-01
83	3.92536E-01	6.50671E-01	2.95844E-01	3.09242E-01	4.64021E-01
84	8.11234E-01	1.09289E+00	4.76130E-01	4.88251E-01	7.80277E-01

TABLE VI (cont)

MASS	U238F	U238HE	PU239T	PU239F	PU239HE
85	7.28003E-01	9.79155E-01	5.78078E-01	6.00345E-01	1.00939E+00
86	1.27144E+00	1.53145E+00	7.62413E-01	7.74539E-01	1.10166E+00
87	1.57446E+00	1.66850E+00	9.96094E-01	1.03616E+00	1.37780E+00
88	2.06468E+00	2.23351E+00	1.37142E+00	1.33482E+00	2.00451E+00
89	2.81902E+00	2.95992E+00	1.69552E+00	1.77142E+00	2.07970E+00
90	3.18874E+00	3.25087E+00	2.12000E+00	2.01616E+00	2.41078E+00
91	4.17402E+00	3.76104E+00	2.50221E+00	2.45005E+00	2.09898E+00
92	4.52876E+00	3.92203E+00	3.03537E+00	2.97577E+00	2.84403E+00
93	4.96569E+00	4.48834E+00	3.92645E+00	3.73231E+00	3.14388E+00
94	4.96754E+00	4.80080E+00	4.46896E+00	4.20733E+00	3.47470E+00
95	5.13504E+00	4.97523E+00	4.91359E+00	4.66816E+00	3.69555E+00
96	5.91702E+00	5.55647E+00	5.12578E+00	4.80583E+00	4.22425E+00
97	5.49417E+00	5.32227E+00	5.36986E+00	5.25276E+00	4.42848E+00
98	5.78597E+00	5.48480E+00	5.87969E+00	5.56377E+00	4.74727E+00
99	6.23957E+00	5.68394E+00	6.15044E+00	6.01452E+00	4.16365E+00
100	6.58804E+00	5.10273E+00	6.83457E+00	6.54341E+00	5.00152E+00
101	6.06974E+00	5.60866E+00	5.92920E+00	6.47320E+00	5.19305E+00
102	6.31128E+00	4.59520E+00	5.99403E+00	6.56174E+00	5.69027E+00
103	6.23064E+00	4.65009E+00	6.94198E+00	6.86456E+00	5.31270E+00
104	4.97666E+00	3.53703E+00	5.93907E+00	6.42421E+00	5.64500E+00
105	3.98270E+00	3.22762E+00	5.35612E+00	5.46011E+00	4.29406E+00
106	2.55039E+00	2.43117E+00	4.26945E+00	4.31966E+00	3.64351E+00
107	1.30684E+00	1.72378E+00	3.37519E+00	3.28275E+00	2.97587E+00
108	6.04333E-01	1.25066E+00	2.18392E+00	2.31403E+00	2.49267E+00
109	3.03155E-01	1.21946E+00	1.64756E+00	1.45739E+00	2.49259E+00
110	1.37784E-01	1.01896E+00	6.03666E-01	6.74236E-01	1.81096E+00
111	7.92755E-02	1.03617E+00	3.08193E-01	3.59002E-01	1.53837E+00
112	5.89575E-02	1.00846E+00	1.10487E-01	1.93049E-01	1.40611E+00
113	5.30790E-02	9.29586E-01	7.77126E-02	1.26950E-01	1.35795E+00
114	3.96584E-02	7.13951E-01	4.55035E-02	9.29484E-02	1.30648E+00
115	4.61394E-02	8.89656E-01	3.65979E-02	8.12383E-02	1.14569E+00
116	4.11696E-02	6.70121E-01	3.39112E-02	5.97602E-02	1.20287E+00
117	3.72340E-02	7.33569E-01	3.33771E-02	6.18806E-02	1.19747E+00
118	4.04084E-02	8.19048E-01	3.33747E-02	6.18669E-02	1.30609E+00
119	3.58360E-02	7.10088E-01	3.55258E-02	5.97662E-02	1.25643E+00
120	3.57984E-02	7.69254E-01	3.55303E-02	6.05186E-02	1.25459E+00
121	4.51905E-02	8.38469E-01	3.82386E-02	6.78148E-02	1.49855E+00
122	3.76486E-02	8.40827E-01	3.87553E-02	6.87114E-02	1.27253E+00
123	4.04911E-02	9.12378E-01	4.46593E-02	8.53981E-02	1.72070E+00
124	4.43963E-02	1.02404E+00	5.58818E-02	1.11278E-01	1.73543E+00
125	4.74756E-02	1.20015E+00	1.11542E-01	1.66725E-01	1.92886E+00
126	6.45733E-02	1.47067E+00	2.02979E-01	2.84100E-01	2.38485E+00
127	1.24117E-01	1.44787E+00	4.95036E-01	5.56731E-01	2.28270E+00
128	4.67922E-01	1.81565E+00	7.59020E-01	9.16971E-01	2.54507E+00
129	1.04958E+00	2.03219E+00	1.50481E+00	1.60194E+00	3.40605E+00
130	1.85993E+00	3.38591E+00	2.38766E+00	2.53176E+00	4.35208E+00
131	3.20617E+00	4.00853E+00	3.87305E+00	3.87895E+00	4.79092E+00
132	5.18227E+00	4.85712E+00	5.41790E+00	5.24327E+00	5.30134E+00
133	6.62973E+00	6.16678E+00	7.03211E+00	6.91830E+00	5.21013E+00
134	7.86669E+00	6.52028E+00	7.66949E+00	7.25771E+00	5.68276E+00

TABLE VI (cont)

MASS	U238F	U238HE	PU239T	PU239F	PU239HE
135	6.81452E+00	5.84695E+00	7.42736E+00	7.50008E+00	5.70464E+00
136	7.04349E+00	5.69042E+00	6.72098E+00	6.98937E+00	5.80777E+00
137	5.99248E+00	4.95662E+00	6.64838E+00	6.51940E+00	4.68209E+00
138	5.64469E+00	4.56819E+00	6.07063E+00	6.07966E+00	4.50909E+00
139	5.92796E+00	5.13925E+00	5.63275E+00	5.52970E+00	4.22136E+00
140	5.94246E+00	4.67251E+00	5.54950E+00	5.37003E+00	3.91939E+00
141	5.37316E+00	4.41956E+00	5.28226E+00	5.32279E+00	3.51967E+00
142	4.70127E+00	4.10629E+00	4.99410E+00	4.83840E+00	3.16364E+00
143	4.52492E+00	3.94497E+00	4.43595E+00	4.30508E+00	2.69473E+00
144	4.50720E+00	3.69968E+00	3.74649E+00	3.68584E+00	2.74309E+00
145	3.73261E+00	3.00160E+00	2.99497E+00	2.97330E+00	2.22044E+00
146	3.37227E+00	2.31256E+00	2.46548E+00	2.44473E+00	1.86584E+00
147	2.52743E+00	2.07081E+00	2.04141E+00	1.98522E+00	1.80432E+00
148	2.07352E+00	1.74117E+00	1.63876E+00	1.63840E+00	1.38595E+00
149	1.60133E+00	1.42696E+00	1.23920E+00	1.26419E+00	1.12930E+00
150	1.25846E+00	1.08083E+00	9.68079E-01	9.89916E-01	1.02055E+00
151	7.96785E-01	6.19134E-01	7.74068E-01	7.83719E-01	7.77271E-01
152	5.18549E-01	5.79926E-01	5.85750E-01	6.11219E-01	5.88043E-01
153	3.95752E-01	3.92330E-01	3.65858E-01	4.38834E-01	4.81264E-01
154	2.12446E-01	2.54857E-01	2.71606E-01	2.80924E-01	3.50250E-01
155	1.31827E-01	1.57414E-01	1.67628E-01	2.21384E-01	2.45598E-01
156	6.81872E-02	1.10644E-01	1.18254E-01	1.53493E-01	2.15464E-01
157	3.84867E-02	6.30798E-02	7.46661E-02	1.10518E-01	1.17839E-01
158	1.67570E-02	4.30525E-02	4.16120E-02	7.09846E-02	7.95135E-02
159	7.69923E-03	2.62130E-02	2.07436E-02	4.01183E-02	5.49542E-02
160	2.94190E-03	1.60392E-02	1.00211E-02	2.58569E-02	4.01435E-02
161	1.29456E-03	8.48644E-03	4.87848E-03	9.66773E-03	1.86432E-02
162	4.87828E-04	6.01261E-03	2.47104E-03	7.11646E-03	9.89232E-03
163	1.19750E-04	3.43892E-03	1.00017E-03	3.44988E-03	3.48055E-03
164	3.89378E-05	2.02075E-03	3.77989E-04	2.17005E-03	1.98836E-03
165	1.49423E-05	1.11136E-03	1.42128E-04	1.09964E-03	8.02202E-04
166	5.34930E-06	6.33095E-04	6.93087E-05	7.65323E-04	5.48050E-04
167	1.58341E-06	3.73379E-04	2.03835E-05	3.31587E-04	2.99153E-04
168	6.77859E-07	2.02642E-04	5.71396E-06	9.50220E-05	1.49283E-04
169	2.22319E-07	1.29806E-04	1.94287E-06	3.20914E-05	6.98179E-05
170	6.78540E-08	6.02195E-05	5.73066E-06	9.52716E-06	5.04510E-05
171	1.89793E-08	3.34758E-05	1.95209E-07	3.20581E-06	3.98934E-05
172	9.89290E-09	2.15484E-05	5.73535E-08	9.50418E-07	2.00173E-05

MASS	PU240F	PU241T	PU241F	PU242F	CF252SF
66	9.81103E-06	1.38065E-07	1.99327E-07	1.90118E-07	2.36981E-09
67	1.47218E-05	2.55458E-07	1.39496E-06	3.80353E-07	1.18338E-08
68	3.43922E-05	5.91926E-07	2.99163E-06	6.65264E-07	3.54845E-08
69	5.40054E-05	1.28092E-06	1.09625E-05	1.42550E-06	1.18337E-07
70	1.37227E-04	4.62975E-06	3.48187E-05	2.85602E-06	4.51438E-07
71	2.45163E-04	6.90617E-06	8.95655E-05	4.75707E-06	1.42055E-06
72	4.89822E-04	2.56664E-05	1.59327E-04	1.04583E-05	4.73190E-06

TABLE VI (cont)

MASS	PU240F	PU241T	PU241F	PU242F	CF252SF
73	9.80793E-04	5.90905E-05	4.97578E-04	1.73698E-05	1.18367E-05
74	1.96277E-03	9.86127E-05	1.19467E-03	4.74651E-05	3.54630E-05
75	3.43493E-03	2.95504E-04	1.99112E-03	9.50848E-05	1.18377E-04
76	6.37972E-03	9.85957E-04	2.98842E-03	2.85366E-04	2.95067E-04
77	1.38695E-02	1.97169E-03	9.97996E-03	9.65134E-03	9.03963E-04
78	2.87313E-02	9.40132E-03	1.89616E-02	1.80629E-02	2.09850E-03
79	5.35005E-02	1.63944E-02	3.69266E-02	3.51735E-02	7.10141E-03
80	8.91665E-02	3.28567E-02	6.68674E-02	6.36944E-02	1.58326E-02
81	1.48610E-01	6.37345E-02	1.09781E-01	1.04570E-01	3.07929E-02
82	2.08273E-01	1.14265E-01	1.69761E-01	1.61645E-01	5.03236E-02
83	3.17914E-01	2.10797E-01	2.49685E-01	2.41281E-01	5.85646E-02
84	4.46624E-01	3.66243E-01	3.69262E-01	3.51740E-01	1.04652E-01
85	5.95234E-01	4.06229E-01	5.08983E-01	4.15009E-01	1.68225E-01
86	7.84349E-01	6.33814E-01	6.69496E-01	6.46656E-01	1.85204E-01
87	1.01320E+00	7.66392E-01	8.79711E-01	8.58361E-01	2.74713E-01
88	1.26966E+00	1.00696E+00	1.12843E+00	1.09061E+00	3.70169E-01
89	1.59749E+00	1.18581E+00	1.37807E+00	1.34601E+00	3.96681E-01
90	1.96507E+00	1.56120E+00	1.75754E+00	1.72939E+00	6.78096E-01
91	2.37043E+00	1.88619E+00	2.11706E+00	2.08315E+00	7.19098E-01
92	2.90489E+00	2.35151E+00	2.56440E+00	2.49698E+00	7.15487E-01
93	3.50895E+00	3.05926E+00	3.14362E+00	3.08543E+00	9.45784E-01
94	4.18250E+00	3.51168E+00	3.74275E+00	3.64787E+00	1.19678E+00
95	4.61764E+00	4.07333E+00	4.48972E+00	4.02836E+00	1.31780E+00
96	4.97424E+00	4.57929E+00	4.69986E+00	4.48681E+00	1.62000E+00
97	5.31140E+00	4.82877E+00	5.11888E+00	4.83449E+00	1.70697E+00
98	5.46007E+00	5.17373E+00	5.40843E+00	5.14031E+00	2.25806E+00
99	5.74788E+00	6.25968E+00	5.48476E+00	5.38334E+00	2.61688E+00
100	6.01451E+00	6.16864E+00	5.94572E+00	5.63095E+00	3.40106E+00
101	5.96677E+00	6.01788E+00	6.01561E+00	5.89565E+00	3.80781E+00
102	5.96679E+00	6.40287E+00	5.91773E+00	5.84258E+00	3.92097E+00
103	5.98669E+00	6.19389E+00	5.99767E+00	5.88584E+00	5.69423E+00
104	5.74023E+00	6.88917E+00	5.86779E+00	5.81332E+00	6.19158E+00
105	5.40450E+00	6.16926E+00	5.63051E+00	5.67952E+00	6.52049E+00
106	5.04881E+00	6.19117E+00	5.24069E+00	5.32554E+00	6.61745E+00
107	4.23632E+00	5.26256E+00	4.91123E+00	5.03114E+00	6.56664E+00
108	3.12742E+00	3.97143E+00	3.72279E+00	4.23319E+00	6.47649E+00
109	2.14806E+00	2.26568E+00	2.77728E+00	3.24962E+00	5.97932E+00
110	1.20211E+00	1.18789E+00	1.69763E+00	2.20439E+00	6.01170E+00
111	5.84533E-01	5.73063E-01	8.98203E-01	1.28751E+00	5.20680E+00
112	2.77406E-01	2.31893E-01	4.19160E-01	6.46639E-01	4.25442E+00
113	1.48613E-01	1.54047E-01	2.19561E-01	3.08845E-01	3.37349E+00
114	9.90741E-02	7.39299E-02	1.39720E-01	1.52103E-01	3.09101E+00
115	9.90838E-02	4.44595E-02	1.09783E-01	1.06169E-01	2.59568E+00
116	8.42146E-02	2.93958E-02	9.98019E-02	9.50687E-02	2.05255E+00
117	8.44465E-02	2.57381E-02	8.98755E-02	9.75395E-02	1.10879E+00
118	7.92594E-02	2.44946E-02	8.58294E-02	8.68600E-02	8.85565E-01
119	7.92591E-02	2.44956E-02	8.48325E-02	8.68631E-02	3.34139E-01
120	8.40876E-02	2.40856E-02	8.47398E-02	8.20347E-02	2.29308E-01
121	8.40866E-02	2.37064E-02	8.97239E-02	8.86913E-02	1.12502E-01
122	9.39817E-02	2.37064E-02	9.27176E-02	9.06608E-02	7.10119E-02

TABLE VI (cont)

MASS	PU240F	PU241T	PU241F	PU242F	CF252SF
123	1.08819E-01	2.50483E-02	9.96925E-02	9.60026E-02	4.25419E-02
124	1.18744E-01	2.93981E-02	1.09677E-01	1.08400E-01	2.36768E-02
125	1.19101E-01	4.19178E-02	7.01704E-02	6.75050E-02	2.21114E-02
126	2.90182E-01	7.70719E-02	2.17663E-01	1.73202E-01	2.71153E-02
127	3.53961E-01	2.29898E-01	3.04341E-01	2.96918E-01	1.00375E-01
128	6.05315E-01	3.56455E-01	5.06775E-01	4.94867E-01	2.07558E-01
129	1.00730E+00	7.79290E-01	8.44836E-01	8.48810E-01	3.90602E-01
130	1.89093E+00	1.65606E+00	1.54845E+00	1.45942E+00	7.21906E-01
131	3.44396E+00	2.96987E+00	3.35100E+00	3.11715E+00	1.50480E+00
132	4.70153E+00	4.39675E+00	4.75305E+00	4.55777E+00	2.00360E+00
133	6.83745E+00	6.75181E+00	6.56081E+00	6.89036E+00	3.28633E+00
134	7.04718E+00	7.70277E+00	7.59376E+00	7.50537E+00	2.94437E+00
135	7.59932E+00	7.22022E+00	7.17235E+00	7.09220E+00	3.97558E+00
136	6.75868E+00	6.93046E+00	6.86831E+00	7.00917E+00	4.07766E+00
137	6.89353E+00	6.77144E+00	6.47165E+00	6.48739E+00	4.81233E+00
138	6.54622E+00	6.72356E+00	6.45383E+00	6.28881E+00	5.47466E+00
139	5.85861E+00	5.91809E+00	6.15747E+00	5.98800E+00	5.84592E+00
140	5.01336E+00	6.04762E+00	5.90773E+00	4.96366E+00	6.08149E+00
141	4.80172E+00	4.92392E+00	5.13397E+00	5.03923E+00	6.13946E+00
142	4.96853E+00	4.95856E+00	4.64512E+00	4.65163E+00	6.09039E+00
143	4.75441E+00	4.64688E+00	4.64042E+00	4.69728E+00	6.18031E+00
144	4.10745E+00	4.27373E+00	3.71182E+00	4.31846E+00	5.94472E+00
145	3.27731E+00	3.30378E+00	3.24664E+00	3.43174E+00	5.45262E+00
146	2.73625E+00	2.82816E+00	2.83721E+00	2.94183E+00	4.78331E+00
147	2.23553E+00	2.33070E+00	2.22100E+00	2.40221E+00	4.43577E+00
148	1.91652E+00	1.96848E+00	2.00038E+00	2.02529E+00	4.42415E+00
149	1.37181E+00	1.51110E+00	1.45166E+00	1.62016E+00	2.84341E+00
150	1.14151E+00	1.23470E+00	1.23241E+00	1.32926E+00	2.47532E+00
151	8.61749E-01	9.30804E-01	9.15999E-01	9.98335E-01	1.85729E+00
152	6.58911E-01	7.40277E-01	7.22440E-01	7.72228E-01	1.53505E+00
153	5.38485E-01	5.41447E-01	6.12007E-01	6.43320E-01	1.30103E+00
154	3.15806E-01	3.92571E-01	3.82938E-01	4.30379E-01	1.07525E+00
155	2.96777E-01	2.37541E-01	3.28987E-01	3.54764E-01	8.97809E-01
156	2.07746E-01	1.73953E-01	2.39264E-01	2.56220E-01	6.60589E-01
157	1.38497E-01	1.34930E-01	1.59510E-01	1.77379E-01	5.32782E-01
158	8.90341E-02	8.67062E-02	1.09664E-01	1.18252E-01	4.76055E-01
159	5.44090E-02	4.79513E-02	6.38032E-02	7.09529E-02	3.54554E-01
160	3.26530E-02	1.92696E-02	3.88841E-02	4.43450E-02	2.76271E-01
161	1.85902E-02	8.45667E-03	2.29298E-02	2.56224E-02	1.99057E-01
162	8.80681E-03	2.50500E-03	1.09316E-02	1.37963E-02	1.78058E-01
163	4.10923E-03	9.03523E-04	6.16203E-03	5.91351E-03	1.48543E-01
164	2.54375E-03	2.90168E-04	3.18035E-03	2.95668E-03	9.71273E-02
165	1.47749E-03	9.06141E-05	1.49378E-03	1.97898E-03	6.75068E-02
166	7.33514E-04	6.07026E-05	5.96325E-04	9.84760E-04	4.45621E-02
167	3.91814E-04	2.74975E-05	2.98558E-04	3.83874E-04	2.45654E-02
168	1.66608E-04	1.25211E-05	1.19231E-04	1.67377E-04	1.22838E-02
169	9.29708E-05	5.29915E-06	5.66868E-05	9.36132E-05	3.43556E-03
170	4.40680E-05	1.54277E-06	1.58943E-05	4.43110E-05	1.35676E-03
171	2.44452E-05	2.88487E-07	5.56489E-06	2.46741E-05	6.31810E-04
172	1.46793E-05	9.62881E-08	1.59075E-06	1.47811E-05	3.98116E-04

TABLE VII

ENDF/B-VC YIELD WEIGHTED QUANTITIES

Fissionable Nuclide	Charge[a]	Neutron[a]	Stable Mass	Stable Charge	Stable A
Th232(F)	90.002	140.681	230.499	96.8875	230.683
Th232(HE)	90.003	138.983	228.800	96.1733	228.986
Np237(F)	93.000	142.390	235.203	98.7622	235.390
U233(T)	91.998	139.526	231.338	97.1983	231.524
U233(F)	92.002	139.591	231.407	97.2143	231.593
U233(HE)	92.004	138.417	230.234	96.7436	230.421
U235(T)	91.979	141.540	233.333	98.0443	233.519
U235(F)	92.000	141.547	233.361	98.0405	233.547
U235(HE)	92.001	139.623	231.437	97.2989	231.624
U236(F)	92.000	142.317	234.131	98.3620	234.317
U238(F)	92.002	143.956	235.772	99.0131	235.985
U238(HE)	91.998	142.581	234.393	98.4558	234.579
Pu239(T)	93.999	143.055	236.868	99.4666	237.055
Pu239(F)	94.003	143.175	236.991	99.5123	237.178
Pu239(HE)	93.999	141.617	235.429	98.8156	235.616
Pu240(F)	93.999	144.000	237.813	99.8543	237.999
Pu241(T)	94.000	145.061	238.875	100.301	239.061
Pu241(F)	94.000	144.758	238.571	100.161	238.757
Pu242(F)	93.999	145.284	239.098	100.376	239.284
Cf252(S)	97.991	149.984	247.791	103.982	247.976

[a] Yield weightings use independent (direct) yields; the last three columns use cumulative mass chain yields.

TABLE VIII

PARAMETERS BASED ON YIELD WEIGHTINGS

Fissionable Nuclide	Charge Deviation (%)	Neutrons		Ave. No. Beta Decays	Q_f	
		Prompt	Delayed[a]		Cal[b]	Eval[d]
Th232(F)	0.002	2.319	0.0402	6.89	157.(194.)[c]	197.
Th232(HE)	0.003	4.017	0.0268	6.17	156.(181.)	---
Np237(F)	0.000	2.610	0.114	5.76	208.(219.)	203.
U233(T)	-0.002	2.474	0.00765	5.20	193.(200.)	198.
U233(F)	0.002	2.409	0.00813	5.21	189.(197.)	---
U233(HE)	0.004	3.583	0.00576	5.74	181.(186.)	---
U235(T)	-0.034	2.460	0.0161	6.04	207.(222.)	203.
U235(F)	0.000	2.453	0.0168	6.04	199.(215.)	---
U235(HE)	0.001	4.377	0.00909	5.30	178.(186.)	---
U236(F)	0.000	2.683	0.0197	6.36	184.(202.)	202.
U238(F)	0.002	3.044	0.0296	7.01	174.(202.)	206.
U238(HE)	-0.002	4.419	0.0222	6.46	174.(195.)	---
Pu239(T)	-0.001	2.945	0.00693	5.47	201.(207.)	207.
Pu239(F)	0.003	2.825	0.00642	5.51	199.(205.)	---
Pu239(HE)	-0.001	4.383	0.00399	4.82	193.(197.)	---
Pu240(F)	-0.001	3.000	0.00837	5.85	200.(208.)	206.
Pu241(T)	0.000	2.939	0.0126	6.30	199.(211.)	211.
Pu241(F)	0.000	3.242	0.0116	6.16	198.(209.)	---
Pu242(F)	-0.001	3.716	0.0118	6.38	195.(206.)	211.
Cf252(S)	-0.009	4.016	0.00488	5.98	218.(223.)	---

[a] Delayed neutrons based on 74 preliminary Pn values; calculations described in T-2-L-2311, letter, England to Schenter, April 29, 1977.

[b] $Q_f = 931.48[M_f + 1.0086652(1-\bar{\nu}_p-\bar{\nu}_d)-\bar{M}_s]$.

Where $\bar{M}_s$ = average mass of stable nuclide,

M_f = mass of fissionable nuclide,

$\bar{\nu}_p, \bar{\nu}_d$ = calculated prompt and delayed neutrons per fission.

[c] Q_f values in parentheses do not use $\bar{\nu}_d$ in above equation.

[d] From R. Sher, EPRI-RP-80, October 1976.

D. Library for Processed ENDF/B Aggregate Fission-Product Spectra (R. J. LaBauve, T. R. England, D. George, and M. G. Stamatelatos)

The ENDF/B-IV fission product files contain neutron cross sections, decay constants, decay energies, and other decay data for 824 important fission products. They also contain fission yields for these fission products produced by one or more fission-neutron energies (14-MeV, fast, and thermal fission) for six important fissionable nuclides: ^{232}Th, ^{233}U, ^{235}U, ^{238}U, ^{239}Pu, and ^{241}Pu. A computer code system[42,43] has been developed at the Los Alamos Scientific Laboratory that uses the ENDF/B-IV fission product data to calculate cumulative delayed beta and gamma spectra on arbitrary energy grids for arbitrary irradiation periods and cooling times. This code system is schematically illustrated in Fig. 17.

Of particular interest is the application of this code system to produce delayed beta- and gamma-spectral data on a fine energy grid (e.g., 150 groups in 0.05-MeV steps from 0 to 7.5 MeV) for irradiation of the above fissionable nuclides with very short pulses (typically 10^{-4}s irradiation time) of thermal, fast, and 14-MeV neutrons. The results can then be further processed into broad groups and fit with functions of the type

$$f_c(t) = \sum_{i=1}^{n} \alpha_i e^{-\lambda_i t} \quad ,$$

as described in Ref. 44.

For convenience, the fine-group results from the LASL code system are assembled into a single library in an ENDF-like format. Definitions for the format for this processed ENDF/B fission product and yield data library (PEFPYD-LIB) are as follows:

MAT: Material number of target nucleus, same as in ENDF/B.

MF: File number, used to identify energy type of incident neutron. We provisionally define the following:

MF=80 - fission induced by thermal neutrons

MF=81 - fission induced by fast neutrons

MF=82 - fission induced by high-energy (14-MeV) neutrons

ENDF/B-IV contains yield data as shown in Table IX

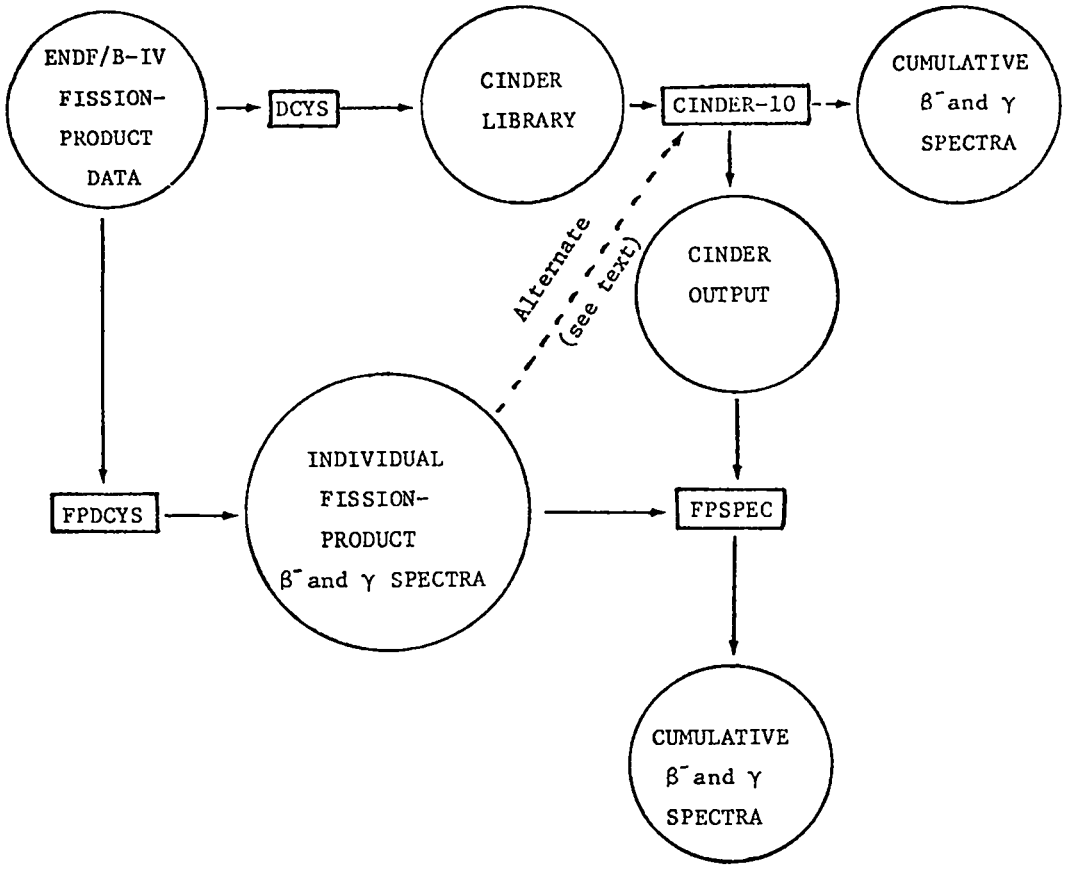

Fig. 17.
LASL code system for generating multigroup β^- and γ fission-product spectra.

TABLE IX

FISSION PRODUCT YIELD DATA AVAILABLE IN ENDF/B-IV

MAT	Nuclide	Thermal Energy (MF80)	Fast Energy (MF81)	High Energy (MF82)
1296	^{232}Th	No	Yes	No
1260	^{233}U	Yes	No	No
1261	^{235}U	Yes	Yes	Yes
1262	^{238}U	No	Yes	Yes
1264	^{239}Pu	Yes	Yes	No
1266	^{241}Pu	Yes	No	No

MT: Section number used to describe the data contents of the section. Provisional MT-numbers are as follows:

MT=801 - delayed energy/fission for β^- + γ summed over all fission products

MT=802 - delayed energy/fission for β^- summed over all fission products

MT=803 - delayed energy/fission for γ summed over all fission products

MT=811 - delayed energy/fission for β^- + γ summed over all gaseous fission products

MT=812 - delayed energy/fission for β^- summed over all gaseous fission products

MT=813 - delayed energy/fission for γ summed over all gaseous fission products.

MT=821 - delayed energy/fission for β^- + γ summed over the noble gas fission products

MT=822 - delayed energy/fission for β^- summed over noble gas fission products

MT=823 - delayed energy/fission for γ summed over noble gas fission products

MT=831 - delayed energy/fission for β^- + γ summed over the halogen gas fission products

MT=832 - delayed energy/fission for β^- summed over halogen gas fission products

MT=833 - delayed energy/fission for γ summed over halogen gas fission products

Other MT-numbers can be defined as needed; for example, MT-numbers could be assigned to the above spectra summed over energy.

The data are given in a TAB2 record with tables of spectra (energy/fission vs. energy) given for a number of cooling times. Interpolation between cooling times (TAB2 interpolation) is not allowed, as the data would have to be extremely detailed to permit use of one of the standard ENDF interpolation schemes. (Note that when the data are placed on a broad-group mesh and fitted with parameters as described in Ref. 44, calculations for any irradiation-cooling time combinations are possible, precluding the need for interpolation on the fine grid.) Histogram interpolation is assigned for TAB1 interpolations.

The assembly of PEFPYD-LIB for ENDF/B-IV is about 90% complete. Upon completion, the library will be sent to the NNDC at BNL for further distribtuion.

Under development is a code, FITPULS, which is an extension of the fitting code described in Ref. 44 that retrieves the fine-group data from PEFPYD-LIB, collapses this data to broad-energy groups (up to 25), and fits the collapsed

group data with linear combinations of functions described above (the parameters are determined by a nonlinear least-squares module). When complete, FITPULS will be made operational at NNDC and it is anticipated that they will respond to user requests for the fits of aggregate fission product spectra for any desired energy group structure. Fits to a broad-group structure in use at LASL that are sufficient for most users will also be supplied to NNDC.

E. Delayed Neutron Precursors [T. R. England, W. B. Wilson, and P. L. Reeder (Battelle Northwest Laboratories)]

Version IV of ENDF/B contains neutron emission probabilities (Pn) for 57 precursors, 34 being measured and the remainder based on a simple fitting model. A new preliminary list of 74 precursors has been completed; of these, 47 have measured Pn values and 27 are based on a least-squares fitting to the neutron emission window (the Q value for beta decay Q_β minus the neutron binding energy B_n of the daughter nuclide) of the measured Pn's. The result is

$$Pn \simeq 1.578\ (Q_\beta - B_n)^{1.577},$$

where Pn is expressed in percent and Q_β and B_n are in MeV. Direct computations of the Pn's based on more elaborate models have resulted in very poor values; without resort to nuclear structure effects, the simple fitted results are preferred.

Table X lists the preliminary Pn values and other parameters for the 74 precursors. The uncertainty column Pn uses 0.0 to distinguish the fitted values. For beta decay energies >1 MeV, these should be accurate within a factor of 2. (Table XI shows a comparison of the model estimates with Pn's measured subsequent to ENDF/B-IV.) The fitted values account for only about 10% of the total calculated delayed neutron emission per fission ($\bar{\nu}_d$); for ^{235}U these account for only 8.9% of the total $\bar{\nu}_d$.

Table XII shows a comparison of calculated $\bar{\nu}_d$ values using the preliminary Version VC yields and the 74 emitters with Version IV calculations and available evaluations. In general, the combination of revised fission yields and Pn values shows a considerable improvement in calculated $\bar{\nu}_d$s over ENDF/B-IV calculations. This work is being continued; there are potential precursors that may improve the $\bar{\nu}_d$s calculated for ^{232}Th and ^{238}U. These calculations are used primarily for integral tests of the yield compilations; however, it is evident that Pn and

TABLE X

PRELIMINARY DELAYED NEUTRON PRECURSORS AND Pn VALUES FOR ENDF/B-V[a]

GP	NUCLIDE	QB	BN	PN(%)	DPN	HL	DHL
4	ZN 300790	8.66	7.65	1.6	0.0	2.74	.04
4	GA 310790	6.06	5.70	0.3	0.0	2.86	.04
4	GA 310800	9.44	8.50	1.4	0.0	1.66	.02
4	GA 310810	7.44	5.13	5.9	0.0	1.23	.01
5	GA 310820	12.55	8.12	16.5	0.0	.60	.01
5	GA 310830	11.41	3.20	44.	0.0	.31	.01
4	GE 320830	8.49	8.11	0.3	0.0	1.9	.4
4	GE 320840	7.54	4.15	11.	0.0	1.2	.3
3	AS 330840	9.99	9.06	0.07	0.02	5.6	.2
4	AS 330850	9.05	4.10	18.	2.	2.031	.008
5	AS 330860	11.35	6.22	5.	1.	.9	.2
5	AS 330870	10.41	4.11	29.	0.0	.5	.2
3	SE 340870	7.27	6.40	.18	.02	5.60	.07
4	SE 340880	6.33	4.85	.56	.05	1.52	.04
5	SE 340890	8.63	6.15	5.	1.5	.44	.04
5	SE 340910	10.31	5.72	21.	10.	.27	.05
1	BR 350870	6.68	5.46	2.4	.1	55.68	.07
2	BR 350880	8.91	7.15	5.3	.2	16.10	.08
3	BR 350890	8.68	5.22	9.6	.5	4.40	.03
4	BR 350900	9.91	6.21	14.	1.	1.86	.04
5	BR 350910	9.18	4.57	11.	2.	.551	.005
5	BR 350920	12.01	6.21	21.	8.	.36	.007
4	KR 360920	5.48	5.06	.033	.002	1.848	.005
4	KR 360930	8.15	6.30	2.0	.1	1.287	.001
6	KR 360940	6.56	4.33	2.2	.8	.209	.006
3	RB 370920	7.94	7.35	.012	.001	4.509	.009
3	RB 370930	6.07	5.14	1.37	.05	5.85	.01
4	RB 370940	9.18	7.17	10.1	.30	2.757	.006
5	RB 370950	7.87	4.64	8.5	.3	.385	.002
6	RB 370960	10.76	6.62	13.7	.6	.201	.001
6	RB 370970	9.03	3.92	28.	1.	.169	.001
6	RB 370980	12.11	6.39	13.3	2.1	.120	.004
6	RB 370990	10.07	3.09	34.	0.0	.076	.005
5	SR 380970	7.10	6.81	0.2	0.0	.4	.03
5	SR 380980	5.37	4.67	0.9	0.0	.75	.04

TABLE X (cont)

GP	NUCLIDE	QB	BN	PN(%)	DPN	HL	DHL
5	SR 380990	8.45	6.16	3.4	2.4	.6	.2
4	Y 390971	5.77	5.22	1.6	.3	1.16	.02
4	Y 390970	5.77	5.22	1.6	0.0	3.7	.1
5	Y 390981	8.26	7.55	4.	2.	.65	.05
4	Y 390980	8.26	7.55	.9	0.0	2.	.15
4	Y 390990	6.51	4.44	1.6	.7	1.48	.09
4	AG 471220	9.17	7.98	2.1	0.0	1.5	.5
5	AG 471230	7.28	5.08	5.5	0.0	.39	.03
5	CD 481280	5.54	5.24	0.2	0.0	.83	.03
3	IN 491271	6.44	5.55	1.3	0.0	3.71	.02
3	IN 491270	6.44	5.55	1.3	0.0	2.0	0.0
3	IN 491280	9.07	7.79	2.3	0.0	5.4	.3
5	IN 491291	7.31	5.32	4.7	0.0	.99	.02
4	IN 491290	7.31	5.32	4.7	0.0	2.5	.2
5	IN 491300	9.69	7.42	5.8	0.0	.58	.01
6	IN 491310	8.39	5.02	11.	0.0	.286	.009
6	IN 491320	12.31	6.97	22.2	0.0	.13	.02
4	SN 501330	7.24	7.11	0.06	0.0	1.50	.06
4	SN 501340	6.07	3.43	17.	3.	1.04	.02
2	SB 511341	8.69	7.35	.091	.008	10.6	.1
4	SB 511350	7.52	3.86	14.1	.8	1.726	.009
5	SB 511360	9.54	5.20	32.	14.	.82	.02
2	TE 521360	4.40	4.02	.76	.01	19.0	.3
4	TE 521370	6.48	5.63	2.2	.4	2.8	.4
4	TE 521380	5.34	3.84	5.6	1.6	1.4	.4
2	I 531370	5.77	4.45	6.2	.3	24.57	.05
3	I 531380	7.48	5.86	2.6	.2	6.49	.04
4	I 531390	6.77	3.89	9.8	.7	2.42	.04
5	I 531400	8.93	5.35	27.	5.	.625	.009
5	I 531410	7.42	3.52	36.	11.	.46	.02
4	XE 541410	5.85	5.79	.043	.002	1.726	.006
4	XE 541420	4.34	3.93	.406	.003	1.24	.01
5	XE 541430	6.65	5.59	1.7	0.0	.76	.02
2	CS 551410	5.06	4.65	.053	.003	24.7	.1
4	CS 551420	7.06	6.20	.118	.008	1.72	.01
4	CS 551430	5.73	4.09	1.75	.09	1.778	.008
4	CS 551440	8.05	6.16	2.6	.2	1.001	.008
5	CS 551450	6.07	3.83	14.1	.7	.585	.004
5	CS 551460	8.54	6.45	14.2	1.7	.299	.006

TABLE X (cont)

Note 1: Notation
GP = Approximate decay group (6 groups).
QB = Maximum beta decay energy of precursor (MeV).
BN = Neutron binding energy in daughter (MeV).
PN = Neutron emission probability (%) of daughter.
DPN= Uncertainty in PN.
HL = Precursor half-life (s).
DHL= Uncertainty in half-life (s).

Note 2:
47 Pn values are based on a weighting of values in a compilation by K.L. Kratz. The weighting and some modification was made by P.L. Reeder. The 27 Pn values having a zero uncertainty (DPN) are estimates based on a fit of A and B using 40 experimental values to the form $A(QB-BN)^{B}$ by T.R. England.

TABLE XI

COMPARISON OF ESTIMATED Pn VALUES
IN ENDF/B-IV WITH RECENT MEASUREMENTS

	Pn %			
Nuclide	ENDF/B-IV Model	Experiment (Average)		ENDF/B-V Model
^{92}Br	26.	21.	8.	25.
^{94}Kr	4.4	2.2	.8	5.6
^{97}Rb	21.	28.	1.	21.
^{98}Rb	26.	13.3	2.1	25.
^{98}Y	0.48[a]	4.	2.	0.9
^{99}Y	3.8[a]	1.6	7.	5.
^{141}I	12.	36.	11.	13.5

[a]Estimate was based on ground state energetics; experimental values not identified as to state.

TABLE XII

DELAYED NEUTRON YIELDS PER 100 FISSIONS CALCULATED VALUES USING PRELIMINARY ENDF/B-V (BC) YIELDS AND Pn VALUES AND ENDF/B-IV COMPARISONS[a]

Fissionable Nuclide[b]	ENDF/B-V(VC) Yields 74 Pn Values	ENDF/B-IV Evaluation	ENDF/B-V(VC) Yields 57 Pn Values	ENDF/B-IV Yields 57 Pn Values
Th232(F)	4.02(4.04)[c]	5.27±.4	3.46	3.93
Th232(HE)	2.68(2.70)	3.0	2.43	----
Np237(F)	1.14(1.19)	--------	1.02	----
U233(T)	0.765(0.788)	0.74±.04	.673	.821
U233(F)	0.813(0.841)	0.74±.04	.721	----
U233(HE)	0.576(0.602)	0.44	.506	----
U235(T)	1.61(1.64)	1.67±.07	1.44	1.60
U235(F)	1.68(1.72)	1.67±.07	1.48	1.48
U235(HE)	0.909(0.938)	0.90	.829	1.09
U236(F)	1.97(2.03)	---------	1.74	----
U238(F)	2.96(3.01)	4.60±.25	2.42	2.93
U238(HE)	2.22(2.28)	2.60	1.96	1.96
Pu239(T)	0.693(0.729)	0.645±.04	.601	.520
Pu239(F)	0.642(0.679)	0.645±.04	.556	.508
Pu239(HE)	0.399(0.431)	0.43	.341	----
Pu240(F)	0.837(0.870)	0.90 ±.09	.724	----
Pu241(T)	1.26(1.31)	1.57 ±.15	1.10	1.05
Pu241(F)	1.16(1.20)	1.57 ±.15	1.01	----
Pu242(F)	1.18(1.21)	---------	1.00	----
Cf252(S)	0.488(0.508)	---------	.424	----

[a] Pn values are tabulated in Table XIII.

[b] T denotes thermal fission, F fast fission, HE fission energies between 14 and 15 Mev, and S spontaneous fission.

[c] Values in parentheses have been corrected for isomeric branching; in addition, ^{98m}Y and ^{129m}In are not in yield set VC and approximate values for these have been added to the total $\bar{\nu}_d$ by assuming that one-half of the cumulative yield to their respective ground states applies to the isomeric state. The net change is likely too large because of the ^{98m}Y and ^{129m}In additions.

yield data already have sufficient quality to predict $\bar{\nu}_d$ within evaluated uncertainties for many fissionable nuclides. The large discrepancy for ^{238}U and ^{232}Th may be a result of the large pairing effect predicted for fission-neutron energies near the fission threshold.

F. Comparisons of Calculated and Experimental Delayed Fission-Product Beta and Gamma Spectra (T. R. England, M. G. Stamatelatos, and N. L. Whittemore

Delayed fission-product beta and gamma spectra following ^{235}U thermal irradiations of 0.015, 1, 10, 100, 20 000, and 28 800 s have been calculated for a number of cooling times. These have been compared to recent LASL, ORNL, and University of Illinois (UI) experiments. Calculations are based on spectra derived from ENDF/B-IV data.[45] Some of these comparisons have been previously reported. They show generally good agreement with experiments and indicate the adequacy of ENDF/B-IV data for such calculation. In particular, these indicate the efficacy of the effort described in Sec. IV.D.

A total of 102 beta or gamma comparisons have been completed. These have now been collated into a report.[46]

G. Processing of Preliminary ENDF/B-V Actinide Cross Sections (W. B. Wilson, T. R. England, and N. L. Whittemore)

Version V of the ENDF/B file will include a separate data set for actinide nuclides. A pre-preliminary issue of this actinide library (Tapes 947-9) was issued by NNDC at BNL for review. Errors and deficiencies in these files detected by participating laboratories are corrected in the recently released preliminary actinide files (Tapes 944-6) describing 46 nuclides in the range $92 \leqslant Z \leqslant 99$.

Of the 46 nuclides included in the preliminary ENDF/B-V actinide library, 36 include cross-section evaluations. These cross sections have been successfully processed with the NJOY code into the PRS 154-group structure, using the PRS Flux Weighting Function. The library of 154-group cross sections has been collapsed with the TOAFEW collapsing code into the EPRI 4-group structure for use in preliminary depletion calculations with the CINDER code.

H. Few-Group Cross Sections for Fission-Product Absorption Calculations (W. B. Wilson, T. R. England, M. G. Stamatelatos, and R. J. LaBauve)

The processing of ENDF/B-IV fission product data into the Power Reactor Spectrum (PRS) 154-group structure with NJOY has been described in previous

progress reports.[46,47] This multigroup library has been collapsed to a four-group structure with the TOAFEW code.[48] Because of interest expressed by a number of users in the attainment of fission-product cross sections in various few-group structures, the library of 154-group cross sections and the collapsing code have been combined in a package for general release. A report describing their production and utilization is in preparation.

Four-group radiative capture cross sections produced in the EPRI four-group structure of Table XIII have been incorporated into a library of fission-product data used by the EPRI-CINDER code in fission-product absorption buildup calculations.[50] These four-group cross sections are listed in Table XIV.

Extensive measurements of fission-product absorption buildup in ^{233}U samples irradiated to ~90% depletion are reported in Ref. 51, along with comparisons with calculations with an unpublished pre-ENDF/B-IV four-group library having the group boundaries of Table XIII. For comparison, the ENDF/B-IV four-group library was modified using the same assumptions regarding flux spectrum and cross-section energy dependence described in Ref. 51.

The resulting comparison, shown in Fig. 18, is given in terms of $\hat{\sigma}_{eff}$, an effective one-group cross section (barns/fission) that, when multiplied by the thermal (4th) group flux, reproduces the total absorption rate.

TABLE XIII

EPRI FOUR-GROUP STRUCTURE

	$1.000\ 000\ 000 \times 10^{7}$ eV
Group 1	
	$8.208\ 499\ 862 \times 10^{5}$ eV
Group 2	
	$5.530\ 843\ 701 \times 10^{3}$ eV
Group 3	
	$6.250\ 600\ 000 \times 10^{-1}$ eV
Group 4	
	$1.000\ 000\ 000 \times 10^{-5}$ eV

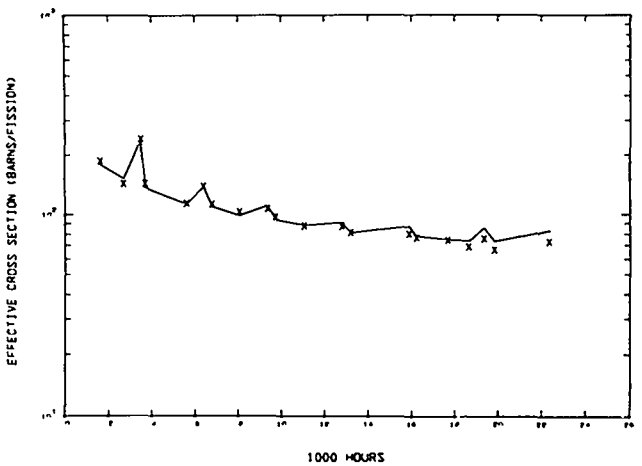

Fig. 18
Sigma-effective comparison, EPRI-CINDER (-) vs BAPL experimental (X).

TABLE XIV

FOUR-GROUP (N,GAMMA) CROSS SECTIONS

NUCLIDE	Z	A	S	MAT	TEMP (K)	GROUP 1 CROSS SECTION	GROUP 2 CROSS SECTION	GROUP 3 CROSS SECTION	GROUP 4 CROSS SECTION	EFFEC.THERM. CROSS SECTION
GE 72	32	72	0	48	1.0E+03	2.099716E-02	5.432289E-02	8.043696E-02	5.476937E-01	9.885840E-01
GE 73	32	73	0	49	1.0E+03	4.379093E-02	1.769910E-01	8.051782E+00	8.381628E+00	1.512879E+01
GE 74	32	74	0	51	1.0E+03	9.484258E-03	3.185640E-02	4.402824E-02	2.141804E-01	3.865945E-01
GE 76	32	76	0	54	1.0E+03	2.668907E-03	9.284226E-03	1.632492E-01	7.941654E-02	1.433464E-01
AS 75	33	75	0	68	1.0E+03	3.174023E-02	2.399267E-01	7.066404E+00	2.408837E+00	4.347936E+00
SE 76	34	76	0	85	1.0E+03	3.043571E-02	1.025647E-01	3.876426E+00	4.754810E+01	8.582406E+01
SE 77	34	77	0	86	1.0E+03	2.397912E-02	2.570206E-01	3.571884E+00	2.346095E+01	4.234688E+01
SE 78	34	78	0	88	1.0E+03	1.233979E-02	4.559968E-02	5.350889E-01	2.234162E-01	4.032650E-01
SE 80	34	80	0	91	1.0E+03	1.224080E-02	4.557911E-02	8.982662E-02	3.412236E-01	6.159067E-01
SE 82	34	82	0	94	1.0E+03	3.747510E-03	1.079513E-02	1.686126E-03	2.513117E-02	4.536163E-02
BR 79	35	79	0	108	1.0E+03	6.182080E-02	4.360678E-01	1.200472E+01	6.222752E+00	1.123203E+01
BR 81	35	81	0	112	1.0E+03	4.217740E-02	2.809681E-01	5.719193E+00	1.503798E+00	2.714348E+00
KR 80	36	80	0	131	1.0E+03	3.268930E-02	1.358841E-01	6.958419E+00	7.974773E+00	1.439442E+01
KR 82	36	82	0	134	1.0E+03	3.209819E-02	1.243721E-01	1.984202E+01	1.685921E+01	3.043078E+01
KR 83	36	83	0	135	1.0E+03	6.710060E-02	3.993954E-01	1.841473E+01	1.119001E+02	2.019790E+02
KR 84	36	84	0	137	1.0E+03	4.472712E-03	1.912670E-02	4.376474E-01	4.633101E-02	8.362721E-02
KR 85	36	85	0	138	1.0E+03	4.363354E-03	2.864559E-02	1.600506E-01	9.295652E-01	1.677860E+00
KR 86	36	86	0	140	1.0E+03	1.108820E-03	3.162755E-03	1.545394E-02	3.441791E-02	6.212414E-02
RB 85	37	85	0	153	1.0E+03	2.080914E-02	2.157803E-01	5.395468E-01	2.576161E-01	4.649955E-01
RB 86	37	86	0	154	1.0E+03	4.296598E-03	9.237312E-02	2.813636E+00	2.735252E+00	4.937115E+00
RB 87	37	87	0	156	1.0E+03	1.287127E-03	8.266649E-03	2.536605E-01	6.710316E-02	1.211208E-01
SR 86	38	86	0	172	1.0E+03	1.688432E-02	4.159945E-02	5.748211E-01	1.588873E+00	2.867907E+00
SR 87	38	87	0	173	1.0E+03	1.669480E-02	7.775602E-02	1.045327E+01	9.270864E+00	1.673386E+01
SR 88	38	88	0	175	1.0E+03	1.329117E-03	1.164227E-03	2.201289E-04	3.248619E-03	5.863738E-03
SR 89	38	89	0	176	1.0E+03	8.295338E-03	2.038847E-02	3.876896E-02	2.348515E-01	4.239056E-01
SR 90	38	90	0	177	1.0E+03	4.920037E-03	1.560162E-02	3.315065E-02	5.026414E-01	9.072648E-01
Y 89	39	89	0	192	1.0E+03	7.136131E-03	2.253723E-02	8.228018E-02	7.165644E-01	1.293395E+00
Y 90	39	90	0	194	1.0E+03	1.138581E-02	1.146555E-01	4.323381E-01	1.954493E+00	3.527849E+00
Y 91	39	91	0	196	1.0E+03	4.217073E-03	3.284697E-02	1.639328E-01	7.827059E-01	1.412780E+00
ZR 90	40	90	0	215	1.0E+03	1.508096E-02	2.520652E-02	1.987868E-02	5.586877E-02	1.008428E-01
ZR 91	40	91	0	217	1.0E+03	1.715130E-02	5.507396E-02	6.700606E-01	5.758814E-01	1.039463E+00
ZR 92	40	92	0	218	1.0E+03	1.042367E-02	3.130879E-02	8.308115E-02	1.452876E-01	2.622433E-01
ZR 93	40	93	0	219	1.0E+03	2.089521E-02	5.150402E-02	3.654891E+00	1.396955E+00	2.521495E+00
ZR 94	40	94	0	220	1.0E+03	5.447404E-03	2.595021E-02	2.019570E-02	3.128906E-02	5.647657E-02
ZR 95	40	95	0	221	1.0E+03	3.771503E-02	1.168058E-01	5.797035E-01	2.741127E-01	4.947719E-01
ZR 96	40	96	0	222	1.0E+03	2.648158E-02	2.165040E-02	6.357653E-01	8.862928E-03	1.599754E-02
NB 93	41	93	0	1189	9.0E+02	1.604464E-02	1.581963E-01	1.036643E+00	6.392347E-01	1.153815E+00
NB 94	41	94	0	238	1.0E+03	5.739899E-03	1.688129E-01	1.173435E+01	7.640611E+00	1.379126E+01
NB 95	41	95	0	240	1.0E+03	5.266054E-02	2.650329E-01	2.503124E+00	8.380113E-01	1.512606E+00
MO 94	42	94	0	264	1.0E+03	1.622583E-02	3.166593E-02	9.483320E-02	8.925915E-03	1.611123E-02
MO 95	42	95	0	265	1.0E+03	3.417280E-02	2.320601E-01	1.257062E+01	8.099988E+00	1.462043E+01
MO 96	42	96	0	266	1.0E+03	1.622694E-02	4.895069E-02	2.259064E+00	5.590317E-01	1.009049E+00

TABLE XIV (cont)

NUCLIDE	Z	A	S	MAT	TEMP (K)	GROUP 1 CROSS SECTION	GROUP 2 CROSS SECTION	GROUP 3 CROSS SECTION	GROUP 4 CROSS SECTION	EFFEC.THERM. CROSS SECTION
MO 97	42	97	0	267	1.0E+03	2.907559E-02	2.248807E-01	1.719731E+00	1.215824E+00	2.194556E+00
MO 98	42	98	0	268	1.0E+03	2.516355E-02	7.168378E-02	7.678803E-01	7.125803E-02	1.286203E-01
MO 99	42	99	0	269	1.0E+03	4.286153E-02	4.063070E-01	2.849176E+00	9.492203E-01	1.713337E+00
MO100	42	100	0	270	1.0E+03	9.074271E-03	5.494819E-02	4.423330E-01	1.111105E-01	2.005538E-01
TC 99	43	99	0	1137	9.0E+02	3.673952E-02	3.614800E-01	3.069278E+01	1.083246E+01	1.955253E+01
RU 99	44	99	0	308	1.0E+03	3.826665E-02	3.753455E-01	1.421606E+01	2.833373E+00	5.114222E+00
RU100	44	100	0	309	1.0E+03	3.858774E-02	1.136596E-01	1.132016E+00	3.239899E+00	5.847999E+00
RU101	44	101	0	310	1.0E+03	2.690347E-02	4.480972E-01	9.421788E+00	1.743797E+00	3.147543E+00
RU102	44	102	0	311	1.0E+03	6.954545E-02	1.577507E-01	3.499625E-01	7.279318E-01	1.313913E+00
RU103	44	103	0	312	1.0E+03	2.468305E-02	3.671989E-01	7.404899E+00	4.301005E+00	7.763290E+00
RU104	44	104	0	313	1.0E+03	3.070218E-02	1.059028E-01	7.196752E-01	2.440178E-01	4.404508E-01
RU105	44	105	0	314	1.0E+03	2.325016E-02	3.233188E-01	6.399468E-01	1.117743E-01	2.017520E-01
RU106	44	106	0	315	1.0E+03	8.344953E-03	5.233637E-02	2.475373E-01	8.153410E-02	1.471686E-01
RH103	45	103	0	1125	9.0E+02	4.648621E-02	5.571160E-01	9.047802E+01	9.701270E+01	1.751074E+02
RH105	45	105	0	334	1.0E+03	9.125643E-02	4.919683E-01	7.002262E+02	4.934551E+03	8.906837E+03
PD104	46	104	0	358	1.0E+03	8.530149E-02	2.169388E-01	2.016123E+00	2.166387E-01	3.910315E-01
PD105	46	105	0	359	1.0E+03	8.900761E-02	7.121473E-01	9.287985E+00	7.843382E+00	1.415726E+01
PD106	46	106	0	360	1.0E+03	4.789705E-02	1.283831E-01	7.720379E-01	1.332195E-01	2.404604E-01
PD107	46	107	0	361	1.0E+03	6.726203E-02	4.894277E-01	7.143654E+00	5.588543E+00	1.008729E+01
PD108	46	108	0	363	1.0E+03	4.149806E-02	1.255796E-01	2.259456E+01	6.845444E+00	1.235599E+01
PD110	46	110	0	366	1.0E+03	1.580939E-02	7.311286E-02	8.358860E-01	1.229825E-01	2.219828E-01
AG107	47	107	0	1138	9.0E+02	8.334117E-02	5.664923E-01	1.210986E+01	2.047736E+01	3.696153E+01
AG109	47	109	0	1139	9.0E+02	4.458553E-02	3.535820E-01	1.302363E+02	5.257063E+01	9.488969E+01
AG111	47	111	0	391	1.0E+03	2.611568E-02	3.334252E-01	1.231271E+01	1.677295E+00	3.027507E+00
CD108	48	108	0	415	1.0E+03	9.591343E-02	1.805074E-01	3.702015E-01	6.153806E-01	1.110758E+00
CD110	48	110	0	417	1.0E+03	1.158785E-01	2.033491E-01	4.663890E+00	6.207640E+00	1.120475E+01
CD111	48	111	0	418	1.0E+03	3.549300E-02	3.246907E-01	5.577368E+00	1.357310E+01	2.449936E+01
CD112	48	112	0	420	1.0E+03	9.319133E-02	1.924481E-01	1.147311E+00	1.230079E+00	2.220285E+00
CD113	48	113	0	1282	9.0E+02	4.035980E-02	2.936839E-01	2.050547E+01	2.727591E+04	4.923287E+04
CD114	48	114	0	423	1.0E+03	9.644373E-02	2.058760E-01	2.208012E+00	1.877895E-01	3.389589E-01
CD115M	48	115	1	425	1.0E+03	3.428619E-02	2.347852E-01	2.226469E+01	1.732369E+01	3.126916E+01
CD116	48	116	0	426	1.0E+03	4.177477E-02	9.279391E-02	2.235261E-01	4.293487E-02	7.749719E-02
IN113	49	113	0	445	1.0E+03	2.409397E-01	5.236885E-01	2.162369E+01	6.590786E+00	1.189633E+01
IN115	49	115	0	449	1.0E+03	1.228192E-01	3.755484E-01	2.854464E+02	1.289674E+02	2.327655E+02
SN115	50	115	0	482	1.0E+03	3.729064E-03	3.183642E-02	2.008304E+00	2.796581E+01	5.047812E+01
SN116	50	116	0	483	1.0E+03	3.175388E-02	4.364059E-02	1.356454E+00	6.732990E-02	1.215301E-01
SN117	50	117	0	484	1.0E+03	3.274490E-02	1.661797E-01	1.984943E+00	1.455753E+00	2.627627E+00
SN118	50	118	0	486	1.0E+03	7.690040E-02	8.667272E-02	6.911670E-01	4.610512E-02	8.321948E-02
SN119	50	119	0	487	1.0E+03	6.371977E-03	4.040596E-02	3.974212E-01	1.284014E+00	2.317637E+00
SN120	50	120	0	489	1.0E+03	1.800320E-02	2.933619E-02	1.337315E-01	7.881781E-02	1.422657E-01
SN122	50	122	0	492	1.0E+03	1.337318E-02	1.827124E-02	7.595520E-02	1.010517E-01	1.823978E-01
SN123	50	123	0	493	1.0E+03	3.947307E-02	8.523844E-02	2.774607E-01	1.845241E-02	3.330650E-02
SN124	50	124	0	495	1.0E+03	1.849913E-02	2.415400E-02	8.102987E-01	7.272250E-02	1.312637E-01
SN125	50	125	0	496	1.0E+03	9.919385E-03	4.686948E-02	1.984130E+00	3.074827E-01	5.550044E-01
SN126	50	126	0	498	1.0E+03	5.678309E-03	7.303296E-03	1.098527E-02	1.677718E-01	3.028272E-01
SB121	51	121	0	511	1.0E+03	1.106325E-01	4.009508E-01	1.677825E+01	3.560680E+00	6.427007E+00
SB123	51	123	0	514	1.0E+03	5.059958E-02	2.100477E-01	8.328224E+00	2.434903E+00	4.394987E+00
SB124	51	124	0	515	1.0E+03	2.543705E-02	5.863286E-01	2.475458E+00	3.630309E+00	6.552687E+00

TABLE XIV (cont)

NUCLIDE	Z	A	S	MAT	TEMP (K)	GROUP 1 CROSS SECTION	GROUP 2 CROSS SECTION	GROUP 3 CROSS SECTION	GROUP 4 CROSS SECTION	EFFEC.THERM. CROSS SECTION
SB125	51	125	0	518	1.0E+03	7.517359E-02	2.103150E-01	2.103414E+00	5.592590E-01	1.009459E+00
SB126	51	126	0	519	1.0E+03	1.848180E-02	3.033790E-01	5.136429E+00	3.247778E+00	5.862222E+00
TE122	52	122	0	538	1.0E+03	1.202321E-01	2.504961E-01	8.412152E+00	1.569423E+00	2.832800E+00
TE123	52	123	0	539	1.0E+03	6.157976E-02	3.666051E-01	4.865476E+02	2.468661E+02	4.455918E+02
TE124	52	124	0	541	1.0E+03	1.104859E-01	1.937552E-01	7.708467E-01	3.808186E+00	6.873755E+00
TE125	52	125	0	542	1.0E+03	2.613155E-02	2.557467E-01	2.647459E+00	8.658353E-01	1.562828E+00
TE126	52	126	0	544	1.0E+03	3.714886E-02	8.357152E-02	1.185596E+00	5.779812E-01	1.043253E+00
TE127M	52	127	1	546	1.0E+03	5.419348E-02	2.648949E-01	4.726406E+00	5.264135E+00	9.501734E+00
TE128	52	128	0	547	1.0E+03	4.529906E-02	8.662364E-02	2.271824E-01	1.202259E-01	2.170070E-01
TE129M	52	129	1	549	1.0E+03	9.472597E-03	8.205984E-02	6.885660E-01	6.142364E-01	1.108693E+00
TE130	52	130	0	550	1.0E+03	3.760774E-03	1.329507E-02	2.826283E-02	1.621755E-01	2.927259E-01
TE132	52	132	0	553	1.0E+03	5.710111E-04	4.443987E-04	7.327881E-05	1.117629E-03	2.017314E-03
I127	53	127	0	565	1.0E+03	5.610752E-02	3.939301E-01	1.539254E+01	3.478504E+00	6.278681E+00
I129	53	129	0	567	1.0E+03	4.800948E-02	2.804701E-01	3.709139E+00	1.510053E+01	2.725637E+01
I130	53	130	0	568	1.0E+03	1.837486E-02	2.696179E-01	1.985659E+01	1.004999E+01	1.814018E+01
I131	53	131	0	570	1.0E+03	9.472026E-03	7.367629E-02	9.685281E-01	3.911037E-01	7.059399E-01
I135	53	135	0	576	1.0E+03	4.684394E-04	5.736313E-04	7.324264E-04	1.118905E-02	2.019617E-02
XE128	54	128	0	1173	9.0E+02	5.312305E-02	2.997089E-01	2.526227E+01	9.969592E+00	1.799506E+01
XE129	54	129	0	589	1.0E+03	5.323277E-02	3.033197E-01	2.522329E+01	1.003302E+01	1.810954E+01
XE130	54	130	0	1174	9.0E+02	3.404525E-02	1.127239E-01	3.154451E-01	3.446107E+00	6.220203E+00
XE131	54	131	0	1175	9.0E+02	1.332154E-02	1.837029E-01	8.832394E+01	5.042924E+01	9.102450E+01
XE132	54	132	0	1176	9.0E+02	1.814070E-02	6.651676E-02	1.568604E-01	2.501073E-01	4.514423E-01
XE133	54	133	0	595	1.0E+03	5.950709E-03	5.286344E-02	3.435562E+01	1.062848E+02	1.918434E+02
XE134	54	134	0	1177	9.0E+02	1.054011E-02	3.432525E-02	3.981692E-02	1.434189E-01	2.588703E-01
XE135	54	135	0	1294	9.0E+02	5.564618E-04	3.218521E-03	3.634285E+02	1.670657E+06	3.015526E+06
XE136	54	136	0	1178	9.0E+02	1.072229E-03	2.288886E-03	1.069663E-02	8.874087E-02	1.601768E-01
CS133	55	133	0	1141	9.0E+02	5.103384E-02	3.777516E-01	3.378401E+01	1.663776E+01	3.003107E+01
CS134	55	134	0	614	1.0E+03	1.286883E-02	3.448577E-01	2.079022E+01	7.828318E+01	1.413007E+02
CS135	55	135	0	616	1.0E+03	3.180215E-03	4.148685E-02	4.381765E+00	4.866696E+00	8.784359E+00
CS136	55	136	0	618	1.0E+03	1.942282E-02	1.635070E-01	3.303652E+00	7.287809E-01	1.315445E+00
CS137	55	137	0	619	1.0E+03	1.502562E-03	5.543158E-03	5.867613E-02	6.142019E-02	1.108631E-01
BA134	56	134	0	634	1.0E+03	3.524396E-02	8.612855E-02	2.724576E+00	1.205309E+00	2.175576E+00
BA135	56	135	0	635	1.0E+03	2.867491E-02	2.214519E-01	1.119982E+01	3.250888E+00	5.867834E+00
BA136	56	136	0	637	1.0E+03	1.312605E-02	3.583927E-02	2.133971E-01	2.289892E-01	4.133242E-01
BA137	56	137	0	639	1.0E+03	7.225130E-03	3.743974E-02	4.969716E-01	2.849852E+00	5.143966E+00
BA138	56	138	0	641	1.0E+03	9.214468E-03	5.529264E-03	1.282347E-02	1.955539E-01	3.529736E-01
BA140	56	140	0	643	1.0E+03	1.689069E-03	3.743996E-03	1.567531E+00	8.912482E-01	1.608698E+00
LA139	57	139	0	657	1.0E+03	6.009337E-03	2.967405E-02	1.244460E+00	5.013105E+00	9.048625E+00
LA140	57	140	0	658	1.0E+03	2.948971E-02	1.295762E-01	7.885135E+00	1.508462E+00	2.722765E+00
CE140	58	140	0	674	1.0E+03	1.703531E-02	1.730715E-02	2.903654E-02	3.190750E-01	5.759285E-01
CE141	58	141	0	675	1.0E+03	4.510816E-02	1.054578E-01	2.342997E+00	1.619745E+01	2.923631E+01
CE142	58	142	0	676	1.0E+03	1.485239E-02	3.294434E-02	5.925282E-02	5.307171E-01	9.579413E-01
CE143	58	143	0	677	1.0E+03	9.577707E-03	7.577132E-02	5.095466E+00	3.349870E+00	6.046496E+00
CE144	58	144	0	678	1.0E+03	1.090923E-02	2.405806E-02	2.314846E-01	5.586255E-01	1.008316E+00
PR141	59	141	0	692	1.0E+03	2.548600E-02	9.959114E-02	2.105239E+00	6.439460E+00	1.162319E+01
PR142	59	142	0	693	1.0E+03	1.604911E-02	2.547168E-01	1.527271E+01	1.117627E+01	2.017310E+01
PR143	59	143	0	695	1.0E+03	4.842014E-02	2.161496E-01	1.913981E+01	4.977789E+01	8.984881E+01
ND142	60	142	0	713	1.0E+03	2.773231E-02	3.127668E-02	7.312854E-01	1.044265E+01	1.884892E+01

TABLE XIV (cont)

NUCLIDE	Z	A	S	MAT	TEMP K	GROUP 1 CROSS SECTION	GROUP 2 CROSS SECTION	GROUP 3 CROSS SECTION	GROUP 4 CROSS SECTION	EFFEC.THERM. CROSS SECTION
ND143	60	143	0	714	1.0E+03	5.923333E-02	1.938598E-01	1.209111E+01	1.773106E+02	3.200445E+02
ND144	60	144	0	715	1.0E+03	4.188978E-02	6.863372E-02	5.867006E-01	2.013982E+00	3.635226E+00
ND145	60	145	0	716	1.0E+03	6.803414E-02	1.983824E-01	2.256161E+01	2.355985E+01	4.252540E+01
ND146	60	146	0	717	1.0E+03	5.710881E-02	1.082823E-01	2.963151E-01	7.827704E-01	1.412896E+00
ND147	60	147	0	718	1.0E+03	5.106341E-02	3.928675E-01	6.013407E+01	2.740049E+01	4.945773E+01
ND148	60	148	0	719	1.0E+03	1.435365E-01	1.318842E-01	2.284639E+00	1.399507E+00	2.526102E+00
ND150	60	150	0	721	1.0E+03	5.230297E-02	1.742186E-01	1.865556E+00	6.713311E-01	1.211749E+00
PM147	61	147	0	733	1.0E+03	1.382808E-01	8.170927E-01	1.918335E+02	9.917021E+01	1.790017E+02
PM148	61	148	0	734	1.0E+03	4.921928E-01	2.574234E+00	2.332976E+03	2.594150E+03	4.682426E+03
PM148M	61	148	1	735	1.0E+03	4.921928E-01	2.574234E+00	3.182157E+02	1.909160E+04	3.446023E+04
PM149	61	149	0	736	1.0E+03	5.268164E-01	2.133433E+00	7.332632E+01	7.811904E+02	1.410044E+03
PM151	61	151	0	738	1.0E+03	1.012214E-03	2.037358E-02	1.742050E+02	3.910634E+02	7.058672E+02
SM147	62	147	0	753	1.0E+03	1.180276E-01	5.432755E-01	7.514796E+01	3.454724E+01	6.235757E+01
SM148	62	148	0	754	1.0E+03	2.023254E-01	2.596780E-01	3.134887E+00	1.509450E+00	2.724549E+00
SM149	62	149	0	1027	9.0E+02	5.637011E-02	9.344686E-01	2.770684E+02	4.841072E+04	8.738108E+04
SM150	62	150	0	756	1.0E+03	1.313093E-01	2.862238E-01	1.160902E+01	5.471646E+01	9.876290E+01
SM151	62	151	0	757	1.0E+03	2.315641E-01	1.356167E+00	2.894601E+02	4.669738E+03	8.428850E+03
SM152	62	152	0	758	1.0E+03	7.520442E-02	2.877061E-01	2.755117E+02	1.173567E+02	2.118261E+02
SM153	62	153	0	759	1.0E+03	2.260670E-04	1.191724E-02	2.418654E+02	1.846696E+02	3.333276E+02
SM154	62	154	0	760	1.0E+03	5.706727E-02	1.425114E-01	3.851160E+00	3.076205E+00	5.552533E+00
EU151	63	151	0	1290	9.0E+02	4.181577E-01	2.402754E+00	2.044278E+02	4.717469E+03	8.515005E+03
EU152	63	152	0	1292	9.0E+02	1.744222E-01	3.245252E+00	3.252586E+02	7.677840E+02	1.385846E+03
EU153	63	153	0	1291	9.0E+02	2.431446E-01	1.539698E+00	1.478631E+02	2.197333E+02	3.966174E+02
EU154	63	154	0	1293	9.0E+02	7.241066E-02	1.875663E+00	2.228416E+02	4.972313E+02	8.974997E+02
EU155	63	155	0	778	1.0E+03	9.062116E-01	1.543263E+00	1.540107E+02	2.258836E+03	4.077187E+03
EU156	63	156	0	779	1.0E+03	5.008924E-04	3.539738E-02	1.016701E+02	2.696344E+02	4.866885E+02
EU157	63	157	0	780	1.0E+03	3.221641E-03	2.526199E-02	8.471598E+01	1.059332E+02	1.912089E+02
GD154	64	154	0	791	1.0E+03	3.041554E-01	6.280531E-01	2.531751E+01	4.755081E+01	8.582895E+01
GD155	64	155	0	792	1.0E+03	1.251320E-01	1.467746E+00	1.313204E+02	1.920502E+04	3.466494E+04
GD156	64	156	0	793	1.0E+03	1.177736E-01	2.925910E-01	1.328447E+01	8.292483E-01	1.496788E+00
GD157	64	157	0	794	1.0E+03	1.068337E-01	7.103253E-01	8.871128E+01	8.261695E+04	1.491231E+05
GD158	64	158	0	795	1.0E+03	4.647452E-02	1.882511E-01	6.519249E+00	1.403779E+00	2.533814E+00
GD160	64	160	0	797	1.0E+03	8.083934E-02	1.503781E-01	9.311768E-01	4.300564E-01	7.762493E-01
TB159	65	159	0	803	1.0E+03	9.138282E-02	7.922879E-01	4.634842E+01	1.437843E+01	2.595299E+01
TB160	65	160	0	804	1.0E+03	1.434563E-03	7.845290E-02	8.018238E+01	2.928139E+02	5.285275E+02
DY160	66	160	0	811	1.0E+03	7.939346E-01	1.200462E+00	1.508596E+02	3.609387E+01	6.514924E+01
DY161	66	161	0	812	1.0E+03	5.945760E-02	1.227134E+00	1.166236E+02	3.112586E+02	5.618201E+02
DY162	66	162	0	813	1.0E+03	2.803023E-01	5.297747E-01	2.471440E+02	1.147570E+02	2.071357E+02
DY163	66	163	0	814	1.0E+03	5.480995E-02	5.190151E-01	1.336405E+02	7.776202E+01	1.403600E+02
DY164	66	164	0	1031	9.0E+02	9.006775E-02	1.905334E-01	2.300536E+01	1.300572E+03	2.347525E+03
HO165	67	165	0	820	1.0E+03	8.922674E-02	8.753142E-01	7.475623E+01	3.753369E+01	6.774810E+01
ER166	68	166	0	823	1.0E+03	1.431152E-01	2.983558E-01	1.481533E+01	1.954315E+01	3.527527E+01
ER167	68	167	0	824	1.0E+03	6.106636E-02	8.024943E-01	1.590069E+02	1.101003E+03	1.987304E+03

NOTE THAT THE EFFECTIVE THERMAL CROSS SECTION IS THE GROUP 4 CROSS SECTION DIVIDED BY SIGMA(1/V), WHERE SIGMA(1/V) IS THE GROUP 4 VALUE OF A 1/V CROSS SECTION EQUAL TO UNITY AT 2200 M/S (.554018)

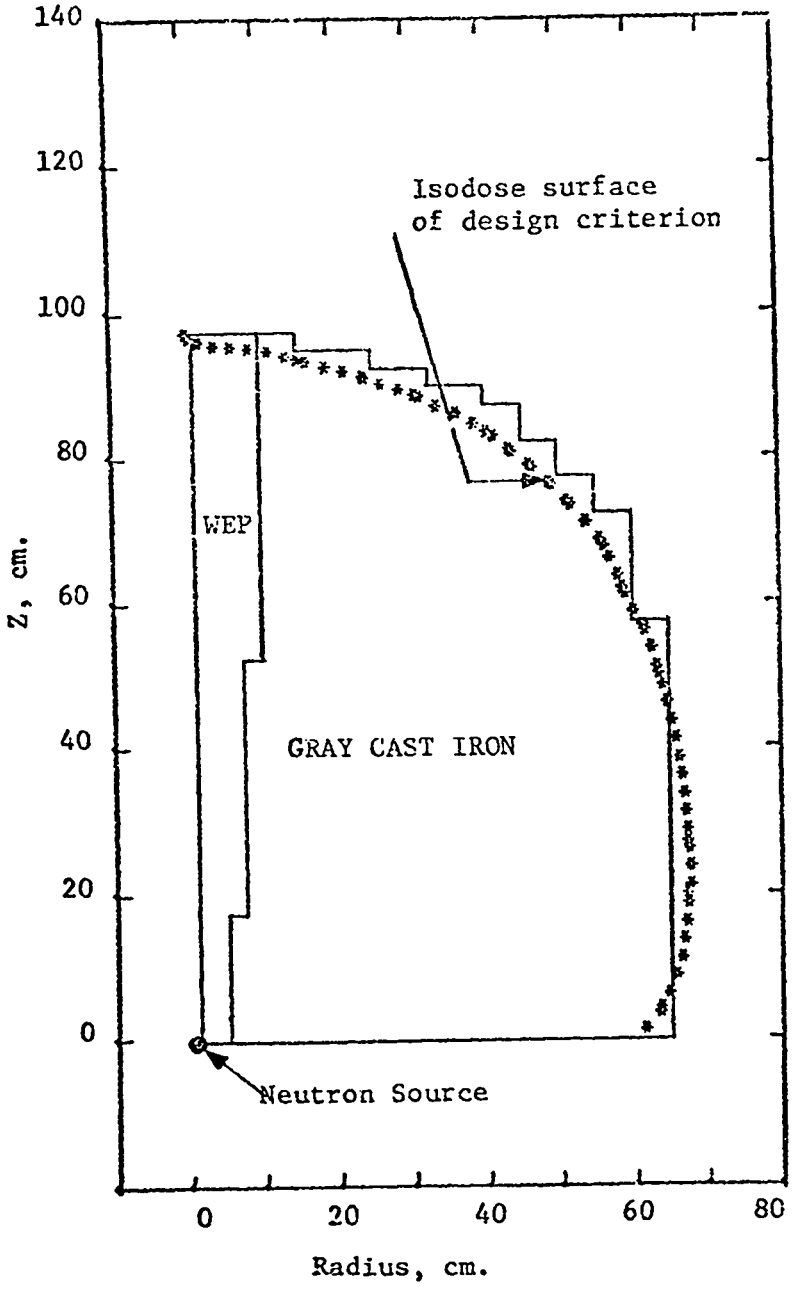

Fig. 19.
Shield design geometry.

V. SHIELD DESIGN FOR MEDIUM ENERGY NEUTRON RADIOTHERAPY [W. B. Wilson, J. B. Smathers (Texas A&M University) and D. R. Harris (Rensselaer Polytechnic Institute)]

The extension of existing programs in neutron radiotherapy to the practical treatment of a large variety of tumors requires the development of a pivoting shield unit of minimum mass and dimension, defining a collimated neutron beam with axis variable from horizontal to vertical. The design of such a unit for the facility at TAMVEC,[52] which uses neutrons produced anisotropically by 50-MeV deuterons on beryllium, has been accomplished (with the use of a 60 energy group nuclear data library previously described.[53]

The design criterion adopted for the shield unit was a neutron dose equivalent rate (NDER) on the shield surface equal to 0.5% of that delivered to the patient in the beam axis, 125 cm from the neutron source. The surface NDER is calculated as the inner product of the neutron flux at the surface and the neutron fluence-to-dose equivalent response function.[54]

The 60-group library energy structure was chosen such that the calculated surface NDER has approximately equal sensitivity to cross sections in each energy group. The 60-group library was collapsed to a 6-group set for use in the two-dimensional transport calculations with the TWOTRAN-II code.[55] Each group of the 6-group library corresponds with 10 groups of the 60-group library, retaining the equal sensitivity feature.

Two-dimensional shield calculations were performed with the 6-group library in cylindrical geometry. A massive gray cast iron shield with collimator inserts of water extended polyester (WEP), B_4C and iron particles (similar to that currently in use at the TAMVEC facility) was first calculated to produce flux values used in defining an isodose surface corresponding to the design criterion. Iterative choices of shield dimensions, transport calculations, and design isodose surface results were made.[55] The resulting geometry of the shield and the isodose surface of the shield design criterion are seen in Fig. 19.

REFERENCES

1. G. M. Hale, D. C. Dodder, J. J. Devaney, and K. Witte, "An R-matrix Analysis of p-^{3}He Scattering Below E_p = 19.5 MeV," Bull. Am. Phys. Soc. 19, 506 (1974).

2. T. R. Donoghue, Ohio State University, private communication (1977).

3. F. Seiler, Universitat Basel, private communication (1977).

4. L. Drigo, C. Manduchi, G. C. Nardelli, M. T. Russo-Manduchi, G. Torneilli, and G. Zannoni, "Polarization in p-^{3}He Elastic Scattering," Nucl. Phys. 89, 632 (1966).

5. P. Cziffra, M. H. MacGregor, M. J. Maravcsik, and H. P. Stapp, "Modified Analysis of Nucleon-Nucleon Scattering. I. Theory and p-p Scattering at 310 MeV," Phys. Rev. 114, 880 (1959).

6. M. Bolsterli and G. M. Hale, "Modified Phase Shift Analysis for p-^{3}He Elastic Scattering," Phys. Rev. Lett. 28, 1285 (1972).

7. G. M. Hale, "R-Matrix Analysis of the ^{7}Li System," Proc. International Specialists Symposium on Neutron Standards and Applications, Gaithersburg, Md (1977).

8. P. A. Moldauer, "Optical Model of Low Energy Neutron Interactions with Spherical Nuclei," Nucl. Phys. 47, 65 (1963).

9. D. Wilmore and P. E. Hodgson, "The Calculation of Neutron Cross Sections from Optical Potentials," Nucl. Phys. 55, 673 (1964).

10. C. M. Perey and F. G. Perey, "Deuteron Optical-Model Analysis in the Range of 11 to 27 MeV," Phys. Rev. 132, 755 (1963).

11. L. McFadden and G. R. Satchler, "Optical-Model Analysis of the Scattering of 24.7 MeV Alpha Particles," Nucl. Phys. 84, 177 (1966).

12. A. Gilbert and A. G. W. Cameron,"A Composite Nuclear Level Density Formula with Shell Corrections" Can. J. Phys. 43, 1446 (1965).

13. J. L. Cook, H. Ferguson, and A. R. Musgrove, "Nuclear Level Densities in Intermediate and Heavy Nuclei," Aust. J. Phys. 20, 477 (1967).

14. L. Milazzo-Colli and G. M. Braga-Marcazzan, "α-Emission by Pre-Equilibrium Process in (n,α) Reactions," Nucl. Phys. A210, 297 (1973).

15. C. I. Baxman and P. G. Young, "Applied Nuclear Data Research and Development Quarterly Progress Report," LA-6893-PR (1977), Sec. I.D, p. 3.

16. D. M. Brink, thesis, Oxford University (1955); P. Axel, "Electric Dipole Ground State Transition Width Strength Fission," Phys. Rev. 126, 671 (1962).

17. E. D. Arthur and P. G. Young, "A New Statistical-Preequilibrium Nuclear Model Code," Trans. Am. Nucl. Soc. 23, 500 (1976).

18. C. Dunford, Brookhaven National Laboratory, private communication (1971).

19. D. M. Drake, Los Alamos Scientific Laboratory, private communication (1977).

20. E. H. Auerbach and S. O. Moore, "Calculations of Inelastic Scattering of Neutrons by Heavy Nuclei," Phys. Rev. 135, B895 (1964).

21. J. M. Blatt and V. F. Weisskopf, Theoretical Nuclear Physics (John Wiley and Sons, Inc., New York, 1952).

22. E. D. Arthur and P. G. Young, "Calculation of 15-MeV Neutron-Induced Charged-Particle Spectra on Stainless Steel Type 316," and "^{59}Co + n Calculations up to Neutron Energies of 40 MeV," Trans. Am. Nucl. Soc. 26, 503 (1977).

23. E. D. Arthur and P. G. Young, "Cross Sections in the Energy Range from 10 to 40 MeV Calculated with the GNASH Code," Proc. of Symposium on Neutron Cross Sections 10-40 MeV, Brookhaven National Laboratory, May 1977.

24. G. J. Pyle, "RAROMP (Regular and Reformulated Optical Model Potentials)," John H. Williams Laboratory of Nuclear Physics Internal Report, University of Minnesota, private communication (1970).

25. Peter Schwandt, Indiana University, private communication (1976).

26. F. D. Becchetti and G. W. Greenlees, "Nucleon-Nucleus Optical-Model Parameters, A > 40, E < 50 MeV," Phys. Rev. 182, 1190 (1969).

27. J. M. Ferguson, "JANE: A Code for Calculating Neutron Compound-Nucleus Cross Cross Sections and Angular Distributions," U. S. Naval Radiological Defense Laboratory report NRDL-CP-68-4 (1968).

28. C. I. Baxman and P. G. Young, "Applied Nuclear Data Research & Development Quarterly Progress Report," Los Alamos Scientific Laboratory report LA-6893-PR (1977), Sec. I.K, p.10.

29. C. I. Baxman and P. G. Young, "Applied Nuclear Data Research & Development Quarterly Progress Report," Los Alamos Scientific Laboratory report LA-6893-PR (August 1977), Sec. IV.B, p.28.

30. Odelli Ozer, Electric Power Research Insitutute, private communication.

31. D. G. Foster, Los Alamos Scientific Laboratory, unpublished data (1973).

32. C. I. Baxman and P. G. Young, "Applied Nuclear Data Research & Development Quarterly Progress Report," Los Alamos Scientific Laboratory report LA-6754-PR (March, 1977), Sec. III, p. 12.

33. D. W. Muir, Los Alamos Scientific Laboratory, private communication (Dec. 1974).

34. S. A. W. Gerstl, "Sensitivity Profiles for Secondary Energy and Angular Distributions," Proc. of the Fifth International Conf. on Reactor Shielding, Knoxville, Tennessee (April 1977).

35. S. A. W. Gerstl, D. J. Dudziak, and D. W. Muir, "Cross-Section Sensitivity and Uncertainty Analysis with Application to a Fusion Reactor," Nucl. Sci. Eng. 62, 137 (1977).

36. A. V. Ignatyuk, G. N. Smirenkin, and A. S. Tishin, "Phenomenological Description of the Energy Dependence of the Level Density Parameters," Sov. J. Nucl. Phys. 21, 255 (1975).

37. J. Terrell, "Prompt Neutrons from Fission," Proc. of the International Atomic Energy Agency Symposium on Physics and Chemistry of Fission, Salzburg, 1965, Vol. II, P. 3.

38. P. A. Seeger and W. M. Howard, "Semi-Empirical Atomic Mass Formula," Nucl. Phys. A238, 491 (1975).

39. D. G. Madland and L. Stewart, "Light Ternary Fission Products: Probabilities and Charge Distributions," Los Alamos Scientific Laboratory report LA-6783-MS (ENDF-247) (April 1977).

40. D. G. Madland and T. R. England, "The Influence of Pairing on the Distribution of Independent Yield Strengths in Neutron-Induced Fission," Los Alamos Scientific Laboratory report LA-6430-MS (ENDF-240) (July 1976).

41. D. G. Madland and T. R. England, "Distribution of Independent Fission-Product Yields to Isomeric States," Los Alamos Scientific Laboratory report LA-6595-MS(ENDF-241) (November 1976).

42. T. R. England, B. Wilczynski, and N. L. Whittemore, "CINDER-7: An Interim Report for Users," Los Alamos Scientific Laboratory report LA-5885-MS (April 1975).

43. M. G. Stamatelatos and T. R. England, "FPDCYS and FPSPEC, Computer Programs for Calculating Fission-Product Beta and Gamma Multigroup Spectra from ENDF/B-IV Data," Los Alamos Scientific Laboratory report LA-NUREG-6818-MS(1977).

44. R. J. LaBauve, T. R. England, M. G. Stamatelatos, and D. C. George, "Approximations to Summation Calculations of Delayed Energy and Spectra from Fission Products," Los Alamos Scientific Laboratory report LA-6684-MS (January 1977).

45. T. R. England and M. G. Stamatelatos, "Multigroup Beta and Gamma Spectra of Individual ENDF/B-IV Fission Product Nuclides," Los Alamos Scientific Laboratory report LA-NUREG-6622-MS (November 1976).

46. T. R. England and M. G. Stamatelatos, "Comparisons of Calculated and Delayed Fission Point Beta and Gamma Spectra from ^{235}U Thermal Fission," Los Alamos Scientific Laboratory report LA-NUREG-6896-MS (1977).

47. C. I. Baxman, G. M. Hale, and P. G. Young, "Applied Nuclear Data Research and Development Quarterly Progress Report," Los Alamos Scientific Laboratory report LA-6472-PR (August 1976), Sec. V.C, p. 60.

48. C. I. Baxman and P. G. Young, "Applied Nuclear Data Research and Development Quarterly Progress Report," Los Alamos Scientific Laboratory report LA-6560-PR (November 1976), Sec. V.C, p. 58.

49. C. I. Baxman and P. G. Young, "Applied Nuclear Data Research and Development Quarterly Progress Reprot," Los Alamos Scientific Laboratory report LA-6754-PR (March 1977), Sec. IV.D, p. 15.

50. T. R. England, W. B. Wilson, and M. G. Stamatelatos, "Fission Product Data for Thermal Reactors, Part 1, A Data Set for EPRI-CINDER Using ENDF/B-IV," Los Alamos Scientific Laboratory/Electric Power Research Institute report LA-6745-MS (to be published); and "Fission Product Data for Thermal Reactors, Part 2, Users Manual for EPRI-CINDER Code and Data," Los Alamos Scientific Laboratory/Electric Power Research Institute report LA-6746-MS (to be published).

51. S. B. Gunst, J. C. Connor, and D. E. Conway, "Measured and Calculated Fission-Product Poisoning in Neutron-Irradiated Uranium-233," Nucl. Sci. Eng. 58, 387 (1975).

52. W. A. McFarlin and A. D. Suttle, Jr., "Fast Neutron Cancer Therapy with the TAMVEC,"IEEE Trans. Nucl. Sci. NS-18, 780 (1971).

53. W. B. Wilson, J. B. Smathers, D. R. Harris, D. G. Foster, Jr., and R. E. MacFarlane, "Neutron Multigroup Cross Sections for Radiotherapy Shielding Applications," Trans. Am. Nucl. Soc. 23, 633 (1976).

54. G. M. Hale, D. R. Harris, and R. E. MacFarlane, "Applied Nuclear Data Research and Development Quarterly Progress Report," Los Alamos Scientific Laboratory report LA-5666-PR (July 1974), Sec. VIII, p. 17.

55. K. D. Lathrop and F. W. Brinkley, "TWOTRAN-II: An Interfaced, Exportable Version of the TWOTRAN Code for Two-Dimensional Transport," Los Alamos Scientific Laboratory report LA-4848-MS (1973).

56. W. B. Wilson, "Nuclear Data Development and Shield Design for Neutrons Below 60 MeV," thesis, Texas A & M University (May 1977).

☆ U.S. GOVERNMENT PRINTING OFFICE: 1977—777-018/127